Welding Research

SPONSORED BY THE WELDING RESEARCH COUNCIL
OF THE ENGINEERING FOUNDATION

W. SPRARAGEN, DIRECTOR

SUPPLEMENT TO THE WELDING JOURNAL, DECEMBER, 1956

TIME-TEMPERATURE DEPENDENCE OF AUSTENITIC STAINLESS-STEEL WELDED JOINT COMPONENTS

Paper enumerates and illustrates the several phenomena involved. Also, a series of corrective procedures are suggested for existing materials

BY J. HEUSCHKEL

Introduction

Austenitic stainless steels tend to retain their tensile strength at elevated temperatures, and welded structures are made of these alloys for such usage. The short-time and long-time mechanical properties of such as-furnished base metals, of the welding heat- and strain-affected zones of the base metal, and of the as-deposited weld metals are not always identical at any one temperature. The yield strength of the rapidly cooled weld metal is usually higher than that of the base metal.[1] An important factor in mechanical structural performance is the manner in which these three components of the welded joints, having similar compositions but nonuniform properties, respond as a unit to nonuniformly applied stress and strain under the imposed orders of temperature and time.

Fabrication and elevated temperature service cracking experiences with some of the austenitic matrix type, Cr-Ni steels have suggested the need for a re-evaluation of the characteristics of these and other high-temperature alloys for applications in the welded condition.[2] The existing metals processing procedures are also open to re-evaluation. The materials involved were usually developed for use in the unwelded condition under corrosive environments at normal temperatures.[3]

These base metals may be brittle over 2450° F in some instances, that is, just under the melting temperature. They may also be embrittled after having been recooled from 2450° F or above.[4] Narrow zones of base metals adjacent to all-metal arc welds are exposed to such high temperatures for brief time intervals. Another short-time temperature zone in which brittleness often exists, particularly in as-deposited weld metals, is between 1700 and 1900° F.[1] Between the 1700 to 1900° F and the 2450° F to melting point zones the metals may be ductile.[5]

The as-welded metallurgical structures may become unstable with time at temperature. Austenitic steels under load at high and medium temperatures tend to decrease in capacity to resist stress and strain with increasing times to rupture.[6] Phase changes, under the impetus of temperature, time and stress, can cause nominally ductile alloys to become fully brittle at high, intermediate, or room temperatures. This introduces the opposite and seldom recognized extreme problem; some of the welding difficulties in austenitic matrix materials arise from cold cracking, for example, in maltreated castings.

The purpose of this paper is to enumerate and illustrate the several phenomena involved. A series of corrective procedures are suggested for existing materials. The long-range future solution lies in the controlled processing of high-temperature alloys which are specially designed for welded applications. Precision control of welding is also necessary.

Detail Considerations

Early weldments of the austenitic Cr-Ni steels were made from metal less than $^3/_8$-in. in thickness and, in such structures, high levels of weld cool-down shrinkage stresses were not usually encountered. For those conditions most of the lower carbon materials were generally satisfactory but even there local cracking was sometimes encountered both in the weld metal and in the stress concentration regions of the heat-affected zones. These phenomena are related to stress.

Carbide precipitation was experienced with the early 0.20% carbon content grades of sheets and plates.[7] The resultant present low-carbon limits and the "stabilized" grades of the Cr-Ni steels are the outgrowth of those early experiences. The usage of the term "stabilized" has proved to be unfortunate in that the original intent of retarding carbide precipitation by selective prevention of chromium depletion near the grain boundaries does not imply over-all attainment of metallurgical stability of all of the several phases

J. Heuschkel is Consulting Welding Engineer, Research Laboratories, Westinghouse Electric Corp., Pittsburgh, Pa.

Paper presented at the ASME Metals Engineering Division Conference held in conjunction with the 1956 AWS National Spring Meeting, May 7 to 11, Buffalo, N. Y.

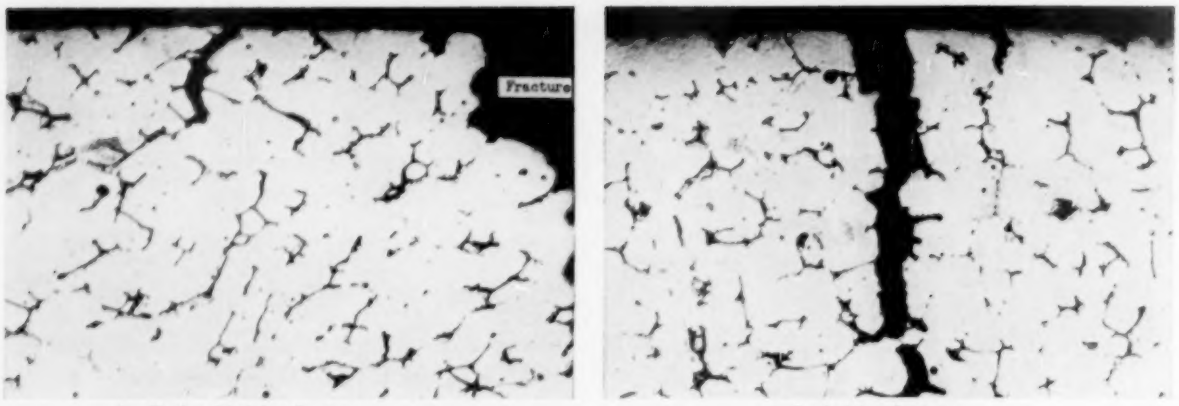

A. Final and incipient fractures

B. Incipient fracture

Fig. 1 Incipient fracture in 25 Cr-12 Ni-1 Nb casting following brittle network (originally delta ferrite). X 100. (Reduced by 1/2 upon reproduction)

which may be present. The niobium (= columbium) stabilized grades have been found to have higher hot strengths and lower hot ductilities.[1] These steels are responsive to heat treatment, but not to the extent that they are quench-hardenable. Some Cr-Ni steel castings can be ductile or brittle, even at room temperature, depending wholly upon the heat treatment of the individual specimen.

In early steam piping applications, ferritic steels were used and some difficulties were experienced as a result of the graphitization phenomena in and adjacent to the welds.[8] Since steam pressures and temperatures have long been expected to continue to increase, it was apparent to the power industry that improved materials for this purpose would be required. Because AISI Grade 347 Cr-Ni steel retained highest strength at elevated temperatures, it was widely used for these applications. More recently, field difficulties have been encountered with the AISI 347 grade steels both in and adjacent to the welds in some individual components operating at or near 1050° F.[2]

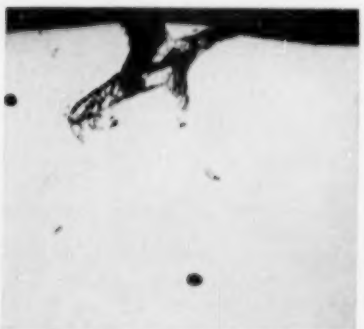

Fig. 2 Incipient crack (surface burst) on room temperature bend test originating from transformed ferrite island. X 500. (Reduced by 1/2 upon reproduction)

Many of the as-cast Cr-Ni steels have a two-phased structure; a three-dimensional network of delta ferrite in an austenitic matrix. Such networks may or may not be continuous. The proportion of ferrite present,[9] its individual particle size and its distribution, are a function of average chemical composition[10] and initial solidification rate. The present technical dilemma is that adjusting the cast composition to the fully austenitic form results in hot brittleness because of contaminated grain boundaries while the ferrite particles in the two-phased compositions subsequently become nuclei of failure at high temperatures. Also sigma and carbides readily form in the ferrite after which the steel is embrittled at and near ambient temperatures. Present deficiencies are only partially rectified by employing vacuum melting techniques and by special alloy adjustments because Fe-Cr compounds form the base of the brittle sigma phase.[11]

It is not yet possible to predict the ultimate performance or the metallurgical requirements of a massive weldment from theoretical considerations alone. Conventional short- or long-time test properties of the unwelded base metal within the usual range of test temperatures have failed to provide the basis for accurate evaluations. Ambient or elevated temperature test properties of any other one component of the welded joints are also inadequate.

The welding materials and procedures being used in the fabrication of austenitic weldments are necessarily being subjected to critical review. The time-temperature dependence of the tensile properties of weld metals deposited in the austenitic Cr-Ni steels have now been partially described.[1, 12] An outstanding characteristic of most weld metals is that a region of short-time minimum ductility exists at or near 1800° F.[1] Highest hot strengths are secured with niobium-bearing weld metals (AISI 347 and other grades). At the 1800° F temperature there is a generally existent inverse relation between weld strength and ductility. However, not all weld-metal compositions exhibit low hot ductility, that is, at temperatures of 2200° F or less. It was therefore necessary to examine the variations observed between the different compositions.

Hot strength of iron-base alloy welds is increased with additions of nickel, manganese, molybdenum, niobium, titanium, carbon and nitrogen. Niobium is the most effective on a percentage-weight basis. Additions of niobium, carbon, nitrogen, oxygen and silicon are sources of compounds which decrease the capacity of the metal to flow in the hot condition. When the product of the adjusted sums of the strengthening and the flow-reducing alloy additions are a minimum, the welds have maximum hot ductility.[1] Conversely, when this product is a maximum, the welds have a minimum hot ductility. Chromium has no significantly-strong influence on either hot strength or ductility; its influence may be negative, positive or neutral and in this paper, for the usually constant amounts involved, is being disregarded.

Fig. 3 Incipient cracking in tensile specimen normal to load direction (origin in transformed delta ferrite). X 500. (Reduced by 1/2 upon reproduction)

Weld-metal hot strength has important implications with respect to stresses and strains imposed upon the metallurgically damaged grain boundaries of the heat-affected zone of the base metal. For any cooling temperature at which the strength of the weld is greater than that of the base metal, the cool-down shrinkage strains are absorbed by the base metal. If the base metal grain boundaries are mechanically weakened by metallurgical changes resulting from their brief exposure to high temperature, macro or microcracking may be induced during cool-down because the high hot-strength weld-metal imposed shrinkage stresses, upon the adjacent base metal, which are above the fracture strength of the grain boundaries. Also, on cool-down, if a brittle phase has previously been formed in the base metal, as in the sigmatization of or carbide formation in the coarse particles of delta ferrite of a casting, the residual welding stresses can readily exceed the average boundary fracture stress and local cracking occurs. Best assurances for avoidance of initial base metal grain boundary cracking are therefore secured by using lower hot-strength weld metal, by using a welding technique that will not impose high shrinkage stresses upon the metallurgically-altered base metal while it is in the dangerously low ductility condition and, preferably, by ultimately having available base metals that are undamaged by brief exposures to submolten temperatures.

In addition to suitable short-time properties, long-time metallurgical stability and capacity to withstand stress under prolonged periods at elevated temperatures are required of the weld metal and heat-affected zone, as well as of the unaffected base metal. Performance of the mechanical structure is determined by the metallurgical component of the joint that is first to rupture.

It is a general characteristic of many metals that both strength and ductility decrease at elevated temperatures with time under static stress. Also, many metals are not metallurgically stable at elevated temperatures, even in the absence of stress. Without an understanding of such phenomena, the probable performance of the joint as a whole cannot be accurately predicted. The industrial problem has been complicated by the fact that much of the necessary information was not and still is not generally available to the engineering profession.

Underbead heat-affected zone base metal cracking has been experienced in both castings and forgings. In wrought products these are austenitic grain boundary separations. Such cracks can form in sheets as well as in forgings. In the absence of clarification, such failures of the base metal have been reported to be due to the presence of grain boundary liquation, initial cool-down microcracks, excessive stresses, hot brittleness, cold brittleness, newly formed phases, improper grain size, or local eutectic formations. No one of these several features need be the sole cause of all of the cracking problems encountered; each may play its part in some particular situation. Cracking may occur in the absence of one or several of these phenomena.

There is a prevalent industrial opinion that, for a particular composition, two grades of forging steel are being furnished; one satisfactory and one unsatisfactory for welding, the criterion being whether or not cracking occurs during or after welding. Variations in preparation of the molten metal, initial ingot pouring temperature, ingot processing, degree of first reduction of ingot in forging and completeness of breakdown of the as-cast dendritic structures may all be more important

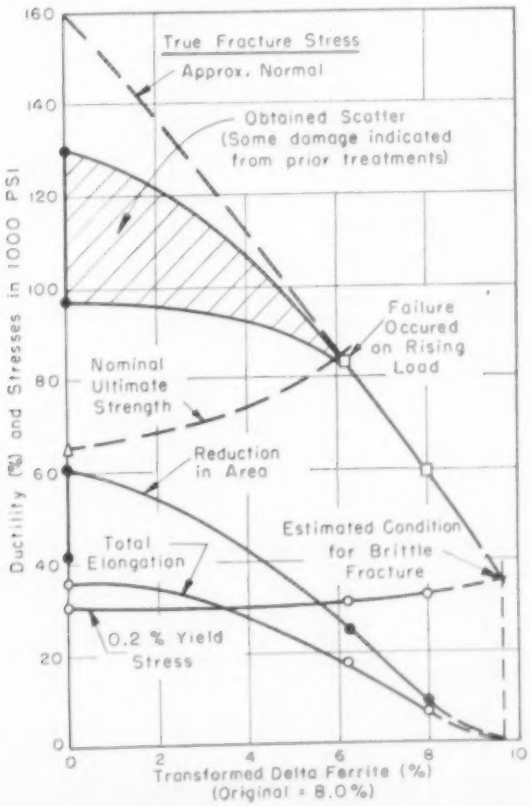

Fig. 4 Influence of brittle transformation products on properties of cast AISI 309 + Cb steel at +80° F

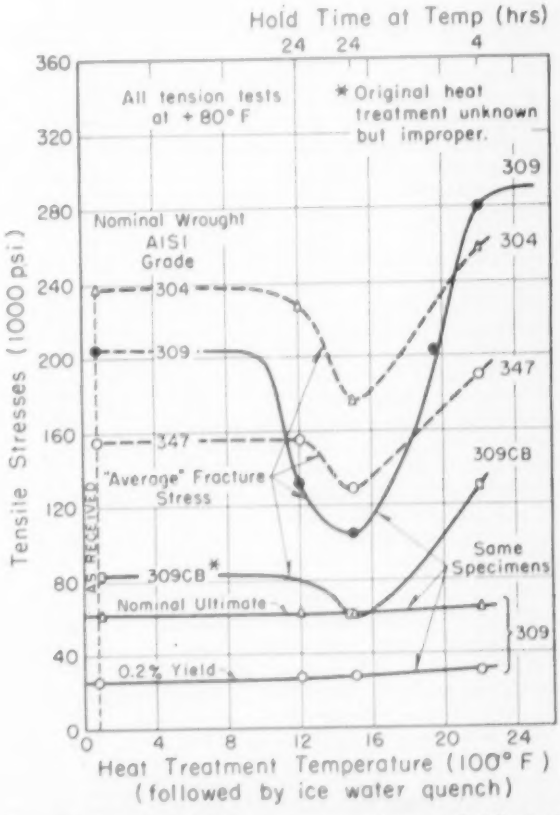

Fig. 5 Relations between grades of some Cr-Ni steel castings, fracture stresses and heat-treating temperature

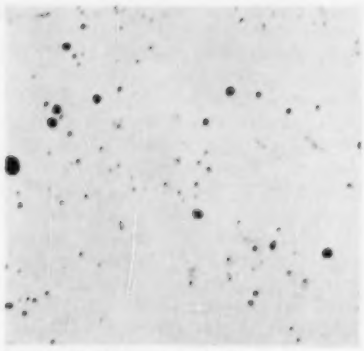

Fig. 6 Inclusions, carbides and eutectic structures in cast 25 Cr-12 Ni-1 Nb steel. X 100, unetched. (Reduced by 1/3 upon reproduction)

factors in controlling forging weldability than compliance with nominal composition or mechanical properties of presently constituted specifications.

Drastic differences in properties, for a given piece of material, can most readily be demonstrated with castings. For selected compositions, a 2200° F solution-treated casting, rapidly quenched, can be shown to be ductile, whereas one heated to 1500° F for 24 hr and quenched is brittle, even at room temperature. Could these readily demonstrable variations be carried over in steel mill ingot processing to cause the two reported conditions in forgings and rolled products? Also, castings may be high or low in inclusion content. With neither the initial inclusion or phase content variables or the degree of breakdown of the cast structure in the forgings being a matter of specification control, it is probable that much of the base metal variation found during or as a result of welding is inherited from the original metal processing. Are present specifications for welded base metals directed toward control of the wrong parameters? If there is an equivalence between metal weldability, hot ductility, stress-rupture characteristics, microstructure, composition and metals-making practice, is it not probable that the last item is the important weldability factor? If so, how is it to be controlled, with due consideration to both the technical and practical aspects of the problem?

Sigma Phase

Sigma phase is considered by the authorities[11] to be made up of a quasi-hexagonally arranged unit cell containing 30 atoms, the end atoms in the hexagons being slightly raised. Its ductility at room temperature is essentially zero. It is formed between 1000 and 1650° F and most readily near 1500° F. Once formed, it can be completely eliminated by heat treatment without detriment to the properties of the steel, provided damaging microcracks were not formed during the period of its presence. Within these limits it is a thermally reversible reaction. The make-up of sigma is not chemically unique but, according to Beck,[11] it may be formed from most combinations of the "1" and "2" groups of elements in Table 1. The elements in column 3 do not participate.

The elements set in italic type are those with which industry is concerned when dealing with the present Cr-Ni steels. The potentialities for the formation of sigma phase, particularly from the Fe-Cr rich delta ferrite, illustrates one facet of the weldability problem inherently different from that of grain boundary liquation, carbide

Table 1

1		2			3	
V	*Cr*	*Mn**	*Fe*†	*Co*		*Ni*
Nb	*Mo*	Tc	Ru	...	Rh	Pd
Ta	*W*	Re	Os	...	Ir	Pt
b.c.c.		h.c.p.			f.c.c.	

* Cubic, complex.

† b.c.c., but this arrangement preferred by Beck.

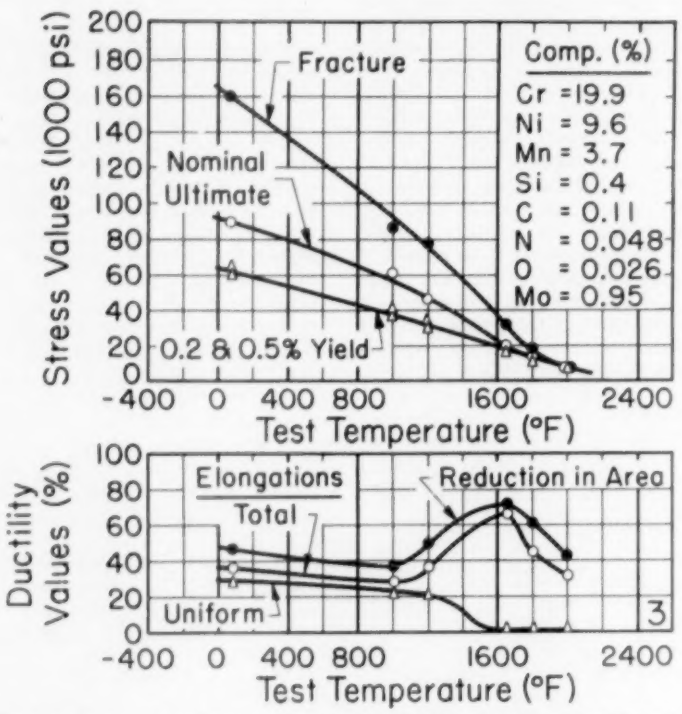

Fig. 7 Influence of temperature upon short-time tension properties of Type 307 weld metal as-deposited with covered electrodes

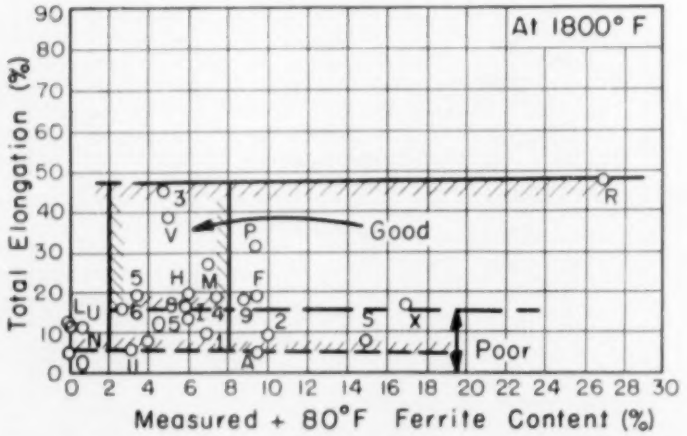

Fig. 8 Relations between as-deposited ferrite content at +80° F and total elongation at 1800° F

Table 2—Properties of Castings (Fig. 5)

Nominal AISI 300 series type:	*304*	*309*	*309Cb*	*347*
Chemical Analysis, Per Cent				
Chromium	19.7	22.2	22.10	19.09
Nickel	8.59	14.0	13.83	11.00
Manganese	1.30	1.13	0.98	0.75
Silicon	0.86	0.21	0.79	0.95
Niobium + tantalum		0.03	1.14	0.91
Carbon	0.07	0.051	0.055	0.054
Nitrogen		0.040	0.029	
Sulfur	0.010			
Phosphorus	0.022			
Molybdenum	...	...	...	0.05
Copper	...	...	...	0.11
Postcasting heat treatment, ° F	2,050	2,050	Unknown	None
Tensile Properties (+80° F)				
0.2% yield stress, psi	29,250	28,200	30,600	31,500
Nominal ultimate stress, psi	70,400	63,000	82,800*	73,000
Fracture stress, psi	226,400	133,000	82,800	154,500
Elong., uniform, %	55.4	27.6	17.6*	39.0
Elong., total, %	67.4	35.4	17.6	45.1
Area reduction, %	74.6	58.1	24.5	57.4
Ferrite, % at R.T.	6.2	2.5	2.0	2.6

* Broke on rising load.

precipitation, and the oxygen-nitrogen compound formation reactions in the presence of the many alloying elements of these systems. On the other hand, it is inaccurate to randomly ascribe all forms of brittleness to the presence of sigma because such brittleness may be caused by the presence of carbides. It is sometimes difficult to distinguish between the two phases.

Castings

Steelmaking starts with the preparation of molten metal for casting the original ingot. Forgings, plates, bars, rods and sheets are processed from such cast ingots. Knowledge of the characteristics, properties, impurities, and weldability of castings, therefore, constitutes an elementary first consideration in the study of the weldability of forged and rolled products.

Even at room temperature castings may be either ductile or brittle. They may be weldable or nonweldable. These properties are determined by the composition, manufacturing procedure, solidification pattern and thermal treatments. Little useful published information is available on this subject.[13, 14]

Most present-day Cr-Ni austenitic type steels are made by electric-arc furnace melting, using from 60 to 70% of alloy steel scrap. Carbon electrodes are used. The molten bath is exposed to an air environment, except for the semiprotection offered by the turbulent floating surface of molten slag which covers the bubbling liquid steel. This accounts for the fact that the nitrogen contents of the Cr-Ni steels, ranging from 0.03 to 0.05%, are higher than the about 0.003% common to open-hearth carbon structural steels. Carbon and other constituents such as silicon are lowered during the final period of the melt by blowing oxygen through the molten mass.[15] This also results in the formation and retention of oxides, including silica and silicate inclusions. The degree of cleanliness of the solidified melt determines the inclusion content of the metal which is later forged, wrought and welded. The original inclusions are elongated, increased in width and decreased in thickness during subsequent working. For research purposes, inclusion identification is simplified by studying the parent casting.

Suitable procedures have not been published for the accurate prediction of the microstructural make-up of Cr-Ni steel castings. Approximate diagrams have been published for the Fe-Cr-Ni system under equilibrium conditions,[16] but commercial alloys involve ten or more significant alloying elements. The Schaffler diagram has been found to be substantially correct for rapidly cooled metal-arc weld metals of essentially constant nominal nitrogen contents.[10] It cannot ordinarily be used for massive castings or for forgings, plates or sheets. Modifications for such usage have been suggested.[17] The AISI 304, 309 and 347 grades are composition types which are often two phased as cast. The original delta ferrite particles are larger in castings than in weld metal (Fig. 1). These larger particles of ferrite, including the ferrite-austenite interface, trans-

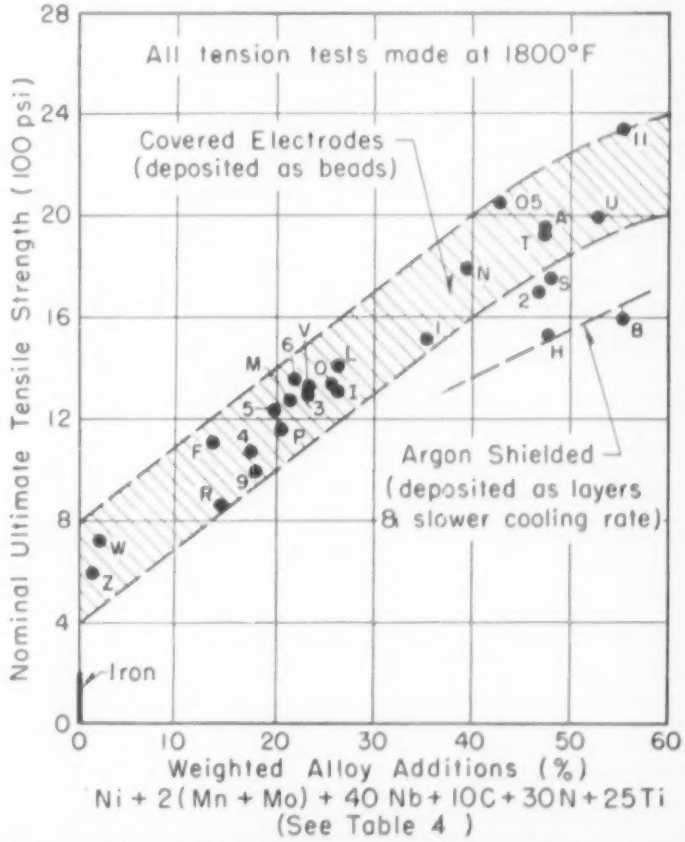

Fig. 9 Tensile strength-composition relations of as-deposited iron-base-alloy metal-arc welds tested at 1800° F

form in part into carbides and/or sigma phase when subject to sustained treatment between 1000 and 1600° F. Both are brittle. Castings therefore become brittle when subject to such treatment prior to, during, or subsequent to welding. Such castings have cracked disastrously at nominal temperatures and stresses. The average fracture stress for one such maltreated material has been shown to be as low as 60,000 psi at room temperature, while for properly heat-treated castings such stresses are from 200,000 to 240,000 psi. The consequences of the low fracture stresses were clearly illustrated by the complete catastrophic rupture which occurred at room temperature after an angular deformation of only 12 deg in a welder's qualification-type bend test. A longitudinal section across the fracture (Fig. 1*A*) shows that cracking originated within the original ferrite regions which had been transformed into the brittle sigma and carbide phases.

In another example, surface bursts found in room temperature bend testing originated in, and were confined to, the brittle phase resulting from transformation of delta ferrite at the tension fiber (Fig. 2). The raised region is the result of the local stiffening by the harder, more brittle phase. The austenitic matrix had a DPH hardness of 195 and companion regions of the brittle phase had hardness values of 519. Hardnesses in the sigma phase as high as 1980 have been reported in the literature.[18]

Longitudinal sections taken through tensile specimens which had been ruptured at room temperature consistently and repeatedly showed the initiation of failure to be in the original ferrite islands which had been transformed into the brittle forms (Fig. 3). The microcracks are normal to direction of load. Such microcracks were not found in sections taken from companion specimens prior to straining. The original larger ferrite islands in the castings permit the microcracks in the brittle phase to become damagingly long under low orders of strain. Such cracks propagate around the more ductile austenitic matrix (Fig. 1 example B). Fracture under these conditions occurs at low orders of strain because local fracture results while the average stress is less than the nominal true fracture stress.

Room-temperature ductility approached zero for this metal in the unnotched tensile condition when all the original 8.0% of magnetic delta ferrite had been converted into the nonmagnetic brittle forms of sigma and/or carbides by heating to 1500° F for 24 hr and ice-water quenching the 0.357-in. diam round (Fig. 4). The fact that, after this treatment, more than 90% of the total volume of the metal was still composed of the ductile austenitic phase had no significance; the essentially continuous brittle phase network completely determined the mechanical characteristics. Solution treatment of companion specimens of the embrittled casting at 2200° F for 4 hr, followed by an ice-water quench, reconverted the brittle phases back into the ductile delta ferrite form. Except for the fact that microcracks had been formed which resulted in permanent damage, the original properties would have been restored. The shaded region of the fracture stress curves (Fig. 4), show some permanent damage had been done to the metal by this treatment. The use of average true fracture stress (final load before rupture divided by final cross-sectional area) as a criterion of suitability of an alloy is therefore a valuable approach.

The conventional measured elongation values in specimens having a brittle second phase may include the summation of all the micro and macrofissures. The unqualified use of such data tends to conceal actual conditions. The variation in reduction of area from 41 to 60% secured by double heat treatments (Fig. 4), placed only a slight doubt upon this lot of metal while the low average true fracture stress values definitely emphasized the deficiencies. The yield stress values showed no striking differences with heat-treating temperatures.

In the usage of an arbitrary specification requiring 180 deg angle of transverse bend without the occurrence of surface bursts, low amounts of sigma or carbide converted delta ferrite are permissible. The number of ferrite particles converted to sigma or carbide per square inch of surface must be no more than the number of surface bursts permitted per square inch. The welding problem is to assure that all of the original ferrite is present as ferrite before welding and that the thermal conditions during welding are such that sigma and carbide conversions do not occur.

The problem of how to specify suitable castings for welded applications has not been fully answered by steel production or foundry metallurgists and should become the subject of joint action by interested technical and scientific organizations. The final problem will be control of the manner for making satisfactory metals and then maintaining suitable thermal and stress gradients during welding with proper atmospheres.

Prior studies have shown that 1500° F is about the center of the sigma forming range.[18] By treating a series of finished tensile specimens from four different castings to 1200, 1500 and 2200° F for sufficient time periods, it was shown that the coarse ferrite particles were converted into a brittle form at and near 1500° F (Fig. 5). Calibrated Magne-Gage determinations on these brittle samples showed reductions in magnetic response. The fracture stress curves show minimum values were secured after the 1500° F treatment. Deficiencies were not readily apparent from either the nominal ultimate or the yield stress values. The welding

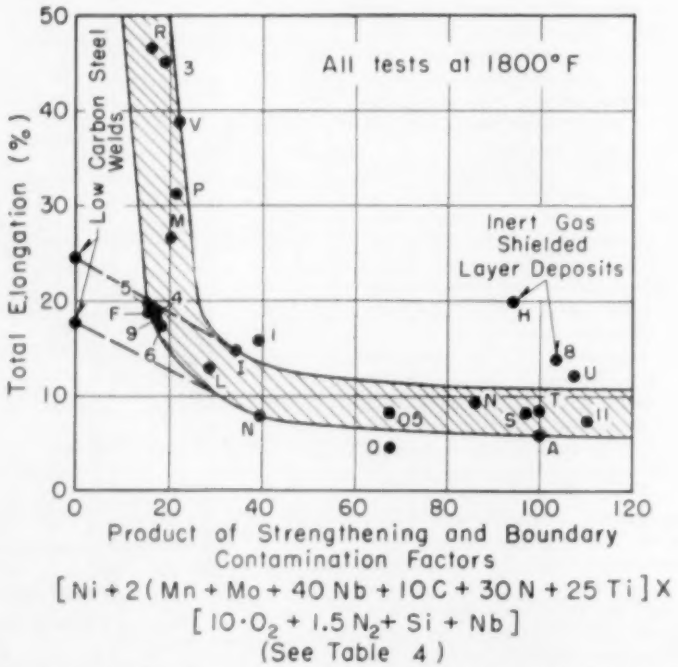

Fig. 10 Tensile ductility-composition relations of as-deposited iron-base Cr-Ni steel metal-arc welds tested at 1800° F

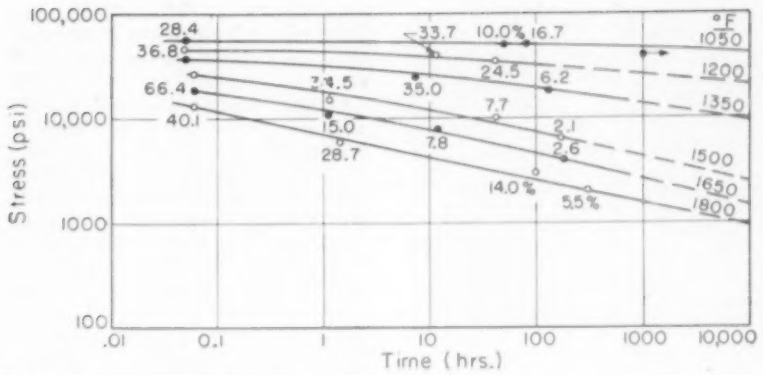

Fig. 11 Stress-rupture data for Type 307 weld metal

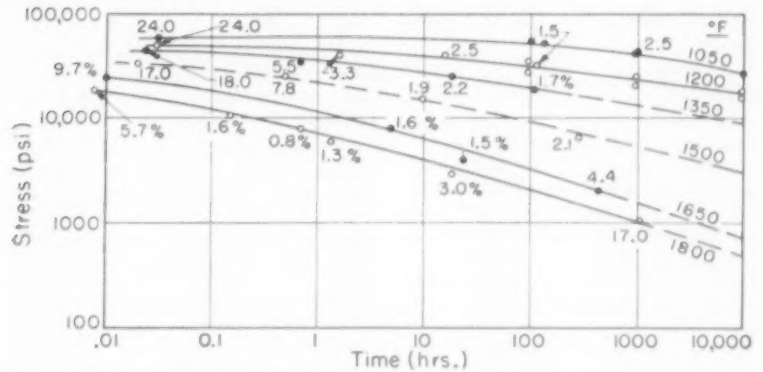

Fig. 12 Stress-rupture data for Type 347 weld metal

and casting industries too often ignore the significant observations which may be obtained from the use of true fracture stress values.

The relative thermal response of four commonly used compositions are also shown in Fig. 5. The 304 grade (Table 2) had the higher fracture stress over the full range of heat treatments, and is known to be the least susceptible to variance in welding. However, even in that alloy, some loss in fracture stress was induced. The 347 grade, essentially 304 with niobium added, was also susceptible to heat treatment and had a lower fracture stress. This was the only item tested as-cast. The 347 grade alloy is also more susceptible than 304 to welding variations. The grade 309 steel, with its higher chromium content, contains more delta ferrite and can be more readily sigmatized. The addition of niobium to this grade is expected to make the steel more susceptible to sigmatization and carbide formation. The 309 Nb example is an extreme case of a casting heat treated so that it is unsuitable for welding. Because of the internal damage caused by the prior treatment, it could not be salvaged by reheat treatment.

Brittle fracture occurs when the cool-down welding stresses build up in magnitude until they equal the fracture stress of the base metal. It is therefore clear why sigmatized castings have repeatedly cracked adjacent to the welds. Several such experiences are known.[18] Cracking of this type occurs on the low-temperature side of the cool-down range as the residual welding stresses increase. Sigma phase is not present at the high temperatures. Sigma-induced cracking is therefore a "cold-cracking" phenomenon independent of the austenitic matrix.

The unetched structure of castings commonly reveals the presence of circular (spherical) or irregular inclusions (Fig. 6). Also revealed by this procedure are the eutectic structures and chromium or niobium carbides.

These test data imply a source of weldability variance which has never been fully evaluated. In large chilled ingots, if the cooling rate and the lowest attained temperatures are such that brittle phases may be formed, cooling and shrinkage stresses in the massive ingots may cause internal rupture bursts. When these same ingots are later reheated for hot rolling and the cracked regions are reconverted into delta ferrite, some of the crack voids probably remain unbonded. These cracks need not fully reweld upon further processing or rolling. The control of ingot processing, therefore, becomes a potential source for variance in ultimate weldability, particularly for compositions which are two-phased upon initial solidification.

From mill observations it is also known that many of the presently produced fully austenitic compositions are crack sensitive during processing, presumably because of excessive contamination at the grain boundaries of the high hot-strength austenitic matrix.

Weld Metal

Each bead or layer of weld metal is continuously arc cast; solidified in intimate contact with the containing mold, while being highly restrained during and subsequent to solidification by the elastic rigidity of that mold. Its properties are therefore substantially different from those of castings of the same nominal composition. The two-phased structures have finer ferrite particles than castings. Coring may be present.

Short-time Tensile Properties

The microstructures, compositions and short-time tensile properties of typical metal-arc weld metals as influenced by temperature have already been reported.[1] Best short-time high temperature properties were secured with a 20% Cr, 10% Ni, 4% Mn, 0.9% Mo composition, known commercially as 307 grade (Fig. 7). This electrode was originally developed for the welding of ferritic armor. Its short-time 1800° F strength is as low as that of the 347 grade forgings and plates and therefore during initial cool-down lower stresses are imposed upon the adjoining thermally-altered and metallurgically-damaged base metal. This becomes important when welding massive forgings, particularly with conventional techniques wherein the highest stress levels are built up in the outer one-third of the depth of the weld groove.

There is, in general, an inverse relation between short-time weld metal strength and ductility at the 1800° F temperature of minimum ductility, but there are significant differences between the several composition grades for each temperature level.[1] Those compositions which have the best combination of strength and ductility are preferred, provided they have acceptable stress rupture and creep characteristics and are metallurgically stable with respect to time. For the present, the time-temperature dependence of stress and strain must be determined for each individual type weld composition. The specification of room temperature short-time properties alone is meaningless.

The heavy dependence industry has placed upon control of the amount of room temperature delta ferrite to inhibit initial cracking in weld metals has not

been fully justified. This is only one of several controlling factors, and its presence may be as harmful as it is helpful. At the critical temperature of 1800° F, for example, the ferrite level has no definite influence upon capacity to strain without rupture (Fig. 8). There is limited substance to the concept of ferrite control; some higher ferrite content welds have lower hot strength and more capacity to flow before rupture.[1] This appears to improve ductility at submolten temperatures. The zero ferrite content welds, that is, the ones fully austenitic at room temperature, tend to be stronger at elevated temperatures but the presence of foreign matter concentrated at the grain boundaries causes weakening at those locations. Such welds have low capacities to flow.[1] Austenitic welds are therefore hot brittle not because they are austenitic but because they have an inherently strong matrix and are "dirty." A clean austenitic weld metal stable for long times at elevated temperatures is needed. A present practical compromise is to use a 2–8% room-temperature ferrite content weld, preferably 3–5%, with composition selected so that it provides deposits, as-made, in the upper portion of the hot-ductility range (Fig. 8).

Low-carbon-steel weld metals have a short-time ultimate strength at 1800° F of about 6600 psi. The introduction of chromium to nickel-free low-carbon steels (Table 3) adds little to the as-deposited strength.

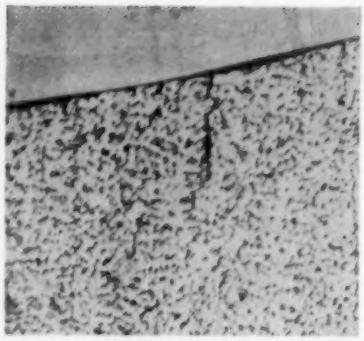

Fig. 13 Incipient crack adjacent to rupture in shoulder of stress-rupture specimen (5000 hr at 1050° F, 0.3% strain). X 100

Table 3

Nominal Cr content, %	*Ultimate strength at 1800° F, psi*	*Total elongation at 1800° F, %*
0	6600	24.7
4	8580	23.5
12	7940	15.0
16	5480	32.2

In a previous paper,[1] chromium was considered to detract slightly from the strength of the austenitic matrix weld metal at 1800° F. That is true in some instances but it appears that chromium alone has little influence on the 1800° F strength. Strength at 1800° F for covered-electrode weld metal and the weld composition can be approximately but usefully, correlated by considering that nickel, manganese, molybdenum, niobium, carbon, nitrogen and titanium all add to the hot strength (Fig. 9 and Table 4). The highest strengths are secured with welds containing niobium which has a powerful effect per unit weight per cent. The niobium-bearing welds of Fig. 9 involve only the 20% Cr 10% Ni type compositions, but other experiments have shown that the same strengthening effect is secured regardless of whether the matrix is fully austenitic or two-phased at room temperature (Table 5).

The mechanism by which niobium produces the powerful effect on hot strength and ductility is not yet fully understood.

Argon-shielded, weaved-layer-deposited, niobium-bearing, weld metals have lesser strength and better ductilities than covered-electrode bead-deposited welds of the same composition. Such welds cool at a slower rate.

It was previously reported that best ductility is secured when the weld strength was a minimum and grain boundary weakening influences were also a minimum.[1] Conversely, mini-

Table 4—Summary of Weld Compositions and 1800° F Properties

Code mark	*1800° F values Tensile strength psi*	*Total elong. %*	*Chemical composition, %* Cr	Ni	Mn	Mo	Si	Nb	C	N	O	Ti	Cu
Z	5,900	24.7	Nil	Nil	0.59	Nil	0.18	Nil	0.10	0.007			
W	7,100	17.6	Nil	Nil	0.86	Nil	0.21	Nil	0.08	0.012	0.005		
R	8,400	46.6	27.3	9.4	1.40	Nil	0.47	0.03	0.10	0.044	0.049	0.03	0.12
9	9,940	18.1	20.4	10.6	1.73	0.064	0.75	<0.05	0.034	0.061	0.011	0.07	0.24
4	10,720	18.8	19.9	10.2	1.59	0.057	0.42	<0.05	0.051	0.069	0.043	0.05	0.13
F	10,950	18.6	20.2	10.0	1.45	...	0.44	0.00	0.05	0.048	0.05	0.06	0.12
P	11,450	31.3	24.7	13.7	1.60	0.11	0.49	0.03	0.08	0.048	0.042	0.05	0.13
5	12,330	19.6	16.5	8.45	2.09	1.47	0.35	<0.03	0.054	0.083	0.027	...	...
M	12,700	26.6	19.6	12.4	1.26	1.99	0.31	0.03	0.06	0.029	0.054	0.02	0.13
3	12,870	45.1	19.9	9.64	3.69	0.95	0.40	<0.05	0.11	0.048	0.026	0.05	0.14
I	13,000	14.5	19.8	11.1	1.66	...	0.71	0.25	0.04	0.055	0.02	0.05	...
V	13,200	38.6	17.3	9.6	1.49	0.13	0.74	0.01	0.07	0.013	0.013	0.34	0.11
O	13,300	5.6	24.5	19.3	1.52	0.10	2.02	0.03	0.09	0.039	0.028	0.04	0.10
6	13,540	17.3	16.4	8.76	2.11	1.44	0.39	0.07	0.058	0.082	0.026	...	...
L	14,200	12.7	25.9	19.8	1.40	0.13	0.41	0.03	0.11	0.035	0.051	0.04	0.20
X*	15,000	17.4	20.9	9.2	1.58	0.46	0.62	0.94	0.11	0.036	0.05	0.03	0.12
1	15,135	15.8	19.6	9.89	1.78	0.014	0.18	0.50	0.051	0.047	...	...	0.09
H	15,300	19.7	19.5	11.2	1.56	...	0.73	0.81	0.04	0.041	0.03	0.07	...
8	15,950	13.7	19.2	11.3	1.76	0.093	0.61	0.96	0.048	0.061	0.014	0.09	0.17
2	17,000	9.1	19.4	10.1	1.51	0.074	0.50	0.81	0.043	0.035	0.042	0.10	0.13
S	17,460	8.4	21.7	9.2	1.61	0.07	0.63	0.81	0.06	0.084	0.04	...	0.11
N	17,800	7.8	17.1	33.0	1.64	0.06	0.52	0.03	.16	0.019	0.028	0.04	0.08
T	18,860	8.4						Repeat of A					
A	19,000	5.7	19.9	9.9	1.56	...	0.69	0.81	0.05	0.046	0.05	0.06	0.14
U	19,520	12.1	19.1	11.6	1.62	0.07	0.59	0.87	0.05	0.085	0.04	...	0.11
05	21,100	8.2	19.3	10.7	1.63	...	0.63	0.66	0.06	0.064	0.05	0.07	0.07
7	22,120	16.5	19.7	9.8	1.52	0.016	0.33	0.59	0.056	0.135	0.019	0.07	0.12
11	23,470	7.1	19.4	10.1	2.81	0.022	0.35	0.89	0.110	0.096	0.026	0.10	0.09

* Also contains 1.40% W.

mum ductility could be expected when both were a maximum. Additional data (Table 4) tend to support this viewpoint (Fig. 10), although at the lower product levels other factors enter into a determination of the hot ductility.

The weighted relations shown in Figs. 9 and 10 need not be considered as exact, final or unique. They do, however, provide an empirical rationalization of the magnitude of the detrimental effect of the presence of oxygen, nitrogen, silicon and niobium in the weld deposits. Item 1, for example, showed that lower silicon and niobium contents improved hot ductility.

Stress-Rupture Properties

One characteristic of the short-time properties of the weld metal is that above about 1500° F, the maximum resisted load, that is, the nominal ultimate tensile strength, is developed at a strain of less than 1%. Above 1500° F there is no strain hardening and flow to rupture becomes continuous at decreasing loads. As temperatures are decreased, flow occurs at constant loads but longer times are required for rupture. This phenomenon is known as time-induced stress rupture. Inadequate capacity to flow plastically may sometimes be a factor in causing early fracture.

The high-temperature stress rupture properties of the 4% Mn, 1% Mo, 307 grade weld metal, when deposited on 347 grade plate, are adequate to assure freedom from initial solidification or postwelding heat-treatment cracking. Such welds have withstood over 6000-hr exposure at 1050° F and 30,000-psi stress without signs of rupture while exhibiting a low secondary creep rate (Fig. 11). The numbers beside the stress-time points on the graphs are the values of elongation recorded at time of rupture.

Table 5

Nominal composition, %			1800° F Short-time properties (strain rate = 750% per hr)			
			Ultimate strength, psi		Total elongation, %	
Cr	Ni	Mo	Without Nb	With Nb	Without Nb	With Nb
25	12	0	11,450	19,140	31.3	14.4
25	20	0	14,200	19,170	12.7	20.1
20	12	2	12,700	21,250	26.6	18.6

For comparison, stress-rupture data are shown in Fig. 12 for one 347 covered-electrode weld deposit in 347 plate. These data have significant relations to field experience. The weld was known to have an elongation of only 5.7% in the short-time tension test at 1800° F with rupture occurring at 19,000 psi. At 1800° F and 11,000-psi stress, a stress-rupture specimen of this weld failed in 0.18 hr after only 1.6% elongation and at 8000-psi stress another companion specimen failed in 0.8 hr after only 0.8% elongation.

Of interest is the ductility inversion at 1000-psi stress, 1800° F in a 1018-hr rupture. This specimen withstood 17% elongation before rupture. It had been shown earlier[1] that solution heat treatment improved 347 type weld hot ductility. The stress-rupture data therefore indicate a tendency for the existence of an equivalence of time and temperature in solution heat treatment. The higher stress, shorter rupture time performance also correlates with industrial experience of observed cracking during heat treatment of massive restrained weldments at or above 1700° F because, to achieve the higher temperatures, the parts must first be heated through the brittle temperature range. In initial heating up through the 1800° F range after welding, the residual stresses in the weldment are often such that the imposed strains exceed the

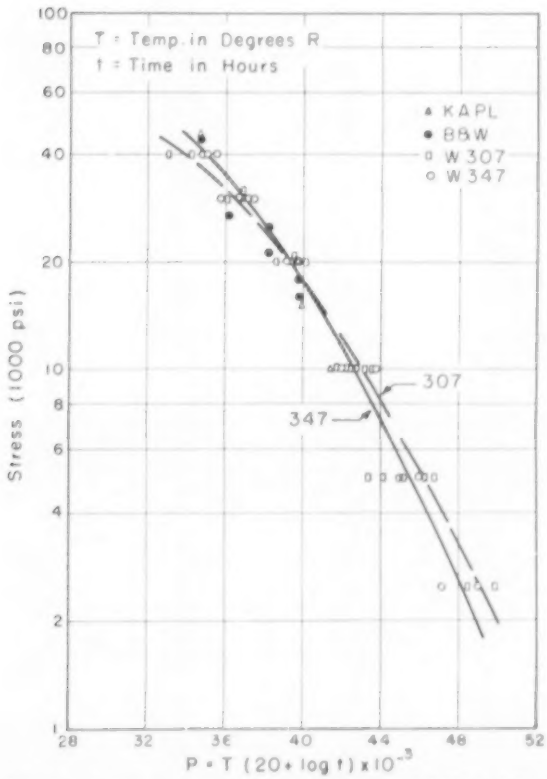

Fig. 14 Rupture strength of Types 307 and 347 stainless-steel weld deposit

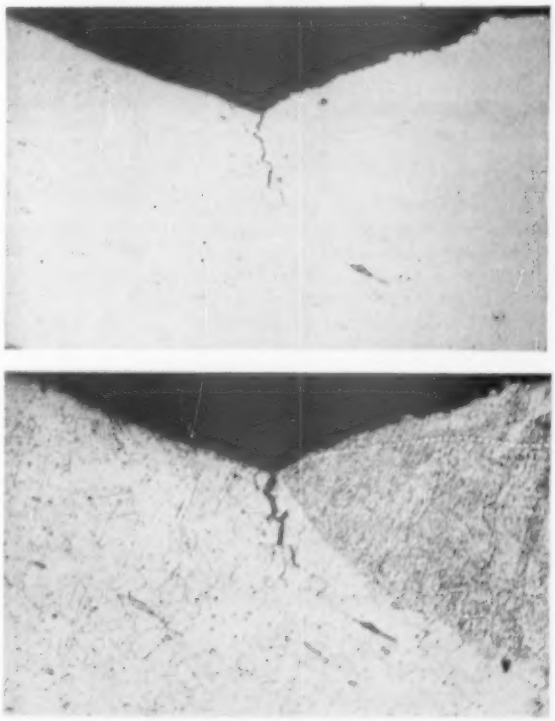

Fig. 15 Crack at toe of fillet weld in Type 347 stainless-steel forging. X 100. (Reduced by 1/2 upon reproduction)

severely limited capacity of the metal to flow and local rupture occurs.

With 30,000-psi stress at 1050° F, rupture started to occur after 5000 hr with only 0.3% strain. The weld contained 10% of delta ferrite in the room temperature as-deposited condition. An average of 5.6% remained after testing; 4.4% had been converted to nonmagnetic phases or compounds within the 5000-hr test period. Rupture occurred in this particular specimen at the shoulder of the specimen, indicating sensitivity to stress and strain concentrations. Secondary cracking, originating in the region which was originally ferrite, existed back of the rupture (Fig. 13).

Engineering parts are designed to operate at lower stresses but a long operating life may be required. The laboratory data therefore again tend to substantiate field experience and, properly timed in advance of engineering design, they serve as an accurate forecast of the ultimate probable performance during the usage of such low-ductility materials.

The stress-rupture data may be usefully related to observations from other materials. By treating the data in accord with the Larsen-Miller parameter,[20] that is,

$$P = T \times (25 + \log t)$$

where T is absolute temperature and t is time to rupture in hours, it was observed that the values of the stresses for the same temperature-time conditions were less than those previously described for 12% Cr steel.[21] The same values, however, were similar to those reported[22] for niobium-bearing weld metal on a parameter of

$$P = T \times (20 + \log t)$$

The KAPL and B & W data of Fleischmann were based upon somewhat longer time intervals at lower temperatures than those of Fig. 12.[22] However, only minor differences were found in the values (Fig. 14). For longer periods of time under stress the magnitudes of stress resisted are lower. This correlates with the known tendencies for all metals. Ferrite conversion to sigma or carbides with increased time may be a factor in these results. The fact that data from three independent laboratories can be correlated as closely as shown in Fig. 14 is scientifically encouraging, although the unanimity in finding low ductility at elevated temperatures may temporarily be discouraging from the practical viewpoint.

The 4% Mn metal, Type 307, has about the same stress-parameter curve, the stress values being slightly lower than for the 347 metal at the lower parameter, i.e., temperature values (Fig. 14). Based upon a comparison of stress to rupture, there is little choice between the Cr-Ni-Nb and the Cr-Ni-Mn-Mo welds under a condition of continuing strain. However, in a substantially static structure, such as a steam pipe, it would appear that the higher capacity of the 4% Mn weld to strain without rupture would provide local adjustments in the composite metals of the welded joint so that rupture would not occur. In this respect, the 4% Mn grade metal is superior to the 1% Nb grade.

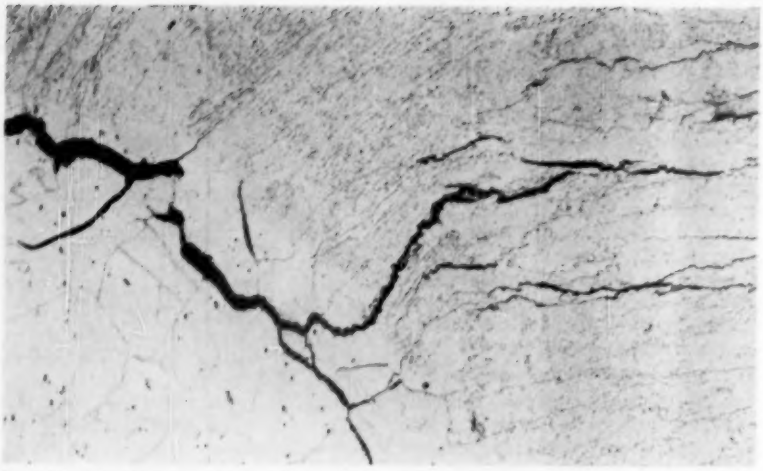

Fig. 16 Service crack in weld and heat-affected zone of 347 steel forging. X 100. (Reduced by 1/2 upon reproduction)

Forgings

Forgings may represent a minimum in reduction and alteration from the original casting and therefore from the cast structure. Unless otherwise specified and required, some of the original cast structure may remain in the final forging, particularly near its central portions. The degree of first and total reduction and the temperatures of those reductions therefore probably become a vital part of the process of producing acceptably weldable materials. While published correlations between these two features are not known to exist, it is probable that ultimately full control of the forging process will be specified for procurement of weldable-grade forgings.

Some cracking difficulties have been experienced during welding, heat treating and service in the heat-affected zone of commercial forgings.

Heat-treatment cracking which occurred in the base metal at the toe of an outside corner fillet weld on a rectangular attachment to a 347 forging is shown in Fig. 15. The crack occurred at the grain boundary either during welding or subsequent heat treatment, probably the latter. Whether or not the crack nucleus occurred at a particularly highly stressed point, at a heavy grain boundary contaminant

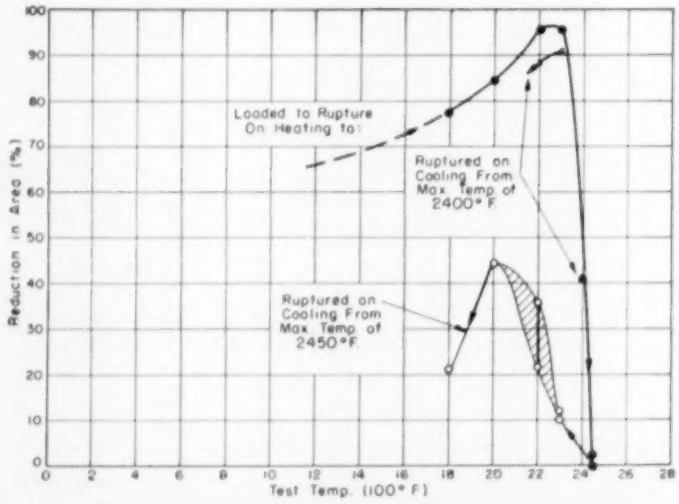

Fig. 17 Temperature-ductility relations found for AISI 347 steel of poor weldability history

concentration region or at a local slag inclusion, the path of propagation was along the austenitic grain boundaries. The forging contained numerous obvious inclusions.

A steam pipe which had been in service for five years at 1050° F developed the crack shown in Fig. 16. Such crack formation and propagation involves weld and base metal properties, joint geometry, residual and imposed stress, temperature, time and metallurgical stability considerations.

Data secured from the Rensselaer resistance-heating hot-ductility test technique[4] on a similar lot of 347 forging which had an unsatisfactory short-time weldability history are shown in Fig. 17. This forging has the composition:

Cr, %	18.6	Mo, %	0.18
Ni, %	10.9	C, %	0.045
Mn, %	1.48	N, %	0.04
Nb + Ta, %	0.56	P, %	0.021
Si, %	0.49	S, %	0.009
Cu, %	0.21		

On heating, the metal exhibited good ductility up to 2400° F. At and above 2400° F, the ductility dropped abruptly when measured by reduction in area or elongation over a gage length corresponding to 0.75 in. When the companion specimens were ruptured upon cool-down from a 2450° F peak temperature, the elongation and reductions in area secured were much less than for the original conditions (Fig. 17, lower curve). The nominal melting point of the Cr-Ni steels is about 2600° F. Achievement of a temperature within 150° F of the melting point therefore was sufficient to result in permanent metallurgical damage to the base metal. Following that damage, the original properties no longer existed. All arc-welded joints contain zones heated to within 150° F of the melting point.

The microstructure of the metal just back of the fracture reveals the presence of substantial amounts of inclusions. Secondary rupture occurred at the higher temperatures at grain boundaries and inclusion nuclei (Fig. 18). In such test specimens the true origin of failure is never known but the inference is that the fracture face is simply the connection of hundreds of local micronuclei. In a cylinder loaded in axial tension, the point of maximum stress is at the center. In a resistance-heated specimen the highest temperature would also be at the center. A further feature in such a test, which involves current densities of the order of 200,000 amp per sq in., is that during resistance heating the grain matrices and boundaries constitute a continuing series circuit through which the electric current passes. If and when the grain boundaries are rich in nonmetallic compounds, their higher resistance promotes localized heating. If the composition and precipitated phases at the grain boundaries are such that they are alloy-rich, their resistance would also tend to be high and their melting point lower. Both factors favor melting, or liquation, at the grain boundaries. These several features combine to cast some question on how to interpret the resistance-heated cylinder type of test. Cross correlation with other methods of heating and test techniques will be necessary. Some form of submolten test, made to accurate control, will probably ultimately become recognized for the pre-evaluation and acceptance or rejection of alloys for welded applications. Such imposed tests will be met only by more accurate control of the metal processing. At present, vendors do not accept such requirements as a basis for furnishing high-temperature alloys.

Sheets and Plates

The aspect of grain boundary separation under tensile stress which occurs through the mechanism of local melting is real, but it is only one part of the problem. This was demonstrated early in the making of spotwelds in thin rolled sheets (Fig. 19), wherein the molten nugget of metal is under an all-directional fluid metal pressure of about 50,000 psi. The regions of grain boundary separations, when they occur, are extruded full of molten metal from the weld ingot and, within the very short time period involved and in the essential internal absence of oxygen, the short duration separations are resealed upon resolidification and subsequent cooling under pressure.

A similar phenomenon in the absence of hydrostatic pressure and compressive

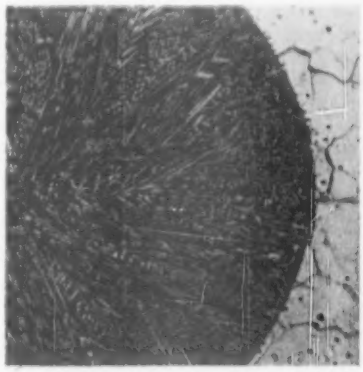

Fig. 19 Peripheral edges of high-current spot-weld nugget showing persistence of grain boundary melting. X 100. (Reduced by 1/2 upon reproduction)

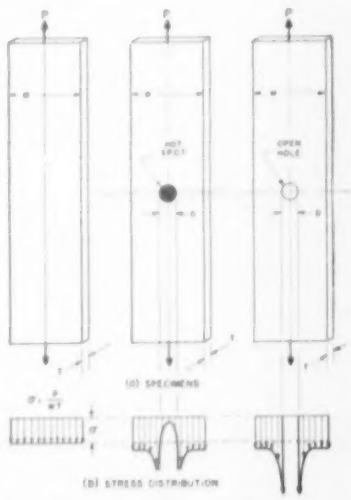

Fig. 20 Center hole specimens

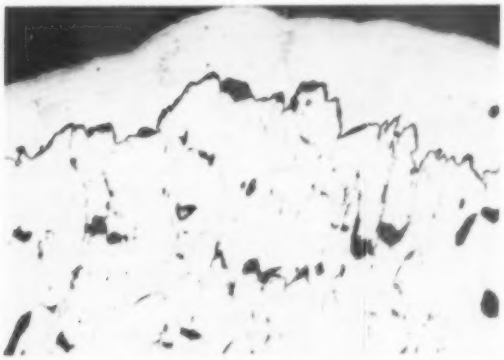

Fracture nickel-plated to protect edge

Fig. 18 Rupture and incipient cracking of 347 forging at 2000° F after cooling from 2450° F. X 100. (Reduced by 1/2 upon reproduction)

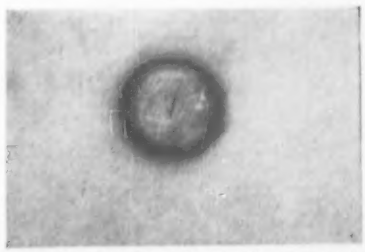

Fig. 21 Cracking back of arc spot in 0.05-in. thick 347 or 310 sheet

stress can result in damaging cracking. Such a condition can be shown to occur for rolled sheets of many compositions. For test purposes, a strip of 0.05-in. thick sheet steel 1.5 in. wide was loaded in simple tension under conditions permitting motion (Fig. 20). When a hole is drilled through such a specimen, stress concentrations exist at the edge of the hole, right view. If, instead of a drilled hole, a welding arc is struck to the center of the sheet so that the metal is heated through the thickness above a red heat, cracks can be observed to form on the reverse side. A typical example is shown in Fig. 21. Color motion pictures of this action clearly show the hot metal, in the region of stress concentrations, to tear progressively into the cooler adjoining metal which has ample capacity to flow, elastically and plastically. Such stress concentrations exist adjacent to the molten crater for all thicknesses of materials. This demonstration-type test has been used by the author for several years but it is not suitable for precise scientific evaluations.

Plates and forgings of the types described do not have a region of short-time low ductility at 1800° F (Table 6); also, they are not damaged materially by holding for 24 hr at 1500° F as was the case for castings (Fig. 5). Their grain boundaries may be damaged by heating to near the melting point, but the ELC 304 grade plates have been found to have excellent ductility even at 2450° F.

Table 6—Tensile Properties of Plates and Forgings at 1800° F

		3/4-In. rolled plates: forgings	
Base metal type:	*304ELC*	*347*	*347*
Proportional limit, psi	4400	10,200	9,560
0.2% yield stress, psi	6680	12,400	11,200
0.5% yield stress, psi	7140	12,800	11,500
Nominal ultimate stress, psi	8500	13,060	12,320
Average fracture stress, psi	8210	14,180	17,650
Uniform elongation, %	11.1	5.05	10.22
Total elongation, %	30.2	31.74	51.25
Area reduction, %	26.90	35.80	51.30

Composite Weld-Base Metal Properties

Longitudinal composite tensile specimens can be used to demonstrate that, in general, the performance of the combination of the three metals involved; weld, heat-affected zone and as-furnished base metal, are determined by the property of the lowest value (Figs. 22 and 23). In some instances the narrow heat-affected zone alone determines the over-all properties. The use of tapered composite specimens can also be used to demonstrate that for initially crack-free welds, fissuring occurs in the region of maximum stress.

Transversely loaded short-time tests tend to fail in either the plate or weld depending which is the weaker. In unusual instances where the fracture stress of the weld is low, the failure may first tend to start in the plate but final fracture will ultimately occur in the weld (Fig. 24). There is often little difference between the weld and heat-affected zone properties.

Summary

If, as now seems probable, there is an equivalence between "weldability," ductility, composition, microstructure and its orientation, it is necessary to also recognize that there is no area of agreement on what constitutes minimum acceptability on any one of those components in the weld or base metal. The "weldability" ideal can be defined as

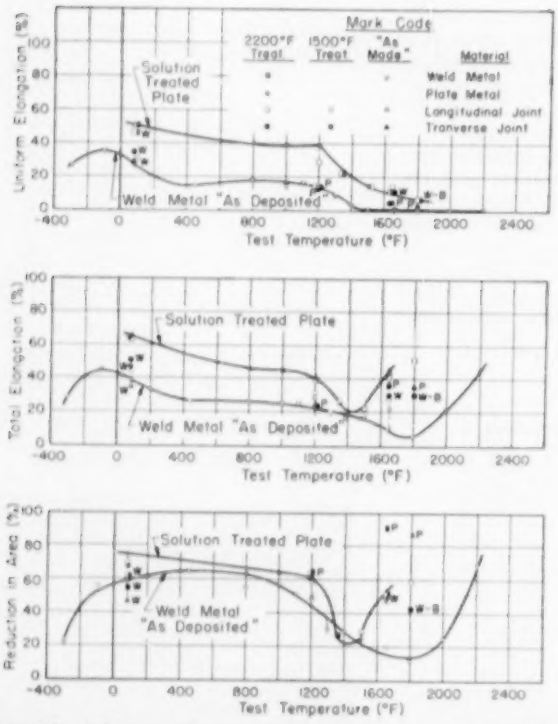

Fig. 22 Influence of test temperature and heat treatment upon ductility of 0.81% Nb weld metal and welded-joint specimens in 0.88% Nb plate

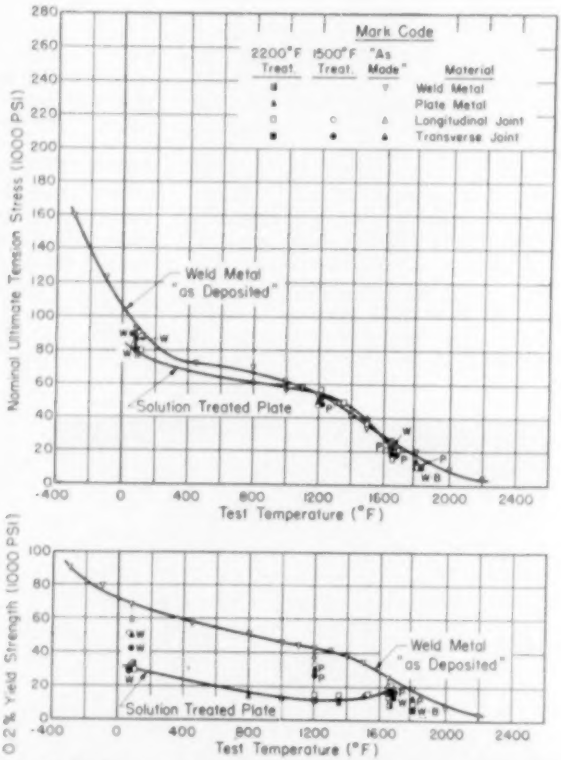

Fig. 23 Influence of test temperature and heat treatment upon yield and ultimate strengths of 0.81% Nb weld metal and welded-joint specimen in 0.88% Nb plate

Fig. 24 *Tension test of transverse joint specimen at +1800° F. (Argon-shielded arc weld 0.26% Nb, plate 0.88% Nb. Failure in weld metal)* X 1.5

freedom from cracks of macroscopic size for the designed life of the structure under the temperature-stress-environmental conditions involved.

To be suitable, even initially ductile metals must exhibit stability with respect to time, temperature and stress before they can be accepted for long-time service at elevated temperatures. Improper processing control of furnace melt, subsequent pouring, ingot processing, and initial and final forging are now such that, in some instances, fully suitable materials are being produced whereas in other instances wholly unsuitable materials are being produced. Under improper acceptability specifications there have been few efforts expended toward the correction of these incongruities.

There is a division of opinion in industry that could have unsuitable long-range consequences. One thought is that the present 347 steel is unsuited for welding, that the necessary control limits are too narrow for suitable production, and that already far too much attention has been given to this subject. The opposite argument is that with that composition it has been repeatedly demonstrated that suitable welds can be made. Apparently two industrial grades are being produced. There is a real industrial and scientific need for learning the true cause of the variations now presumably being secured. Control studies must start in the furnace and all the following steps in processing must be directed within the limits which produce a steel suitable for arc welded applications under rigidly restrained conditions.

The best short-time weld-metal hot ductility secured up to the present was with the 307 grade, 4% Mn, 1% Mo composition (Fig. 7). The strength-ductility combination obtained has a significant usefulness. Lower stresses are imposed upon the damaged base metal at the temperature of lowest resistance to strain. By converting time-temperature relations of the weld cooling cycle to temperature-stress relations, for both the weld and base metals, it is possible to determine the safest conditions for any specific joint.

The deficiencies encountered by using only ferrite content control in weld metal were further confirmed. At present, industry does not have a wholly stable and clean grain boundary austenitic weld metal. The high-ferrite content weld metals must be avoided because of tendencies for the formation of sigma phase and/or carbides. A compromise is to secure a deposit having a 2 to 6% average ferrite content *and* a minimum short-time tensile elongation of about *15%* at 1800° F (Fig. 8). For extended service at elevated temperatures and for postwelding annealing applications, there must also be the assurance that the stress-rupture properties are adequate within the most brittle portions of the heat-treating cycle. To illustrate, the weld metal of Fig. 12 could not be expected to withstand the solution heat treatment operation at 1950° F, as commonly used, or any higher temperature, because of its low capacity to strain at 1800° F. In a massive weldment stress rupture would occur upon initial heating into the 1800° F range.

For intermediate temperature applications, it is essential that the stress-rupture properties of all components of the welded joints be adequate to assure freedom from service cracking.

Acknowledgments

The studies described could not have been conducted without the support of the Westinghouse Steam Division, upon the recommendations of Messrs. N. L. Mochel and J. R. Carlson, and of the Atomic Equipment Division upon the recommendation of A. L. Cooper. All welding was done by P. T. Ehrhardt; heat treatment by H. C. Foust; tension testing up to 1800° F by Messrs. E. T. Wessel and W. H. Pryle; tension testing above 1800° F by E. Vandergrift and R. J. Dunegan of Materials Engineering; stress rupture testing by T. Hengstenberg and E. Van Antwerp; optical metallography by R. L. Anderson; X-ray diffraction by P. S. Stoll of Materials Engineering; oxygen analyses by F. H. Hickman; chemical analyses by F. Byrne and J. Penkrot of Materials Engineering; hardness and magnetic tests by C. J. Dorsch. Facilities for testing above 1800° F were designed by M. J. Manjoine. Specially extruded electrodes were provided by Messrs. E. H. Turnock and L. K. Birinyi of the Westinghouse Arc Welding Department. The Rensselaer hot ductility tests were made by that school under an arrangement negotiated with Dr. E. F. Nippes.

References

1. Heuschkel, J., "Initial Characteristics of Chromium-Nickel Steel Weld Metals," The Welding Journal, **34** (10), Research Suppl., 484-s to 504-s (1955).

2. Poole, L. K., "The Incidence of Cracking in Welding Type 347 Steels," *Ibid.*, **32** (8), Research Suppl., 403-s to 412-s (1953).

3. Zapffe, C. A., *Stainless Steels*, American Society for Metals (1949).

4. Nippes, E. F., *et al.*, "The Heat-Affected Zone in Arc-Welded Type 347 Stainless Steel," The Welding Journal, **34** (4), Research Suppl., 169-s to 179-s (1955).

5. U.S.S., "Steels for Elevated Temperature Service," Fig. 38, p. 82, Third Printing (1952).

6. ASM Committee on Creep, "Creep and Creep Rupture Tests," *Metal Progress*, **68** (2-A) 175–184 (esp. Fig. 7, p. 179).

7. Bain, E. C., *et al.*, "Nature and Prevention of Intergranular Corrosion in Austenitic Stainless Steels," *Am. Soc. Steel Treating, Trans.*, **21** (6) 481–509, (1933).

8. Austin, C. R., and Norris, B. S., "Effects of Small Amounts of Alloying Elements on Graphitization of Pure Hypereutectoid Steels," *Trans. Am. Soc. of Metals*, **30**, (6) 425–454 (1942).

9. Emerson, R. W., and Morrow, M., "Welding High-Temperature Austenitic Steel Piping," The Welding Journal, **30** (1), Research Suppl., 15-s to 39-s (1951).

10. Metals Progress, 680-B, November, 1949.

11. Greenfield, P., and Beck, P. A., "Intermediate Phases in Binary Systems of Certain Transition Elements," *Journal of Metals*, **8** (2) 265–282 (1956).

12. Wylie, R. D., *et al.*, "Stress Rupture Properties of Cr-Ni Stainless Steel Weld Deposits," *Trans. ASME*, **76** (7), 1096–1106 (1954).

13. Anger, E. M., *et al.*, "How to Weld High Alloy Castings," *The Welding Engineer* (April, May, September, 1953).

14. "Recommended Practice for the Welding of Steel Castings," Steel Founder's Society of America (September 1951).

15. Hilty, D. C., et al., "Observations of Stainless Steel Melting Practice," *J. Iron Steel Inst. (London)*, 180, 116–128 (1955).

16. Metals Handbook, 1260–1261, 1948 Edition.

17. Puzak, P. P., *et al.*, "Hot Cracking of Stainless Steel Weldments," The Welding Journal, **35** (1), Research Suppl., 9-s to 17-s (1956).

18. Experiments on Etching Procedures for the Identification of Sigma Phase in Austenitic Chromium-Nickel Stainless Steels, Appendix, Subcommittee VI of A-10 of the ASTM.

19. Emerson, R. W., private communication.

20. Larsen, F. R., and Miller, James, "A Time-Temperature Relationship for Rupture and Creep Stresses," *Trans. ASME*, **74**, 9, 765–775 (1952).

21. Newhouse, D. L., *et al.*, "Some 12% Chromium Alloys for 1000° F to 1200° F Operation," *Trans. ASME*, **76** (7), 1107–1122 (1954).

22. Fleischmann, W. L., Discussion, *Trans. ASME*, **76** (7), 1104–1106 (1954).

CONSIDERATIONS AFFECTING FUTURE PRESSURE-VESSEL CODES

Authors indicate tentative basic principles for revision of the ASME pressure-vessel codes to a broader base to suit the wide variations in service and economic demands

BY J. J. MURPHY, C. R. SODERBERG, JR., AND D. B. ROSSHEIM

ABSTRACT. Code requirements for pressure vessels are presently associated with extremely ductile materials and safety factors sufficiently ample to limit consideration to principal stresses evaluated by simple formulas. Advancements in physics have extended present knowledge of the fundamental behavior of metals, and metallurgical progress has provided new, improved, and special-purpose materials, many with physical properties enhanced by chemistry, heat treatment, or cold work with concurrent reduced ductility. The horizons of both analytical and experimental stress analysis have been vastly extended. Also new and improved inspection techniques and equipment are available. Since World War II, pressure vessel demands of the process, power, and other industries have rapidly increased in number, size and complexity. In many cases this requires more precise design and fabrication, with attendant justification of lower safety factors and improved economics. This trend toward balanced or adequately proportioned pressure vessels is further accentuated by new critical materials whose greatly increased cost justifies the objective of higher working stresses as obtained from improved design, fabrication, materials, and inspection. It is the aim of this paper to indicate tentative basic principles for revision of the ASME pressure-vessel codes to a broader base to suit the wide variations in service and economic demands.

I. Introduction

In a discussion of pressure-vessel codes we must start with a recognition of the purpose of a code. Our explanation for the existence of such a document is that it permits various fabricators to compete with each other and still protect the public by defining a minimum standard of safety. This fact was recognized by the ASME when it published its first issue of the code some forty years ago. In 1934 the joint API-ASME Code introduced a lower safety factor for more stringent design and fabrication requirements which was accepted by the ASME in the early forties and required a general redraft of the rules. This revision continued the simplified principal stress basis but extended the rules by increasing the detail design requirements. This constituted an acceptance of a design code as contrasted to an inspection code of maximum simplicity tailored to the needs of the shop inspector.

The year 1956 seems an appropriate time to reassess this industry because of the tremendous strides made in new material properties and in evaluating their limitations. Some of these advances have been recognized in the ASA Code for Pressure Piping. Here the allowable stress range for expansion effects has been extended for better design details. This revision was made because the fabrication industry recognized that it could reduce overall costs by increasing the engineering costs.

The needs of the process and power industry have multiplied as is shown by the fact that supercritical boilers are now a reality. These increased needs are forcing designers toward maximum use of present materials as well as contemplation of wider horizons with new materials. All materials can be economically used if it is recognized that lower factors of safety are possible when the "weak links" of catch-all safety factors in the present designs are eliminated. Actually we believe that far safer vessels are possible if balanced requirements for material, design, fabrication, and inspection are used rather than the present reliance on catch-all "factors of ignorance." For severe service or complicated vessels this balance approaches an optimum use of materials: for simple vessels, more generous use of materials outweighs the engineering costs of precise design.

The objective of this paper is to examine the factors involved and to formulate a philosophy which can be used as a basis for a next major change in the pressure-vessel codes.

II. Discussion of Code Requirements and Possible Modifications

The ASME Boiler and Pressure Vessel Code has admirably served the interests of the public, as well as those of industry and enforcement agencies, in providing uniformly acceptable and safe pressure vessels for average service when fabricated from ductile carbon steel. We appear to be on the threshold of a new era brought about by new materials of high strength, improved corrosion resistance, and, unfortunately, lesser ductility. Changing labor-material cost ratios; increased availability and lower costs of nondestructive examination; and increased understanding, ability, and willingness on the part of designers of vessels for critical service, require and permit more comprehensive, flexible, and balanced rules. Proportioned design, improved materials, proper fabrication, and thorough inspection requirements will achieve maximum effectiveness at a minimum over-all cost, without lowering safety standards.

In Section III of this paper the results of the PVRC programs relative to pressure-vessel materials and design, and other investigations in this field, will be reviewed with particular emphasis on the influence of ductility and high yield to ultimate stress ratio on the relative fatigue performance of pressure-vessel materials in the low-cycle range.

The objectives of this section are: 1, to point out the inadequacies of the present code as to the requirements for a proportioned design to balance materials, fabrication, and inspection; 2, to indicate the refinements required for pressure vessels with a lower nominal

J. J. Murphy is Manager, Mechanical Section, Development Division; **C. R. Soderberg, Jr.**, is Assistant Manager, Design Engineering Department; and **D. B. Rossheim** is Chief Mechanical Engineer, of the M. W. Kellogg Co., New York, N. Y.

Paper presented at the ASME Metals Engineering division Conference held in conjunction with the 1956 AWS National Spring Meeting, May 7–11, 1956, Buffalo, N. Y.

safety factor; and, 3, to provide a definite relationship of the design and construction requirements to service hazards and demands.

A. General

The ASME Code for Unfired Pressure Vessels does not provide complete guidance as to minimum requirements for other than mild or average service and simple design, although the detail-design requirements have been necessarily expanded to a considerable degree. The effectiveness and adequacy of the inspection for complex vessels is subject to question. Because of the improvement in detail design, the degree of reliance on the safety factor has been reduced. However, general criteria are still lacking for the many forms of loading or details for which specific rules or formulas have not been provided. In general, this is true of all provisions; e.g., nozzle welds, regardless of service, are subjected only to visual examination, except for special materials such as Hastelloy and 18-8 stainless. The same safety factor prevails around openings whether the main seams are fully or randomly radiographed.

One possibility would be to expand the rules to include every form and variation of loading for all conceivable geometries, but such an approach appears impractical because of its complexity and the fact that it would restrict the flexibility and ingenuity used in handling complex details. On the other hand, if the code is modified to recognize that the best interests of safe construction will be served by defining the extent and general methods of analyses, with explicit limits for secondary or localized stresses, the code no longer need assume gigantic proportions. Certain design formulas are of basic significance, such as those for the shell and head thickness, and these should continue in the main body of the code with the results entered on the vessel data sheets. However, the many special details—such as flanges, intersections, lugs, skirts, and similar details of fabrication and materials—could be treated in the appendixes where frequently used formulas could be given. References to applicable texts or literature could be cited for assistance in handling less common problems. However, all calculations would follow the basic criteria stipulated in the body of the code, and could be made by competent vessel designers without reference to other developments or formulas. With this approach, average vessels would be designed as readily as they are at present; more complex vessels would require competent knowledge, which they do even now, but could then be accomplished without numerous arbitrary restrictions. Many requests for code interpretations and revisions can be avoided by an approach which recognizes principles and avoids arbitrary detail.

Responsibilities of the manufacturer and inspector would be more adequately indicated, and the user's responsibility would also be defined to prevent confusion and ambiguity. In many applications the vessel manufacturer has little or no access to the design of the general plant in which the vessel is incorporated, so that he can hardly be expected to appreciate, much less be responsible for, the correct assessment of the operating conditions or structural loading. Therefore, the separate responsibility of a "vessel designer" is a definite part of more complex construction. The code should establish the qualifications for, and functions of, the "vessel designer." For average or well-recognized vessels the fabricator would be able to assume this additional responsibility as he does at present; whereas, with the more complicated designs of the future, the vessel designer's role should be clearly established. A necessary adjunct to vessel designer responsibility would be the approval and inclusion of the essential design drawings and calculations as a part of the vessel data records.

B. Service and Loadings

The ASME Code for Unfired Pressure Vessels nominally considers only steady static loading, inasmuch as it contains no provisions recognizing cyclic effects, either mechanical or thermal, which can lead to fatigue failure. The initial Safety Factor (SF) of 5 evidently provided a margin sufficiently ample for most services, as shown by the number and operating life of the vessels built under Par. U-68, U-69, and U-70 limitations. The service experience with a safety factor of 4 is less definitive in point of time or number of vessels because much API and Par. U-200 and U-201 construction initially was to more refined design and fabrication requirements than that permitted by present code minimum construction. However, the postwar period of almost 10 years is representative of designs with appreciable stress intensifications, and tends to justify the conclusion that ductile carbon steel with principal stresses based on a safety factor of 4 does not undergo fatigue failure during a lifetime of 10,000 cycles, e.g., of full service pressure and/or temperature change. For this number of cycles, localized stresses need not be kept below the endurance limit, but rather can exceed the yield stress with a restricted amount of repetitive plastic deformation as demonstrated by the tests of the Welding Research Council's Pressure Vessel Research Committee (PVRC) described in Section III herein. For a larger number of cycles or for a higher basic allowable stress, as proposed for fully radiographed construction, the possibility of fatigue failure must be evaluated. This can be accomplished in routine design without much difficulty by following the present approach of the ASA Code for Pressure Piping. The stress or strain range is usually a function of the atmospheric and operating temperature yield points, and can be associated with a stress-cycle curve similar to fatigue under mechanical loading at constant temperature. An aspect not appreciated is that temperature gradients associated with changes in operation, or thermal expansion, are a common source of frequent and appreciable repetitive plastic deformations. At present, there is no restriction on the use of lap-welded or otherwise marginal construction for rapidly repetitive service.

High pressures are not adequately covered by the simplified rules of the present code, particularly as to shell thickness and nozzle reinforcement. The elastic distribution of stress through a thick wall is of less significance than the average stress in the wall with respect to initial and continued yielding, but retains significance from a fatigue viewpoint. As to openings, it is obvious that, even if a small opening is reinforced by the present code requirements, it still induces a stress intensification. It is also difficult to obtain satisfactory attachment weld designs with the present nozzle requirements. On the other hand, with a proper expression of principles, flexible rules could be applied without restriction as to pressure, thickness, or size, so that arbitrary limits could be dropped.

Service hazards in the operation of pressure vessels may be grouped as: (*a*) overpressure; (*b*), overtemperature; and (*c*), other effects.

At present, only the first of these is formally recognized, and the second is taken care of for fired steam boilers only by special code sections. Other effects include explosions, resonance (flow and structural), deterioration by nuclear fission products, dynamic effects of the structure (including acceleration effects), heat transfer, and temperature change—many of which are listed for design consideration in the code, but without assistance as to design methods or criteria.

With regard to overpressuring of pressure vessels, the design limits are straightforward. The main difficulty is in defining the requirements for safety valves or other devices which will definitely limit the pressure on a vessel under all conditions. Overtemperature relates mainly to heat transfer or to an internally insulated vessel. With excessive heating rates or ineffective insulation, a higher shell temperature may be attained. Heat release from

exothermic reactions, electrical power sources, or nuclear fission may similarly raise metal temperatures. Proper design assumptions and protective devices or details need attention because, at present, each design organization is guided by its individual views. For example, some internally lined vessels are designed so that, with failure of the lining, the short-time properties of the shell are sufficient to prevent immediate failure. However, this is not a general practice.

The present approach for designs having the possibility of an internal explosion is similarly varied. Some applications are designed for the full explosion pressure corresponding to a stoichiometric mixture; in others, the explosion pressure is checked by limiting primary stresses induced by the explosion to the yield strength; and in some instances there is no recognition whatsoever of such a hazard.

It is essential in the initial stage of reorientation of the code to incorporate mandatory requirements as to service. It is suggested that vessels be divided into at least the three general classifications shown as Classes C, G, and N, in Table 3. Class C would be suitable for the most critical services, and thus would require the highest quality and most searching examination and evaluation of materials, design, fabrication, and inspection. Vessel Class G would apply to average service, with present membrane stress level subject to certain limitations on temperature, cycles, contents, and the like, while recognizing commensurate reduced requirements for design, materials, and inspection. Vessel Class N would apply to comparatively small vessels in relatively nonhazardous service, with the design membrane stress established sufficiently low to justify use of simple design checks and minimum quality controls for fabrication and inspection. Vessel Class N must be definitely restricted to ductile carbon steel, in which the stored energy is limited by size and pressure for compressible gases, or which is essentially noncyclic, nonshock, and is not subject to rapid temperature changes, and the like.

Experience has indicated that Class G vessels of ductile materials can be used with reasonable safety for all services, except those involving more than a nominal number of cycles, or extremes of temperature and/or pressure, and whose contents are lethal or otherwise hazardous. A size limitation has been considered but is difficult to establish in view of the many large-size low-pressure vessels which have been constructed to this vessel class over the past 15 years. A more logical restriction would be in terms of stored energy, similar to the isolation requirements of explosives, with a suggested limit of 25,000,000 ft-lb. Class G vessels are not proposed for low ductility—0 to 8%—or for severely air-hardening materials, and would be restricted when made from medium—9 to 15%—ductility materials by requiring appreciable excess thickness—100% suggested—to minimize plastic deformation during test or in service. For materials enhanced in strength by thermal treatment, this vessel class would be permitted only for simple cylinders with centrally located and contoured end connections. Or, if the ends contain other openings, the head thickness must be doubled to provide integral reinforcement. This is predicated on seamless construction. If welded assemblies are to be accepted, consideration must be given to the reshaping necessary to remove distortion at longitudinal welds, to heat treatment after fabrication as contrasted with the use of heat-treated materials, to more extensive inspection, and to other details.

Class C vessels would be essentially unlimited as to service, materials (except quality), or contents. The single exception presently contemplated is with respect to ductility which, when medium—9 to 15%—or low—0 to 8%—would require added thickness of the order of 50 and 100% respectively, to minimize plastic deformation.

All of the foregoing discussion pertains to services at operating temperatures below the creep range, where performance depends on the fatigue and short-time tensile properties of the material which can be tangibly related to a "safety factor." This covers the entire temperature range of vessel Classes G and N; for Class C, temperature is limited only by individual material suitability as to strength and stability, so that at higher operating temperatures a constant rate of deformation as a function of time, or creep, occurs. The basis of the ASME Code for Unfired Pressure Vessels allowable stresses is stated in Appendix "P" to be the lower of the following for the indicated temperature: (*a*) 25% of the ultimate tensile strength (UTS); (*b*) 62½% of the yield strength (YS) for 0.2% offset; (*c*) the stress corresponding to 1% creep in 100,000 hr; and (*d*) 100% of the stress producing rupture in 100,000 hr.

It is contended that the present criteria for creep rate and rupture life are a minimum for lengthy safe operation, which code construction should provide. This view accepts creep-rate and rupture-life test data as of direct quantitative significance, and emphasizes that the present values are proved by service, and any alteration upward would be speculative as to performance. Opposed to this is the opinion that creep-rate and rupture-life test data are essentially qualitative and serve only to compare materials with ductile carbon steel as a service-proved base line. In support of this reasoning, attention is invited to applications, such as oil-refinery still tubes, of which many installations have been designed to 1% creep in 10,000 hr, and yet have given satisfactory service over periods

Table 1—Calculated Fatigue Performance for Various Materials with Different Design Bases (N Calculated from Equations (2) and (3))

DESIGN BASIS FOR S_a	ITEMS	MATERIAL				
		A285 or A201 55,000 UTS 30,000 YS	A212 70,000 UTS 38,000 YS	TI 105,000 UTS 90,000 YS	A302 80,000 UTS 50,000 YS	A225 75,000 UTS 43,000 YS
.25 UTS	$\mathfrak{G}$	3	3	3	3	3
	N	655,000	154,000	70,000	362,000	101,000
.25 UTS	$\mathfrak{G}$	4.35	3.42	3	3.94	3.19
	N	70,000	70,000	70,000	70,000	70,000
.333 UTS	$\mathfrak{G}$	3	3	3	3	3
	N	116,000	27,400	12,400	63,000	18,100
.333 UTS	$\mathfrak{G}$	4.35	3.42	3	3.94	3.19
	N	12,400	12,400	12,400	12,400	12,400
.333 UTS	$\mathfrak{G}$	2	2	2	2	2
	N	1,320,000	311,000	141,000	720,000	206,000
.333 UTS	$\mathfrak{G}$	1.5	1.5	1.5	1.5	1.5
	N	7,450,000	1,750,000	795,000	4,050,000	1,160,000
.625 YS	$\mathfrak{G}$	3	3	3	3	3
	N	101,000	24,600	720	24,400	11,600
.50 YS	$\mathfrak{G}$	3	3	3	3	3
	N	386,000	93,800	2,750	93,800	44,400

$\mathfrak{G}$ = DESIGN LOCAL STRESS FACTOR
N = NUMBER OF CYCLES TO FAILURE
E = 30,000,000 PSI

of 10 or 20 yr. The validity of rupture-life predictions as extrapolated from tests of a few thousand hours duration is not considered established.

Similarly, these comments apply to the critical extent of deformation which establishes useful life. On the one hand, some hold that safe deformation is limited to a few per cent, others point to ductile carbon-steel simple vessels in which creep as extensive as 5 to 10% or more has occurred without instability or other distress. Undoubtedly, the results of short-time yielding and long-time creep render proper interpretation of service deformation difficult because individually they are not readily distinguishable.

The present code requirements do not distinguish between elastic and creep service, permitting the same details for minimum heads, nozzle reinforcement, fillet and blind-root welds. For example, there is no temperature limit on lap-welded construction of main seams. There is no recognition of stress intensification which results from local interruption of a stress pattern resulting from flaws or sharp changes in contour, and increased stress at locations, resulting from the local contour of the surface of revolution. The latter probably assumes a more favorable contour with little deformation. In general, the extent of local plastic flow which can be tolerated is no doubt related to the complexity of the entire structure and the interdependence of the overstressed area and the remainder of the structure. There is certainly some evidence that service cracks are more prevalent in high-temperature service.

Cyclic temperature and/or mechanical loading apparently increase the creep rate, and would be expected to exert a similar influence on rupture life although, insofar as the authors are aware, this has not been demonstrated by actual tests. Fatigue-test investigation has been essentially limited to constant temperature. An exception is the work of Coffin. Also, the influence of time, or the duration of each cycle, has been explored only for very short periods.

The foregoing amply supports the need for concerted effort toward an understanding of the high-temperature behavior of complex structures, as represented by present code construction. Much progress can result from critical reasoning and realignment of fundamental knowledge employing the special factors found by experimentation to be peculiar to pressure vessels. This can also serve to guide the limited and relatively expensive supporting experimental investigations necessary for reasonably sound conclusions. For the present, two alternate philosophies of high-temperature vessel design are possible:

Table 2—Cyclic Pressure Effects on Vessels with Flat Heads—Test Results vs. Cycles Estimated by Calculation (See Fig. 3)

REFERENCE	HEAD DETAIL (FIG. 3)	MATERIAL	CYCLIC PRESS. CHANGE PSI	NO. OF TESTS	NO. OF CYCLES TO FAILURE			CALCULATED VALUES	
					MIN.	MAX.	AVG.	S*	N**
GROSS (12)	A	MILD STEEL	2950	7	56,000	109,800	71,000	58,000	130,000
	B	"	2950	4	63,300	335,000	158,000	54,900	118,000
	C	"	2950	5	604,400	1,283,000	879,200	48,770	238,000
MUTUAL (13)	D	"	73	1	-	-	7.8×10^6	21,600	32×10^6
ECOLE POLY. (PVRC)	E	A201	3850	1	-	-	16,200	76,200	17,600
	E	A302	7000	1	-	-	1,952	134,700	2,800

* LOCAL LONGITUDINAL BENDING AND LONGITUDINAL MEMBRANE STRESS IN SHELL AT HEAD.

** CALCULATED FROM EQ. (2) FOR MILD STEEL AND EQ. (3) FOR A302.

1. Continue present high-temperature stress criteria, but with construction requirements of vessel Class C for the elimination of present weak areas.

2. Advance the limits for principal stress in recognition of the greatly reduced local stresses of vessel Class C requirements. An increase of 33% to correspond to that proposed for temperatures below the creep range would accelerate creep for carbon steel and most ferritic materials roughly to 1% in 24,000 hr, or 4.2% in 100,000 hr.

The first, and conservative, alternative has been incorporated into the proposed basic principles of Section IV of this paper. It is reasoned that the assessment of the factors involved should proceed to much more definite indications before a more liberal approach as to primary stress is sanctioned, particularly in consideration of doubts concerning the present details and the adequacy of the existing code approach for local areas. However, this may also be taken to emphasize that local stress far outweighs primary stress as the critical factor of high-temperature design. An increase in the former and a drastic reduction in the latter provides capacity at least equal to present code design for the total structure to resist and absorb plastic flow or creep, with a reasonable expectation of over-all improved safety and freedom from crack initiation.

The present code lists essentially all loadings which are encountered in pressure vessels. These, with some additions, could be classified as to type of stress and related criteria. For Class N vessels only primary pressure loads would be considered; for Class G vessels all types of primary loadings, as at present, would be considered for non-cyclic service, with secondary stresses evaluated on the new approach to a stress-range basis for cyclic service; and for Class C vessels all types of loadings and both primary and secondary attendant stresses would be controlled to suitable limits.

C. Design

Before classification of pressure-vessel stresses is made we would like to propose two definitions. A direct stress is a stress which is constant throughout the thickness. A bending stress is a stress which varies from positive to negative across the thickness. The stresses encountered in a pressure vessel may then be classified as:

1. Primary Stress. Primary stresses are the direct or bending stresses generated by the imposed loading and which are necessary to satisfy the simple laws of equilibrium between forces external to the shell and stresses within the shell.

2. Secondary Stress. Secondary stresses are by definition local stresses which exist only in a small portion of the vessel. Direct or bending stresses which exist in a length less than $3\sqrt{Rt}$ are secondary stresses.

The longitudinal, circumferential, and radial pressure stresses are primary direct stresses, although the radial stresses are commonly ignored for usual dimensions. An example of a primary bending structural stress is the longitudinal structural stress in a vertical vessel exposed to wind forces. Another example is the bending stress in a flat head under pressure loading. The stress superimposed on the primary direct stress at a nozzle is a secondary stress caused by pressure. The longitudinal and circumferential stresses caused by pressure in a shell at its intersection with a flat head are secondary stresses because they reduce rapidly with distance from the intersection.

These stresses can be caused by two types of loading—external forces or strain loadings. They are caused by the former if the loading is independent of the deformation and thus capable of causing complete fracture. They are the result of strain loading if the load and strain are interdependent, and plastic strains can relieve the loads.

Essentially, the present ASME Code for Unfired Pressure Vessels considers

only primary direct and bending stresses, and hence is suited only for substantially static (noncyclic) service. This approach is continued by the destructive type of code proof tests. For other types of proof tests, a part which previously has been cold worked by a preliminary application of twice the design pressure is only required to be free of yielding in the formal test. Thus no check of initial yielding is obtained by this test. Brittle coatings and destruction tests do not satisfactorily indicate local areas of high stress but, rather, react more nearly to average stresses. The requirement for strain-gage measurements in most highly stressed zones, in the alternate tests which may be used, seems out of place with the general code approach. The destruction test often has shown the surprising result that local areas of high stress undergo only limited strain and can develop the full static-pressure rating of the basic structure, allowing the failure to occur elsewhere.

There is no distinction between external force and strain loading, and only the flange rules recognize a difference between bending and direct stress, inasmuch as they permit the hub bending stress to exceed the code allowable by 50%. Actually, this inherently recognizes a further increase of 50% resulting from the longitudinal pressure stress, which is not included, and so leads to a stress intensification factor of 2. Localized stresses may be altered by slight yielding to a stronger contour, or the moment effects may be redistributed. However, the strain range which such a vessel fiber undergoes on repetitive cycles of load may undergo little change, and this is the significant aspect insofar as fatigue is concerned. The expansion and flexibility rules of the ASA Code for Pressure Piping have led the way in connecting fatigue life with a design "allowable stress range," and these provisions can conveniently be used as a limit for shell-bending stresses at nozzles, skirts, and lugs, as well as cyclic thermal gradient stresses and intersection effects. There is no attempt to regulate the stress-raising potential of abrupt contour changes or attachment details. Fillet and blind-root welds are widely used in nozzle reinforcement, and sharp or lightly radiused corners and abrupt changes in section are common.

The effects of structural loadings, including wind and earthquake, are left to the individual designer, with many varying approaches as to the total allowable stress.

The present code approach has evolved from experience with extremely ductile materials which, by incorporation of ample safety factors, permits a design by the calculation of principal stresses to simple formulas and yet achieves virtually 100% safety. To permit lower nominal safety factors and the use of less ductile or otherwise sensitive materials, and to afford a practical basis for the design of special complex details, or demanding services (in particular of a cyclic nature), and at the same time retain or improve, if possible, the code safety record, it is necessary that the code design approach be broadened to include direct recognition of all stresses, with logically related criteria for their individual and combined limits. The PVRC and related investigations have now reached a stage at which general guidance can be obtained to establish this complete design, including the effects of fatigue. When translated into consistent requirements for these vessel classes, the more predictable performance which results for all vessels should reduce the hazard of controllable failure to a minimum.

The inherent stress factors listed in Table 3 are intended to indicate a reasonable expectation of the influence of flaws remaining in the base material and welds and of the maximum stress level including localized effects. When material or design of lesser quality is used, the advantage of complete examination of welds or emphasis on any other fabrication or inspection step at additional cost is limited, and is similar to strengthening the stronger members of a mechanism containing a weak link. Therefore, the inherent local stress factor is a starting point in logically relating the requirements necessary for a specific class or quality of vessel. The nominal safety factor—minimum UTS

Table 3—Suggested

ITEM						PRESSURE VESSEL CLASS - FERROUS MATERIALS		
						C	Q	H
1. OBJECTIVE						TO PROVIDE A FABRICATED PRESSURE VESSEL DEVELOPING THE FULL POTENTIAL OF THE BASE MATERIAL	TO PROVIDE A FABRICATED PRESSURE VESSEL DEVELOPING THE AVERAGE POTENTIAL OF THE BASE MATERIAL	TO PROVIDE A FABRICATED VESSEL FOR LIMITED SERVICE IN WHICH ADDED THICKNESS OBVIATES REFINED DES. & FAB.
2. SELECTION OF VESSEL CLASS	SERVICE PERMITTED FOR					CRITICAL	GENERAL	NON-HAZARDOUS
	SERVICE LIMITS	PRESSURE				NO RESTRICTION	SEE CONTENTS	SEE CONTENTS
		TEMPERATURE				NO RESTRICTION	750°F MAX.	300°F. MAX.; 20°F MIN.
		CYCLES (1)	MAXIMUM INHERENT BY VESSEL CLASS REQUIREMENTS			60,000	6,000	1,000
			FOR GREATER NUMBER			AS PERMITTED BY TABLE 4	AS PERMITTED BY TABLE 4	NOT PERMITTED
		DUCTILITY BASE MATERIAL				15% MIN.	15% MIN.	15% MIN.
	MATERIALS	ANALYSIS	ASME SECT. IX		LIMITING THICKNESS			
			GROUP P-1			NO RESTRICTIONS	1 1/2" MAX.	1/2" MAX.
			GROUP P-3			NO RESTRICTIONS	1" MAX.	NOT PERMITTED
			GROUP P-8			NO RESTRICTIONS	1/2" MAX.	NOT PERMITTED
			OTHER GRPS.			NO RESTRICTIONS	NOT PERMITTED	NOT PERMITTED
	CONTENTS	LETHAL				NO RESTRICTIONS	NOT PERMITTED	NOT PERMITTED
		NON-FLAMMABLE LIQUIDS				NO RESTRICTIONS	NO RESTRICTIONS	300#/SQ. IN.
		NON-FLAMMABLE GASES				NO RESTRICTIONS	600#/SQ. IN.	100#/SQ. IN.
		OTHER CONTENTS				NO RESTRICTIONS	300#/SQ. IN.	NOT PERMITTED
		STORED ENERGY (MAX. SIZE)				NO RESTRICTIONS	25,000,000 FT-LBS.	36" DIA. X 10'-0" LG.
3. DESIGN	LOCAL STRESS FACTOR β (FOR FATIGUE)					1.5	3.5	6.0
	(2) NOMINAL SAFETY FACTOR (UTS) UP TO 750°F INCLUSIVE					3.0	4.0	5.0
	(2) BASIS FOR HIGH TEMPERATURE STRENGTH OVER 750°F					PRESENT ASME CODE SECT. VIII, APPEN. P	NOT PERMITTED	NOT PERMITTED
	(3) WELDED JOINT FACTOR					100%	100%	WELD STRENGTH (100) FOR DOUBLE BUTTWELD
	ALLOWABLE STRESS	EXTERNAL LOADINGS	LONG TIME	PRIMARY STRESS	PRESSURE + STRUCTURAL	S_a	S_a	S_a
				PRIMARY PLUS SECONDARY DIRECT STRESS		1.5 S_a	1.5 S_a	1.5 S_a
				PRIMARY PLUS SECONDARY BENDING STRESS		2.5 S_a	2.5 S_a	6.0 S_a
			SHORT TIME	PRIMARY STRESS	PRESSURE + STRUCTURAL INCL. WIND OR EARTHQUAKE	1.25 S_a	1.33 S_a	NOT REQUIRED TO BE EVALUATED
				PRIMARY PLUS SECONDARY DIRECT STRESS		1.875 S_a	2.0 S_a	NOT REQUIRED TO BE EVALUATED
				PRIMARY PLUS SECONDARY BENDING STRESS		1.875 S_a	4.66 S_a	NOT REQUIRED TO BE EVALUATED
	STRESS LIMITS	TOTAL STRAIN PLUS EXTERNAL LOADINGS	LONG TIME	ANY LOCATION	PRESSURE + STRUCTURAL & THERMAL STRESS	3/4 ($S_{aHOT}+S_{aCOLD}$)	1.75 ($S_{aHOT}+S_{aCOLD}$)	NOT REQUIRED TO BE EVALUATED
			SHORT TIME	ANY LOCATION	PRESS. + STRUCT. INCL. WIND OR EARTHQUAKE & THERM. STRESS	1.25 X 3/4 ($S_{aHOT}+S_{aCOLD}$)	1.33 X 1.75 ($S_{aHOT}+S_{aCOLD}$)	NOT REQUIRED TO BE EVALUATED

(1) NUMBER OF CYCLES OBTAINED FROM EQUATION (1) SECTION 161 WITH SAFETY FACTOR OF 1G ON NUMBER OF CYCLES AND AS RELATED TO A MILL PLATE SURFACE.
(2) BASIC ALLOWABLE STRESS (S_a) TO BE LOWER OF UTS/SAFETY FACTOR, 5/8 YIELD STRENGTH, 1% CREEP 100,000 HRS. AND 100% STRESS RUPTURE 100,000 HRS.
(3) WELD STRENGTH RELATIVE TO PLATE, NEGLECTING FLAWS, NON-DESTRUCTIVE EXAMINATION AND POST-HEAT TREATMENT.

divided by allowable membrane stress—is related to the inherent local stress factor and the number of service cycles expected. With perfect materials, design, and welding, the local stress factor would be 1 and the safety factor could probably be as low as 2 provided a satisfactory margin against general yielding still existed, and under these conditions the maximum local stress would not exceed levels which are justified by experience. For the more practical value of 1.5 for the local stress factor, a proportionate safety factor would be 3.

The interdependence of the local stress factor and safety factor is obvious from simple mathematics because in combination they control the maximum level of localized stress relative to material properties on which the code allowable stresses are based. Because of lack of direct recognition and regulation of localized stress, this obvious interrelation is not adequately appreciated. The PVRC and other investigations reviewed and commented on in Section III herein have given at least qualitative demonstration of:

(*a*) The significance of localized stresses on fatigue performance, as evidenced by the École Polytechnique's tests, in which failures occurred earliest and predominantly at areas involving high local stress caused by design details, rather than at purposely introduced notches.

(*b*) The interdependence of the local stress factor and nominal membrane stress in relating tests of different geometry and materials, and translation of these experimental data into possible design parameters.

(*c*) The relative fatigue performance of the materials tested is not reflected by their comparative YS. Comparative tensile strength (TS), although better than yield ratios, also overestimates the fatigue resistance of the higher strength materials. An index considering actual yield, and tensile and elongation properties will be suggested in Section III.

There has always been considerable opinion that the basic allowable membrane stress can be simply related to the YS, exclusive of the UTS and other properties. The authors reason that no single physical property reliably predicts over-all performance. Rather the influence of each must be separately considered—including UTS, YS, elongation, fatigue resistance, transition temperature, creep, and the like. The PVRC fatigue tests show that to be guided merely by TS or YS, or both, would seriously overweigh fatigue performance. On the other hand, the yield stress cannot be ignored for reasonable dimensional stability and avoidance of general yielding in service and during test. Current practice requires a 1.5 factor for hydrostatic test although lower factors are permitted for special reasons or in other countries. The value of the hydrostatic test as a check on fabrication or design is recognized as extremely limited and it can be expected to disclose only gross errors. It tells nothing at all about fatigue failure potential. A test factor of 1.5 would require that the basic allowable stress not exceed about 0.625 yield.

The present attitude ignores the high level of localized stress permitted by code requirements and, in particular, thermal stresses resulting from temperature gradients or restrained expansion which may involve high strain ranges which can be a function of fluctuations in operation and thus involve many cycles for each full operating cycle of the vessel. Section III clearly shows that the fatigue aspect becomes far more critical as membrane stresses are increased.

The preceding discussions of the influence of secondary stresses considers the fatigue aspects as related to the peak cyclic strain range. Usually areas of high localized stress involved bending stress superimposed on direct stresses. A typical example is the case of a sharp conical head junction under internal pressure at which there are direct longitudinal and circumferential stresses and superimposed bending stresses. The peak strain for fatigue consideration involves the combined effect. However, the direct stress, which is also the average stress across the wall thickness, should be controlled and preferably limited by the basic allowable stress the same as other membrane

Basis for Code Modification

ITEM			PRESSURE VESSEL CLASS — FERROUS MATERIALS								
			C			B			A		
4. MATERIALS	GRADE — MINIMUM		FIBEROS - IMPROVED			FLANGE			STRUCTURAL		
	EXAMINATION		ENTIRE AREA SCANNED FOR INJURIOUS DEFECTS BY ACCEPTABLE MEANS			VISUAL EXAM. OF ALL SURFACES & CUT EDGES FOR INJURIOUS DEFECTS			VISUAL EXAM. OF ALL SURFACES FOR INJURIOUS DEFECTS		
	INJURIOUS DEFECTS		TO BE DEFINED IN MATERIAL SPECS.			TO BE DEFINED IN MATERIAL SPECS.			TO BE DEFINED IN MATERIAL SPECS.		
	PROVISION AGAINST BRITTLE FRACTURE	CURRENT (BUT NOT BELOW -20°F)	TRANSITION TEMP. AT OR BELOW - 20°F			CONTROLLED C/Mn FOR ALL THICKNESSES. FINE GRAIN SIZE FOR THICKNESSES OVER 1".			NONE		
		BELOW -20°F	TRANSITION TEMP AT OR BELOW SERVICE TEMP.			CHARPY TEST 15 FT. LBS AT SERVICE TEMP.			NOT USED		
	FATIGUE TESTS OF MATERIALS		FOR FUTURE CONSIDERATION			NONE			NONE		
	CORROSION, DETERIORATION AND IMPAIRMENT		USER RESPONSIBILITY WITH CODE GUIDANCE			USER RESPONSIBILITY WITH CODE GUIDANCE			USER RESPONSIBILITY WITH CODE GUIDANCE		
	OVERLAID MATERIALS		HARDNESS CHECK AND INSPECTION FOR CRACKS			NOT USED			NOT USED		
5. FABRICATION	MAIN SEAMS		DOUBLE BUTT WELDED OR EQUIVALENT			DOUBLE BUTT WELDED OR EQUIVALENT			BUTT OR LAP WELDED		
	NOZZLES AND ATTACHMENTS		DOUBLE BUTT WELDED (NOT CORNER WELDS)			AS PER PRESENT CODE			NO RESTRICTIONS		
	FIT UP		MANDATORY CHECK BEFORE WELDING			AS PER PRESENT CODE			LIBERALIZE PRESENT CODE		
	CONTOUR TOLERANCES		MORE COMPLETE REQUIREMENTS, 1/45 DIA. FOR SHELLS			AS PER PRESENT CODE			LIBERALIZE PRESENT CODE		
	WELD DISTORTION		MORE COMPLETE REQUIREMENTS, 1 1/2% DIA. AT NOZZLES			AS PER PRESENT CODE			LIBERALIZE PRESENT CODE		
	REFORMING AT LONGITUDINAL SEAMS		REQUIRED			NOT REQUIRED			NOT REQUIRED		
	HYDRO TEST		1 1/2 D.P. BUT PERMITTED TO .9 Y.S.			1 1/2 D.P.			1 1/2 D.P.		
	AIR TEST		1 1/4 D.P.			1 1/4 D.P.			NOT PERMITTED		
	FATIGUE TEST OF WELDS		FOR FUTURE CONSIDERATION			NONE			NONE		
	WELD SURFACE		GROUND SMOOTH & CONTINUOUS - 1/16" MAX. REINFORC.			ASME PRESENT LIMITS OF OVERLAY			REASONABLY WORKMANLIKE		
	VESSEL TEST PLATE		REQUIRED			NOT REQUIRED			NOT REQUIRED		
	UNDERCUTTING		MUST BE REMOVED			ACCEPTED TO SAME EXTENT AS SIMILAR DEFECTS			MUST NOT BE WIDESPREAD		
6. INSPECTION			MAIN SEAMS	NOZZLES & ATTACH.	MAIN SEAMS	CRIT. LOCATIONS	NOZZLES & ATTACH	MAIN SEAMS	CRIT. LOCATIONS	NOZZLES & ATTACH
	RADIOGRAPHIC		100%	100%	RANDOM	COMP.	RANDOM	NOT REQ'D.	NOT REQ'D.	NOT REQ'D.
	FERRITIC AUSTENITIC OR NON-FERROUS	MAGNETIC POWDER PENETRANT DYE OR EQUIVALENT	100%	100%			100%	NOT REQ'D.	NOT REQ'D.	NOT REQ'D.
	ULTRASONIC FOR VESSELS OVER 1" THK. OF SIX HARDENING OR HIGH STRENGTH MATERIALS		100%	100%				NOT REQ'D	NOT REQ'D.	NOT REQ'D.
	VISUAL	INDIVIDUAL VESSELS	100%	100%	100%	100%	100%	COMP. RANDOM	COMP. RANDOM	LIMITED RANDOM
		MASS PRODUCED VESSELS								RANDOM MASS PRODUCED VESSELS
	DESTRUCTIVE									

effects, although a somewhat higher limit can be justified because of the limited width of the stressed zone and the establishment of a favorable residual stress system of opposite sign, should local yielding occur.

A safety factor of 3 on the UTS represents a considerable potential advance in the economic use of costly materials; and, more important, with the design and quality controls specified, it provides better quality construction for critical services at what would seem to be a nominal increase in cost. Thus, with a Class C vessel, the extra cost of butt-welded connections and additional quality control would in large part be offset by approximately 25% reduction in weight and related savings in material and fabrication. With a vessel of Class G there would be a similar economic gain with a 100% joint factor. Also it would be recognized that full radiographic examination overemphasizes weld quality for this vessel class. For Class N vessels, further design easements would be justified; e.g., smaller head-knuckle radii, greater limits for unreinforced openings, and the like. In addition, the joint efficiencies would be adjusted to reflect only minimum strength, with attendant improved economics in proportion to the higher values agreed upon for the joint factors.

The objective of the code must be to provide the maximum safety which can be obtained at nonprohibitive costs. One-hundred per cent safety is a desirable goal, but can never be completely attained because of the considerable expenditures involved in raising the safety record the last few hundredths of 1% if such perfection can ever be achieved. On the other hand, a very few failures can equal the total cost of many pressure vessels. A good example of an economic and sensible safety requirement is afforded by random radiographic examination. Its use exerts a tremendous psychological effect because the manufacturer, boilermaker, welder, and inspector realize their work is under scrutiny, and much more uniform weld quality is achieved than with visual examination alone. With proper rules to treat such examination as "sampling," utilizing statistical quality control without unfair demands for conditioning of welds, and with realistically interpreted standards which accept occasional unfusion and lack of penetration, the extra fabrication and inspection costs should be merely a few per cent, a small price for the improved safety achieved. Table 3 also indicates a requirement for examination of critical locations, such as weld intersections, which would likewise be desirable and should not be too costly when adopted as a standard approach.

One aspect of the proposed code reorientation which deserves exceptional emphasis is the goal of "uniformly proportioned vessels." Present code requirements accept the existence of higher and not-closely-controlled local stresses at nozzles, changes in shape, and other discontinuities, with the result that the material in the shell proper is not utilized to its fullest advantage. Although this is generally appreciated, progress in the art of welding and techniques for nondestructive examination of main-seam welds has led to relatively high code radiographic standards and a trend toward expecting even higher quality by rigid interpretation during inspection. As a result, the quality of vessel main-seam welds, whether fully or random examined, far exceeds that attained by the materials, fabrication, and design details as a whole. For example, the nozzle design details permitted, together with the absence of examination of nozzle welds, other than visual, makes them a focal point of vessel construction vastly inferior to the main seams. The PVRC is well aware of this situation and much of the effort of its divisions is aimed at extending knowledge pertaining to the evaluation and significance of localized or secondary stresses, as well as the effect of fabrication operations, notches, and specification material quality.

D. Materials and Metallurgy

The ASME Code for Unfired Pressure Vessels has achieved an outstanding accomplishment in providing a consistent and logical tabulation of basic allowable stresses. This provides a ready vehicle around which complete stress criteria can be established, with factors for individual or combined types of stresses. The significance and effect of ductility on general safety is still lacking. In comparing materials of different character, ductility appears to have an influence on fatigue performance. It is equally important that the useful ductility which prevails in the fabricated vessel under average combinations of stress allow plastic deformation in distorted or inaccurately shaped areas to occur without failure. The ductility should also permit reduction of local stress at flaws or at changes in contour by plastic deformation. Proper requirements for materials of zero or low ductility are lacking.

The effect of time (aging) and similar metallurgical phenomena—particularly on copper and aluminum alloys—should be more adequately covered.

Impact and fatigue tests could well be justified for vessels where the full potential of the materials is to be approached. Also effort should be directed at improving the transition temperature of ferritic materials for average service.

The cleanliness, uniformity, and absence of flaws should be related to the degree of severity to which the material will be subjected. For the highest vessel class and attendant stress level, the material should be of firebox quality, with flange and structural quality permitted for average and nonhazardous services. In addition, the highest quality material should be examined for injurious internal and external defects by an acceptable means related to the thickness. In particular, the standard for acceptability of minor laminations or small string-like inclusions needs further study to avoid controversy. Material specifications should be improved by establishing the relative quality of firebox, flange, and structural grades; and, most particularly, by formulating a usable definition of injurious defects. It should be made clear whether the physical properties and chemical analysis specified will be achieved only in the selected test locations, or whether these properties are to be considered as representative of the material at any location; and, if not, tolerances should be established below which the material would be considered substandard.

Corrosion, deterioration, and impairment of materials and welds can have serious effects on the safety of pressure vessels. It appears illogical to emphasize the initial integrity of a vessel and leave inspection in service and proper appreciation of safety in operation entirely up to the user without all possible guidance. The ASME Boiler Code Committee constitutes an excellent forum for the collection and dissemination of information on this subject and should provide this information as a code appendix in a "recognized good practice" category. Mandatory requirements as to inspection in service and for precautions or prohibitions as to the use of certain materials, fabrication procedures, and the like, are well justified.

E. Fabrication and Inspection

For maximum utilization of material with refined design, it becomes essential to control and assess fabrication operations and to incorporate tests and inspection requirements which assure that the desired mechanical properties and soundness are met in the fabricated vessel. For basic allowable stresses of $^1/_3$UTS, the material must be thoroughly checked for soundness, such as by descaling and examining by the magnetic-particle method, radiographing, or ultrasonic testing. When physical properties are dependent upon heat treatment or cold work, they must be checked on the finished vessel by thorough hardness checks and by representative mechanical tests on material simultaneously treated. All pressure-holding seams, including nozzle welds, should be of the double butt-welded type, or equivalent, and fully radiographed.

Welds for major nonpressure attachments, including supports, should be of the same design and inspection or the shell should be locally thickened. Welds for minor attachments should be critically examined by the magnetic-particle method after the vessel hydrostatic test. The inside of a vessel requires critical inspection, as well as the outside; hence, vessels in which this is not practical should be more conservatively designed. Abrupt changes in contour resulting from forming, fit-up, and the like, must be avoided; and, whenever unequal thicknesses are involved, a maximum slope of 1:4 is recommended. Undercutting is a problem which is essentially avoided by its flat prohibition; similarly, the smoothness and contour of weld surfaces is not satisfactorily established. Possibly the use of an inert-gas tungsten-arc cover pass may produce an acceptable contour without grinding, and which is free of undercutting.

For Class G vessels which are to be used under fatigue conditions, some of the foregoing applies. In addition, some details—in particular, fillet welds—deserve consideration as to their stress-raising potential. Otherwise, for the most part, present code fabrication and inspection is entirely adequate for Class G, with some liberalization deserving consideration. For Class N vessels the requirements should be appreciably reduced.

Fabrication requirements should be proportioned to the vessel class, with the closest tolerances for fit-up, forming, and distortion applied to the most refined class of vessel. For this highest class of vessel, the weld surfaces would be ground smooth, the present code surface requirements maintained for the average class of vessels, and the weld surface requirements made more generous for the lowest class of vessel.

The weld tests as presently constituted are of limited value, in the opinions of the writers. The procedure test is made only once, qualifying the fabricator forever afterward to perform welding to that procedure, and there is wide latitude in grouping materials, electrodes, and other variables. Operator qualifications also allow wide latitudes for materials, to which they apply and place almost entire reliance on guided-bend tests. No tests are made to check the weldability of the base material or weld rod for a specific vessel. The procedure tests merely indicate that a satisfactory weld has been accomplished with the base material and rods which were selected because the successful tests may have been the best of several tests. The operator tests indicate only the operator's capacity for depositing sound welds and, in the opinion of the writers, is much inferior to radiographic examination, sectioning, or similar means which will provide more assured knowledge of the subsurface condition. In any case, operator qualification tests serve only to assist the fabricator in his initial selection of welders, inasmuch as they do not contribute to quality control. The expenditure for such tests could probably be directed more effectively at production quality control.

The fit-up of nozzles and attachments has considerable influence on the effectiveness of the attendant welding. However, such fit-up is not presently specified and, consequently, satisfactory requirements should be provided.

The necessity for, and advantages of, stress relief need examination. There is some opinion that stress relief is of secondary importance, and that the real benefit of so-called thermal stress relief is in the reduction of air hardening with possibly some subcritical grain refinement in the plastically strained heat-affected zone. Opposed to this is the view that stress relief decreases the locked-in fabrication stresses which cannot be removed by the hydrostatic test without yielding the entire vessel. A special task group of the ASME Boiler Code Committee is examining the requirements for thermal stress relief and the possibility of mandatory vs. suggested requirements for preheat. The final evolution of logical stress relief, preheat, and postheat requirements can be achieved only through a better understanding of the fundamental benefits which they provide.

The value of pressure testing of vessels is likewise subject to considerable variation of viewpoint. Hammer testing may initiate cracks at local zones of weakness with little chance of revealing small flaws. Similarly it can be reasoned that the hydrostatic test may initiate or propagate flaws particularly on a non-stress-relieved vessel. Some benefit may be derived however such as the possibility of some reshaping of the vessel in inadequately formed or distorted areas that will effect some measure of mechanical stress relief. However, the stress level is too low for a check on design or fabrication unless gross errors have been made and it can reveal nothing as to a vessel's fatigue failure potential. Weighing the relative costs and very limited benefits of hydrostatic testing, the tentative conclusion is reached that more effective assessment of performance can be arrived at by more accurate design and full use of nondestructive examination and details adapted to such examination with pressure testing limited to a tightness test at the working pressure or with air at moderate pressure. By virtue of long-standing practice the hydrostatic test probably has assumed a safety stature in the eyes of the public out of proportion to its true value. It is time to recognize the more effective safety value of good details and searching inspection.

The inspection of vessels would benefit from more definite requirements as to a minimum extent of inspection and by more information on inspection procedures. For example, misalignment of plates at welds can be judged only before performance of the welding, inasmuch as it is difficult to measure weld alignment after the joint has been completed.

Magnetic-powder and ultrasonic examinations are increasing in use to such an extent that the ASME Boiler Code Committee should be active in the preparation of rules for their employment. For radiographic examination satisfactory requirements have not yet been evolved for random examination because of the tendency of demanding quality closely approaching that of fully radiographed construction wherever an examination is made. This only serves to defeat the purpose of the sampling approach, which random examination is intended to cover.

III. Fatigue Aspects—Discussion of the PVRC and Related Investigations

The Pressure Vessel Research Committee was formed in 1945 under the guidance of the Welding Research Council. Its activities are grouped under three divisions, viz., Design, Fabrication, and Materials. These activities have been aimed primarily at extending the knowledge pertaining to the evaluation and effect of: (1) secondary stresses; (2) fabrication operations; and, (3) notches on the performance of established and new materials for pressure-vessel application.

The PVRC Design Division has made an outstanding contribution in the analysis and experimental verification of the stresses in heads. Its report[1] not only is an exhaustive technical treatment, but includes a helpful historical background on the evolution of the code rules and a discussion of their practical aspects. This division is continuing with other complex design problems. The initial results of an analysis of the stresses caused by local external loadings on cylindrical shells has recently been released[2, 3, 13] and a supporting experimental program is currently in progress. Other studies in progress include cooperative projects dealing with stresses around openings.

With appreciation of the magnitude of peak local stresses common to the design details and flaws acceptable under present code rules, and realization that the attendant strain range involves yielding with each application of loading, the PVRC set out to explore the fatigue resistance of current and projected ferrous materials, with emphasis

on cyclic strains extending into the plastic range. Test data have been obtained on both laboratory test specimens and small pressure vessels. The results of laboratory specimens tested at the University of Illinois and Lehigh University have been reported in several papers.[6, 7, 10] The authors will briefly present significant observations which have a bearing on pressure-vessel construction, as follows:

1. The strain range per cycle is the essential index of performance in the plastic-elastic range such as may be encountered at peak stress locations on present code pressure vessels. With a fatigue life (failure) up to about 100,000 cycles, which covers the great majority of applications, it is not necessary to consider the initial state of stress or the mean stress, as would be the case with a larger number of cycles approaching the endurance limit for such items as machine parts where peak strains are well within the elastic range.

2. Fatigue tests on plate having a polished surface finish, when compared with tests on plate having a scaled or pickled "mill" finish or containing fabrication punch marks, indicated the latter finishes involve an effective stress intensification of the order of 1.3 to 1.45. Notches contoured to a calculated stress intensification factor of 2.9 (as compared to a polished bar) or 2.15 (as compared to a mill surface) showed on test about 2.0 and 1.5, respectively. This leads to a conclusion that the notches did not reach their full stress-raiser potential.

3. The relative fatigue performance of the high-tensile steels as compared to conventional, more ductile, carbon steels is shown by the reference papers to be more nearly in proportion to their tensile strengths rather than their yield strengths. However, the ratio of the tensile strengths is not an accurate index to relative cyclic life, particularly when tested in the notched condition, and would overrate the high-strength materials as can be seen from Figs. 15 and 16 and Table 3 of Bowman and Dolan.[5] Elongation seems to have some influence and the authors find that the following comparative index comes much closer to correlating with the notched data, as it is reasonably close for A 225 and T_1, but low for A 302:

$$\text{Relative fatigue-life index} = \frac{[(T8 + Y8)/(2)]\ (\text{elongation})\ (\text{of material being compared})}{[(T8 + Y8)/(2)]\ (\text{elongation})\ (\text{of material to which compared})}$$

It can only be stated that this appears to be better than the tensile ratio for data so far available.

4. The influence of heat treatment and prestraining to considerably enhance the physical properties of A 212, A 201, and A 302 was shown by tests to improve fatigue performance as the tensile strength was raised. A prestrain of 10% was provided for the tests, with a remaining elongation of at least 15% still available in the least ductile specimen. It is presumed that this prestrain was obtained uniformly along the specimen, so that it is not to be compared to localized yielding, which would tend to lower the additional available deformation without instability at that location.

The result of the tests of small vessels made at École Polytechnique have not been published up to the present, and are given only in progress reports to the PVRC Fabrication Division. These 12-in.-ID by $^3/_8$-in.-thick vessels of A 201 and A 302 materials were subjected to periods of cycling with the internal pressure slightly below, slightly above, and considerably above the pressure producing general yielding of the shell. Some vessels had $1^1/_2$-in.-ID welded nozzle connections, and machined notches similar to those of the specimens of the other laboratories. A comparison of the results to date on vessels G and H (A 201) and vessels L and M (A 302) with the laboratory tests on the same materials is of interest. The authors find that their performance follows the trend of the University of Illinois notched plate tests, with lower values. To illustrate the comparison most clearly, Fig. 1 has been prepared by replotting the University of Illinois data on a log-log basis, choosing a straight line which fits the notched plate data reasonably well, drawing parallel lines for the unnotched plate and polished plate to correlate

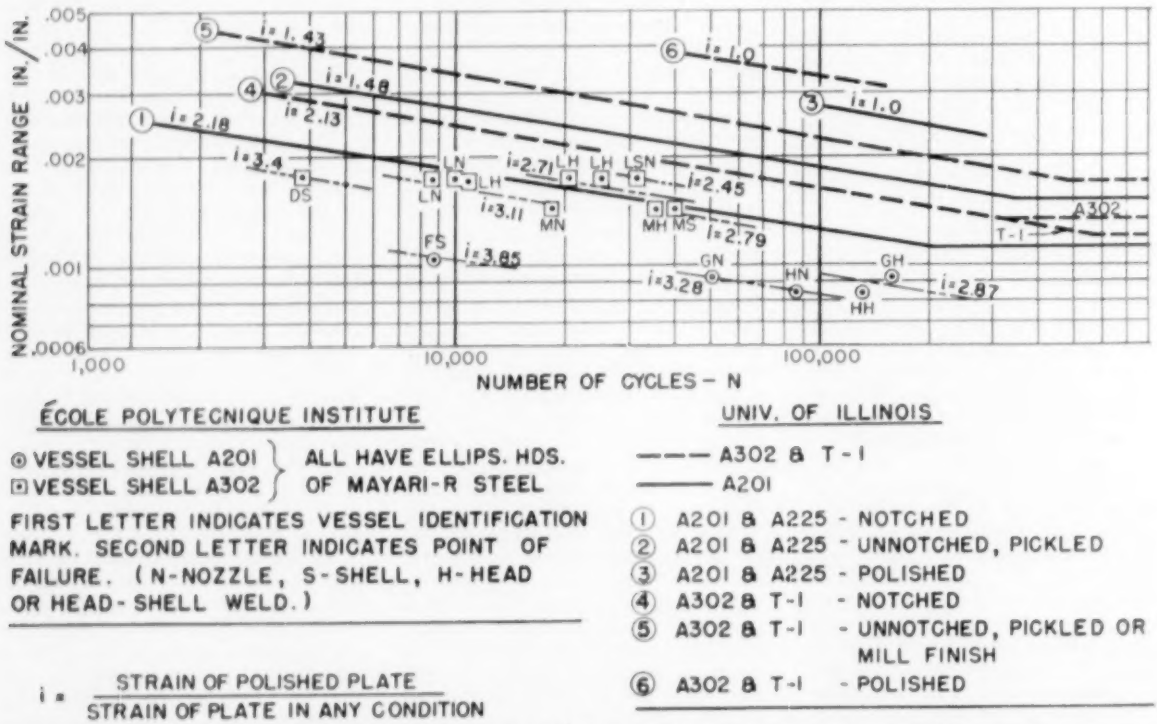

Fig. 1 Trend of University of Illinois biaxial fatigue tests and École Polytechnique Institute model vessel fatigue tests

with the test at about the 100,000 cycle point, and relating all curves for the same material by assigning a unity strain intensification to polished bars. The i factors marked on the other curves are obtained by dividing the strain for the polished plate by the nominal strain for the curve in question for a given value of N.

The tests at École Polytechnique provide a convincing demonstration that, from a fatigue standpoint, stress concentrations which result from customary design practices are the weakest points in a vessel. The earliest ruptures were experienced at flat head-to-shell connections and then at openings, with failures at head-to-shell welds or in the head-knuckle regions after the earlier weak points were reinforced. Few failures have occurred so far at the purposely introduced notches in the shell plates. Although there are not enough test points for a conclusive indication, a review of Fig. 1 shows that vessels G, H, L, and M would fall fairly in line with the University of Illinois results if the nozzles were assigned an i factor of 3.2 and the elliptical heads an i factor of the order of 2.8. These are not unreasonable considering that the fabricated plate surface condition is taken to involve an i factor of about 1.45. This would then indicate a design stress-intensification factor of 3.2/1.45 = 2.2 for the nozzles and 1.93 for the heads as compared with mill plate. This head factor seems high as the PVRC report[1] indicates only 1.4. However, the heads were of Mayari R which may have lower fatigue properties, or in their small diameter and relatively heavy thickness local thin or otherwise weakened areas may have developed.

Also spotted on Fig. 1 are 2 test points for vessels D and F which were cycled at pressures well in the plastic range. Inasmuch as different pressures were used for different portions of the test, the plotted point represents an approximate "equivalent" number of cycles at the starting pressure, which was arrived at as follows:

$$N_e \text{ (at pressure } P_1) = N_1 + N_2\left(\frac{P_2}{P_1}\right)^6 + \cdots + N_n\left(\frac{P_n}{P_1}\right)^6$$

Because the plastic strains in these tests were undoubtedly greater than the nominal values, these points are significant largely in the relative position of the A 302 and A 201 test points which conforms to the general trend. An additional comparison of École Polytechnique's test results on flat-head closures will be discussed later in connection with Table 2. It is of interest to note that tests on model vessels of T-1 steel are scheduled to be made at École Polytechnique.

The curves on Fig. 1 can be mathematically expressed by the following equation:

$$N = 10{,}000\left(\frac{e_r}{ie}\right)^n \qquad (1)$$

Where
- N = number of cycles to failure.
- e_r = strain range for failure in 10,000 cycles for polished specimens ($i = 1$), inches per inch.
- i = strain intensification factor.
- e = nominal strain range imposed per cycle, inches per inch.
- n = constant for the material, as determined by test.

Appropriate values for the Fig. 1 curves are:

- e_r = 0.00526 for A 302 or T1 steel.
- e_r = 0.0040 for A 201 or A 225 steel.
- n = 6 for the 4 materials compared.

For practical design purposes it would be preferable to have the equations in terms of the nominal design membrane stress (S_n) and the design stress factor (β) as related to the "mill" surface condition [$\beta = (i/1.45)$]. The statement then is as follows:

$$N = 10{,}000\left(\frac{0.00363E}{\beta S_n}\right)^6 \text{ for A 302 or T1} \qquad (2)$$

$$N = 10{,}000\left(\frac{0.00276E}{\beta S_n}\right)^6 \text{ for A 201 or A 225} \qquad (3)$$

Where
- E = Young's modulus of elasticity for the material at the test temperature.

The validity of using elastic stress analysis for application in an empirical equation of this kind when dealing with strains in the plastic range can of course be questioned. The authors would consider this not as an index of the actual stress or strain but only as a useful comparative index for different conditions and have found it to work reasonably well in other cases such as the correlation of fatigue test results on commercial expansion joints cycled well into the plastic range.

The important trend indicated is that

$$N \propto \left(\frac{e_r E}{\beta S_n}\right)^6$$

which permits estimation of the effect of separately or jointly changing: (1) the basic design allowable stress; (2) the maximum design stress concentration factor; and (3) the material.

For example, in comparing a vessel of A 201 steel with one of T1 steel we would get:

$$\frac{N_{201}}{N_{T1}} = \left(\frac{0.00276\beta_{T1}S_{T1}}{0.00363\beta_{201}S_{201}}\right)^6 = \left(\frac{\beta_{T1}S_{T1}}{1.32\beta_{201}S_{201}}\right)^6 \qquad (4)$$

From this, it follows that:

(*a*) For an equal fatigue service life

$$\beta_{T1}S_{T1} = 1.32\beta_{201}S_{201}$$

which indicates that from fatigue considerations the design stress for T1 steel cannot be increased to more than 1.32 times that for an A 201 vessel unless the design is more refined, i.e., lower level of local stress—or a lesser number of service cycles is acceptable.

(*b*) For the same design practice ($\beta_{T1} = \beta_{201}$) the reduced cycles:

$$N_{T1} = N_{201}\left(\frac{1.32S_{201}}{S_{T1}}\right)^6$$

Illustrative comparative results for different materials and design bases are shown in Table 1 to demonstrate trends. A generous safety factor—probably equal to 10—would have to be placed on the value of N to allow for the sensitive sixth-power relationship, and for scatter and other uncertainties. The tabulation points up the trend that, for a fixed stress factor β, the resulting level of the total local stress, rather than the basis used for selecting the basic allowable stress as a function of yield or tensile strength, establishes fatigue performance. Material characteristics are secondary to the strain range, so that even for materials of moderate strength increase, now recognized in the codes, considerable spread in probable fatigue performance is indicated.

The authors are cognizant that the curves of Fig. 1 interpret the test data on an idealized basis, and that their slope and position could be altered somewhat to affect the constants and figures cited. However, it is contended that the general trend which has been illustrated is a valid interpretation, as it hinges largely on the ratio of the allowable strains for different materials for a constant number of cycles and the exponent n. The strain ratio for T1 compared to A 201 in the notched condition as listed in Table 3 of Bowman and Dolan[5] compares well with the 1.32 value used in this correlation as a representative value.

It is of interest to examine some test data from other sources. Of particular significance is the fatigue test data on commercial carbon-steel piping assemblies (ASTM A 106 grade "B") reported by Markl.[9] The curves for pipe with a clamped edge condition, or having butt welds with as-deposited reinforcement, and for pipe with commercial surface finish but free of fabrication or design stress raisers, are shown in Fig. 2 and compared with the A 201 data taken from Fig. 1. Markl's curves are related by a stress intensification factor for commercial pipe of about 1.5. The polished bar data could not be represented by a straight line on the plot and, therefore, could not be used as a basis. The composite correlation presented in Figs. 1 and 2 is considered reasonably good for tests conducted under different conditions. Although the slopes of Markl's curves and the Fig. 1 curves are slightly different, a common slope could easily be selected which would fit both sets of data reason-

ably well. The slope also agrees reasonably well with tests on structural steel reported by Harris, Nordmark and Newmark.[17] Markl's data have been utilized for the revised rules of the ASA Code for Pressure Piping for the design of piping subjected to cyclic thermal-expansion strains. At present, these are the only rules in a standard pressure-equipment code which recognize the fatigue aspect for design.

The cyclic test data reported by Coffin[1, 11] are of comparative interest, for these tests involve cyclic strains resulting from restrained thermal expansion when subject to temperature cycling. Although applicable to a different material (Type 347 stainless steel) and thin polished tubular specimens, data for specimens with and without stress raisers are included in Fig. 2. The trend is similar, although the strain range for a given N value is greater. Coffin's tests show that cyclic strains, whether produced by thermal or mechanical loading, have similar effects, and can be treated in a common design approach.

As a random check of the proposed correlation the authors have compared the results of fatigue tests on small vessels with flat heads, as reported by several investigators, with the number of cycles predicted by entering the calculated maximum local stress in empirical eq (2) or (3). A comparison of the reported test values for fatigue failure with the calculated results is tabulated in Table 2. It can be seen that the calculated cycles to failure follow the trend of the experimental investigations remarkably well. The fact that detail c was better in performance than predicted can be attributed to the generous corner fillet radius which was ignored in the stress evaluation. The stress-raising potential of the weld details is unpredictable, and can very well both influence some reduction in the minimum number of cycles and also add to the scatter of the test results. Apparently the weld quality, proportions, and locations are such that, for the majority of these tests, the welds are less critical as stress raisers than the designed intersection stresses. The authors consider that this comparison demonstrates the value of the empirical fatigue correlation index for comparative evaluation of different designs and relative performance of different materials, even though present limited data was used to establish its numerical value. Undoubtedly, as more test data of this type are obtained, a more accurate correlation can be achieved.

Although the majority of reported fatigue tests have been conducted at atmosphere temperatures, a limited amount of fatigue testing at higher temperatures or under cyclic temperature change, as reported by Coffin, indicates that the ability of steel to take cyclic plastic strain is of the same order at high temperature as at low temperature. A few PVRC tests at 500 and 650° F showed a slight increase in capacity to absorb such strain. However, this conclusion cannot be validly extended into the temperature range where creep is a factor. Fatigue under combined cyclic strain and creep can be extremely complex when the influence of time, creep properties, and strain concentrations are considered in the manner discussed in Demoney and Lazan[14] and Robinson.[15] The design practice inherent in the ASA Code for Pressure Piping to assure adequate flexibility for thermal expansion in high-temperature service has been established by more than 20 years of widespread application. These rules provide an allowable stress range proportioned to prevent repetitive plastic flow on successive cycles. Relaxation on the first cycle self-springs the line and provides a stable residual stress system which predominates in the cold or offstream condition, and is within the short- and long-time capacity of the material for the repetitive applications involved. This has been accomplished in a practical manner by connecting the allowable stress range with the basic allowable stresses for the material at atmospheric and operating temperatures.

IV. Suggested Basic Principles for Code Modification

As a final step, the authors will attempt the challenging task of suggesting the major basic principles for a modified ASME Code for Unfired Pressure Vessels which would emphasize balanced requirements to achieve maxi-

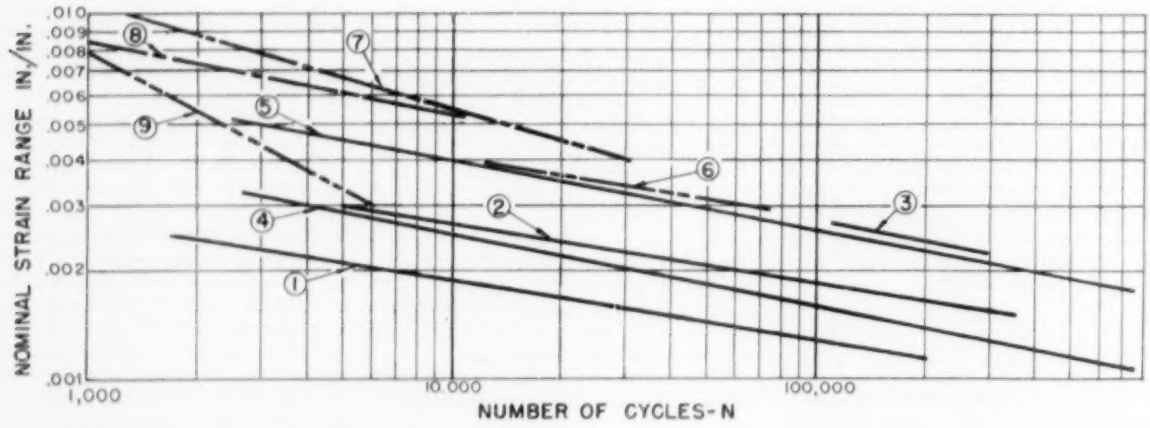

Fig. 2 Comparison of fatigue tests on plate materials with fatigue tests on piping materials

mum economic safety, and which would also provide a broad base for effective utilization of new materials and designs toward satisfying the challenging demands of our widening industrial horizons. It is obviously beyond the capacity of an individual or limited group to appreciate and assess all factors, so that the suggested basic principles which follow are humbly offered as a vehicle for broad examination and agreement. For clarity the presentation is in summary form supported by a tabular comparison (Table 3), and omits repetition of supporting reasoning.

A. General

1. *Philosophy of Code.* The objective would be to establish essential basic principles for the guidance of the user, vessel designer, vessel fabricator, inspector, and enforcement agencies toward accomplishing maximum economic safety for pressure vessels by balanced and flexible requirements for design, materials, fabrication, and inspection, as well as indicating the selection of requirements to suit the specific service hazards and demands of each application.

2. *Format of Code.* The last revision of the ASME Code for Unfired Pressure Vessels (1952) provides a logical arrangement and subdivision, and mandatory and nonmandatory appendixes for the detailed treatment of specialized subjects. It is proposed that the main body of the code be limited to basic principles and requirements, including only those formulas which are common to practically every vessel. More involved or less frequently used detailed requirements would appear in mandatory appendixes. Insofar as practicable code design requirements should avoid arbitrary limitations by stating objectives, parameters, and criteria, without detailed formulas, except for frequently used components. Guidance for solutions can be by reference to accepted textbooks or literature for fundamental and detailed approaches utilizing accepted basic theories.

3. *Responsibilities.* The following clearly recognized responsibilities would be established:

(*a*) Selection of material and material protection (corrosion, deterioration, and impairment by contents): user.

(*b*) Maintenance and operation (in service and design provisions for): user.

(*c*) Establishment of operating requirements (operating temperature, pressure, cycles, and hazards, and the like): user.

(*d*) Establishment of design requirements (design temperature, pressure, cycles, hazards, and the like; selection of vessel class and detailed requirements; and performance of specialized calculations): vessel designer.

(*e*) Detailed design (to establish design requirements): vessel fabricator.

(*f*) Approval of detailed design (formally approved drawings bearing signature of vessel designer to form part of data reports): vessel designer.

(*g*) Fabrication to approved detailed design: vessel fabricator.

(*h*) Materials to specification and free of injurious defects: supplier and vessel fabricator.

(*i*) Inspection and stamping to approved design drawings and to Code: qualified inspector and vessel fabricator.

The inspector would not be expected to verify the entire detailed design, but would have additional responsibilities to perform checks of the design items entered on the data sheet or basic to the vessel class. The user may exercise his responsibilities through a consultant or engineering organization. The vessel designer must be thoroughly acquainted with the process unit or other use for which the vessel is intended, and must be a qualified designer registered with the ASME Boiler Code Committee. The vessel designer may be a consultant, an engineering organization, or a vessel fabricator. The responsibility for establishment of design requirements is distinct and apart from that of detailed design to these requirements. The vessel designer is responsible for both, and the fabricator only for the latter, unless also qualified to and acting as the vessel designer.

B. Service and Loadings

Closer design can be accomplished only with adequate consideration of service and loadings. Repetitive stressing and possible resulting fatigue failure involve all forms of loading, but usually reach a maximum strain range and frequency for thermal effects, such as temperature gradients or restrained thermal expansion which can occur under operating conditions, particularly with relatively minor but rapid changes in pressure and/or temperature.

The influence of service on safety must include evaluation of hazards not only resulting from overpressure, but also overtemperature and other effects, such as explosion, resonance, and dynamic effects (flow and structural), deterioration by nuclear fission products, corrosion, and other impairment of materials and welds, as well as temperature gradients, and thermal expansion. The objectives of this paper do not permit detailed treatment of these aspects of vessel design.

Types of loadings are fairly adequately covered by present code requirements. They can be classified into types and criteria as shown in Table 3.

C. Selection of Vessel Class

The second section of Table 3 summarizes the service, material, and fluid-content limitations of the 3 proposed vessel classes. Class N represents construction as presently provided for in the code for a safety factor of 5. Class G is a more balanced random examined construction which continues the present safety factor of 4. Class C would be a new construction representing an optimum use of materials in view of proportionately controlled materials, design, fabrication, and inspection. Vessels for high-temperature service in the creep range would be placed in Class C or in a separate classification as discussed in Section II.

D. Design

1. *Stress Evaluation.* In keeping with the objective of more accurately assessing performance, it is recommended that the effective stress be evaluated by the shear strain energy theory or the Mises-Hencky criterion of yielding at least for Class C vessels. One of the main advantages of the Mises-Hencky criterion is that it permits the calculation of two functions called the intensity of stress and intensity of strain in a two- or three-dimensional state of stress. The intensity of stress and strain are directly related to quantities measured on a simple tension test. For heavy thickness and/or high temperatures, stress formulas based on the stress distribution which prevails in the plastic state or under steady-state creep conditions can be utilized for temperatures below and within the creep range, respectively. In connection with such more liberal analysis, the authors wish to point out that, from a fatigue-resistance standpoint, it is the strain range per cycle at the critical fiber which determines performance. A measure of

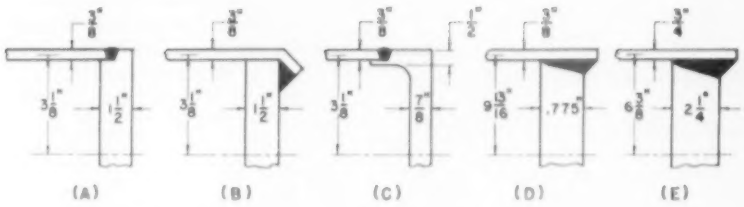

Fig. 3 Details of head tests compared in Table 2

this strain range is most conveniently obtained from elastic stress analysis.

2. *Stress Criteria.* The proposed allowable stresses and allowable stress ranges for long- and short-time loading are given in the third section of Table 3, and must be associated with the safety factor assigned to each vessel class. In general, these are related to the following basic principles:

(*a*) Primary stresses resulting from pressure and sustained external loadings are kept within the basic long- or short-time allowable stress. The direct and bending stresses caused by occasional loadings, such as wind and earthquake, when combined with these primary stresses, are allowed to exceed the basic allowable stress in nominal degree in recognition of their occasional occurrence.

(*b*) Localized stresses are divided into two categories. The localized direct stresses plus the primary stresses are kept within the long- or short-time yield strength. Localized bending stresses plus the primary stresses are limited by the fatigue life of the material for the particular service.

(*c*) Thermal strain loadings, in combination with external loadings, are controlled for long- and short-time conditions to a strain range well within the sum of the cold and hot YS for service below the creep range, and within the sum of the cold YS and the basic hot allowable stress for service in the creep range, similar to the ASA Code for Pressure Piping rules. This is on the basis that yielding or creep relieves the initial stress in the hot condition and establishes a residual stress system of opposite sign in the cold condition. This principle can be applied more broadly to other types of strain loadings or secondary stresses whenever the result of any hot plastic flow is to establish a cold stress of opposite sign; it is merely an application of the strain-range fatigue criterion with consideration of hot and cold material properties.

3. *Cyclic Loadings.* For each class of construction a working fatigue life is associated with the specified design basis, materials quality and extent of inspection.

It is not intended that Class N be used for recognized cyclic service. Classes G and C are shown as limited to 6000 cycles and 80,000 cycles, respectively, unless the working stress range at the maximum stressed areas is reduced similar to the new ASA Code for Pressure Piping rules for piping flexibility (see Table 4).

The basic number of cycles associated with each vessel class in Table 3 have been arrived at by utilizing eq 2 or 3 of Section III for materials likely to be used in each vessel class, and by applying a safety factor of 10 to the number of cycles. Inasmuch as the indications in Section III are that, for the same nominal design basis, this table will not be a constant for materials of different properties, the values used tend to reflect the lowest expected performance. A more precise approach would entail working directly (for each material) with some such criterion—eq 2 or 3.

Table 4—Stress-Range Reduction Factor for Increased Number of Service Cycles

Factor by Which Cycles Are Increased	*Stress-Range Reduction*
1	None
10	0.68
20	0.60
40	0.55

4. *Safety Factors.* The safety factor, as related to the ultimate tensile strength, is the same as used for many years for construction equivalent to vessel Classes G and N. Vessel Class C represents a higher quality level than heretofore defined in the Code, the details of which have been selected to justify a safety factor of 3.

5. *Local Stress Factors.* The values selected and given in Table 3 are justified by the service experience with present similar construction for vessel Classes G and N. For vessel Class C the value selected appears practical and consistent with the details specified.

6. *UTS vs. YS.* Pending the evolution and agreement on a parameter which can be demonstrated as representative of the PVRC and other fatigue-test data when various types of materials are compared under elastic and plastic strain ranges, it is considered advisable to retain the UTS as the basic short-time property on which allowable stresses are based for service temperatures below the creep range with the additional limitation on YS of the present code. It is anticipated that an added parameter for fatigue resistance can be worked out which may bear an approximate relation to the total energy of deformation and which will involve the UTS, YS, and elongation.

E. Materials and Metallurgy

For more economic use of materials, the quality requires definition and assured maintenance by specification provisions as to injurious defects and mandatory examination. The consequence of even very occasional failures resulting from unsatisfactory transition temperature would more than justify any economic means which can assure their avoidance.

Fatigue is an important and revealing property of materials, and research on specimens of sufficient size could contribute valuable guidance as to the most desirable metallurgical condition and the significance of defects. Its further use as a means of quality control deserves consideration.

Corrosion, deterioration, and impairment of materials and welds can have serious effects on the safety of pressure vessels. Instead of limited treatment of inspection and occasional warning flags as to special phenomena, complete treatment of this subject seems essential for reasonable guidance of the user and enforcement agencies.

F. Fabrication

For the vessel class with a proposed safety factor of 3, fabrication requirements deserve careful consideration, particularly with respect to the distortion resulting from welding. This class of construction has been limited to butt welding of nozzles and attachments; also fatigue tests of welds are proposed for consideration. Routine tests of base materials and electrodes would seem desirable because there is no present quality control of these items to assure their continuous suitability.

G. Inspection

The application of available nondestructive means for inspection should be established in accordance with the class, design approach, and service. Whenever less than complete examination can be justified, any partial examination should be directed toward the most critical areas. Specific proposals are included in Table 3.

Glossary

β	= Design stress factor
ϵ	= Strain range imposed per cycle, inch per inch
ϵ_r	= Strain range for failure in 10,000 cycles for polished specimen ($i = 1$), inch per inch
E	= Young's Modulus of Elasticity
°F	= Degrees Fahrenheit
ft-lb	= foot pounds
i	= Strain intensification factor as associated with polished bars
ID	= Inside diameter
n	= Constant for material determined by test
N	= Number of cycles to failure
N_e	= Equivalent number of cycles
N_1, N_n	= Number of cycles
p	= Internal pressure
P_1, P_n	= Pressure
psi	= Pounds per square inch
R	= Shell radius
S_n	= Nominal design membrane stress
SF	= Safety factor
t	= Thickness
TS	= Tensile strength
UTS	= Ultimate tensile strength
YS	= Yield strength

References

1. "Report on the Design of Pressure Vessel Heads," PVRC Design Division, The Welding Journal, 32, Research Suppl., 31-s to 51-s (1953).

2. Bijlaard, P. P., "Stresses from Local Loadings in Cylindrical Pressure Vessels," ASME Paper No. 54-PET-7 (Sept. 1954).
3. Bijlaard, P. P., "Stresses from Radial Loads in Cylindrical Pressure Vessels," ASME Paper No. 54-A-101 (Dec., 1954); THE WELDING JOURNAL, 33 (12), Research Suppl., 615-s–623-s (1954).
4. Bowman, C. E., and Dolan, T. J., "Biaxial Fatigue Properties of Pressure Vessel Steels," *Ibid.*, 32 (11), Research Suppl., 529-s–537-s (1953).
5. Bowman, C. E., and Dolan, T. J., "Studies of the Biaxial Fatigue Properties of Pressure Vessel Steels," *Ibid.*, 34 (1), Research Suppl., 51-s to 59-s (1955).
6. Gross, J. H., Tsang, S., and Stout, R. D., "Factors Affecting Resistance of Pressure Vessel Steels to Repeated Overloading," *Ibid.*, 32 (1), Research Suppl., 23-s to 29-s (1953).
7. Gross, J. H., and Gucer, D. E., and Stout, R. D., "The Plastic Fatigue Strength of Pressure Steels," *Ibid.*, 33 (1), Research Suppl., 31-s to 39-s (1954).
8. Stout, R. D., and Gross, J. H., "Mechanical Properties and Weldability of Six High-Strength Steels Applicable to Pressure Vessels," paper for presentation to a session on pressure vessels during the 20th Midyear Meeting of the American Petroleum Institute's Division of Refining, St. Louis, (May 1955).
9. Markl, A. R. C., "Fatigue Tests of Piping Components," *Trans. Am. Soc. Mech. Engrs.*, 74 (3), 287–303 (1951).
10. Coffin, L. F., Jr., "A Study of Cyclic Thermal Stresses on a Ductile Metal," ASME Paper No. 53-A-76 (Dec. 1953).
11. Coffin, L. F., Jr., "The Problem of Thermal Stress Fatigue in Austenitic Steels at Elevated Temperatures," ASTM Paper No. 100A (June 1954).
12. Gross, Nicol, "Researches on Welding Pressure Vessels and Pipelines," *Brit. Welding J.*, 1 (4), 149 (1954).
13. Mutual Boiler Insurance Co. report (unpublished).
14. Dempsey, F. W., and Lazan, B. J., "Dynamic Creep and Rupture Properties of an Aluminum Alloy under Axial Static and Fatigue Stress," ASTM Paper No. 71 (June 1954) (and additional references listed therein).
15. Robinson, E. L., "Steam Piping Design to Minimize Creep Concentrations," ASME Paper No. 54-A-186 (Dec. 1954).
16. Gross, J. H., and Stout, R. D., "Plastic Fatigue Properties of High-Strength Pressure-Vessel Steels," THE WELDING JOURNAL, 34 (4), Research Suppl., 161-s to 166-s (1955).
17. Harris, L. A., Nordmark, G. E., and Newmark, N. M., "Fatigue Strength of Butt Welds in Structural Steels," *Ibid.*, 34 (2), Research Suppl., 83-s–96-s (1955).
18. Bijlaard, P. P., "Stresses from Radial Loads and External Moments in Cylindrical Pressure Vessels," *Ibid.*, 34 (12), Research Suppl., 608-s to 617-s (1955).

DISCUSSION BY R. W. SCHNEIDER

This paper has been read and studied with a great deal of interest; undoubtedly the authors have presented subject matter on the design of vessels which gives food for thought. This is particularly true for pressure vessels of unusual design or where the present Code is inapplicable. It is evident that a great deal of thought and preparation have gone into the writing of this paper. It would seem, however, that such a presentation would be incomplete without at least a few comments from a representative of the group classified as "qualified inspectors."

In view of the fact that the qualified inspector has been mentioned and his abilities or activities questioned a few objective comments may lead to some clarification of this phase of the over-all picture.

It is generally known that the shop inspector is faced with many problems related to the design and construction of pressure vessels from those of extremely high pressures to those of atmospheric pressure. Under the present Code it is inconceivable that a vessel will be stamped without the design being reviewed in one way or another; otherwise there would be no certainty that the vessel complied with the Code requirements. The Code as it now stands covers vessels up to a maximum allowable working pressure of 3000 psi. The scope of the existing Code is limited when compared with that proposed in the subject paper. Even though the present Code covers a limited pressure range a great many problems continue to arise in the industry. These problems are frequently answered by the ASME Boiler Code Committee by means of interpretations or by placing the responsibility on the qualified inspector to resolve the question. Frequently the latter arrives at an answer by consultation with the designers to make certain that both agree as to the intent of the Code. The present paper does not seem to resolve this situation excepting that in specialized designs the onus of responsibility appears to shift from the inspector to a "qualified designer."

Simplifying the Code to the extent that it will contain only the basic shell and head formulas and by adding an authorized bibliography whereby the designer or inspector may find the answer to a particular question still does not resolve these difficulties. If the latter idea was adopted, interpretations would probably be required to clarify the listed references, unless, of course, the formulas and their application were also included. This would evidently result in the need for an unbiased authority such as the Boiler Code Committee or someone deputized by the committee such as a "qualified inspector."

In the development of the paper considerable stress has been placed on the individual defined as a "qualified vessels designer." It is assumed that this individual will be qualified by passing examinations, experience or by some other yardstick. This is somewhat the same procedure as is used to certify a qualified inspector or for that matter a qualified welder. In the latter case he is subjected to the possibility of being made to reprove his ability by a repeat examination. The qualified inspector is responsible to the various authorities. The question is "who would the qualified designer be responsible to?"

It is recognized in saying this that in an industry such as the authors represent this problem would take care of itself. However, it must be recognized that there are a great number of pressure vessel manufacturers where control inherent in the organization would not apply and who do not confine themselves to the simpler types of vessels. This statement is not intended to belittle the smaller pressure vessel manufacturers with limited engineering facilities and in terms of quantity it is probably this group which manufactures and sells the most pressure vessels.

There are many cases where manufacturers or their designers of both groups have difficulty in interpreting or adhering to the present code which is, in general, simple and rather straightforward.

If, as the authors propose, the secondary stresses are limited to a constant times the primary shell stress the problem of the manufacturers adhering to the new Code will be increased manyfold.

For example, the majority of vessels fabricated will probably fall into the Class G and N category, according to Table III the local stress factor "B" is 3.5 and 6.0, respectively. This then means that local or secondary stresses may be permitted to be as high as 3.5 and 6.0 times the primary shell stress. The question immediately arises how many manufacturers of Class G and N pressure vessels employ designers who are sufficiently versed in stress analysis to evaluate the secondary stresses which exist? It appears that they must be able to evaluate the secondary stresses before a crosscheck can be made of B times Sa which is the permissible secondary stress level.

While Class G and N vessels are "run of the mill" the design calculations are not. The above also applies to the Class C vessel but this is the critical service vessel and as brought out in the paper requires a close check on design and fabrication.

There is one last comment which concerns the foundation upon which the new Code will be built. When the paper was presented in 1955 to a session on pressure vessels during the 20th Mid-

R. W. Schneider is associated with The Travelers Insurance Co., Hartford, Conn.

year Meeting of the American Petroleum Institute's Division of Refining, it was mentioned that the year 1955 seemed an appropriate time to reassess this industry because of tremendous strides made in new-material properties and in evaluating their limitations.

There is one basic point which has always been rather perplexing and questionable, namely, the selection of a working or design stress. The design stress for ferrous materials at room temperature is usually taken as the ultimate strength of the material divided by some factor; this factor being designated as the safety factor. If a design is based on maximum principal stress the pressure at which the vessel will start to yield and the pressure commensurate with rupture bear little if any direct relation to the design stress whereas it appears that the yielding pressure, rupture pressure or any simple fraction of these pressures are more definitive of the true state or condition of the vessel.

This point is mentioned realizing that this will probably be the foundation upon which future Codes are built.

It is encouraging to read this paper and realize the work behind it; it shows that the pressure vessel industry is dynamic and willing to look over the accomplishments of the past with a critical eye and prepare a more realistic design for the future commensurate with present day material and technology.

AUTHORS' REPLY

With regard to Mr. Schneider's first comment on the added responsibility imposed on the inspector by a new code, we heartily agree. Because of this we have suggested an added individual who would assume part of this burden. A "qualified vessel designer" would be a professional man who has been licensed in a similar fashion to "professional engineers." The vessel designer would assume the burden of certifying that the vessel design is proper and in accordance with the code, and therefore free the inspector for the specific task of checking and certifying all facets of the manufacture.

Mr. Schneider has also asked the question as to whom would the vessel designer be responsible. Professional engineers are bound by a set of professional ethics but licensed by each state. We believe that the same procedure would be suitable for governing the qualifications and responsibilities of the vessel designer with vessel drawings carrying the designers seal similar to present practice on structural drawings.

With regard to the complexities of the calculations for evaluating secondary stress, we believe these exist now under the present Code rules. Unfortunately, presently permissible details such as nozzle reinforcements permit extremely high secondary stresses. Our beliefs are that the Code could contain empirical and simplified rules for limiting these stresses for certain commonly used details, but as in all cases of empirical rules, would fit only average cases and can err in either direction for special applications. It would, however, be possible to make more precise calculations of the secondary stresses, and in the case of Class C vessels, these calculations would be mandatory when not suitably provided for by the rules. For vessels in critical service, it seems only reasonable that a thorough investigation of stress concentration be made by competent engineers. Responsible manufacturers do this to a considerable degree even under the present Code rules recognizing that the rules do not adequately cover all aspects.

With regard to the selection of working or design stresses, we have felt that safety factors as related to static loading should be based upon the bursting strength of a vessel. Various rather thorough investigations have shown that the bursting pressure is very closely (though not exactly) dependent upon the ultimate tensile strength. This involves following the material through the elastic range and into the plastic zone. Use of the maximum shear theory or some other yielding criterion such as that of Mises Hencky give different results but never varying by more than 15%.

All vessel services involve some repetitions of loading; the degree varying considerably with different applications. Fatigue, in its broadest sense to include failures under relatively few as well as a large number of cycles, therefore becomes a consideration. Tensile strength has been well proved to yield better correlation with fatigue performance than yield strength but it alone is not adequate; ductility enters in to some degree, particularly for structures where local plastic flow adjustments may be necessary. The allowable stress must be selected to adequately assess all factors for a specific set of design rules, material, inspection and service requirements.

Welding Research Council Bulletin No. 31

Stainless Steel for Pressure Vessels

by A. Grodner, Alloy Fabricators Division, Continental Copper and Steel Industries, Inc.

An interpretive report prepared for the Materials Division of the Pressure Vessel Research Committee, discusses chemical composition, mechanical and metallurgical properties and fabrication characteristics of wrought and cast stainless steels used for pressure vessel construction.

This Bulletin is priced at $1.00 a copy. Copies may be ordered from the American Welding Society, 33 Wes 39th Street, New York, 18, N.Y.

METAL FINISH SEAM WELDING

Considerable similarity found between the schedules for mash seam welding and finish seam welding. It is also demonstrated that, with proper conditions, a good finish surface can be consistently maintained on one side of sheets

BY W. J. ALLEN AND M. L. BEGEMAN

Introduction

The increased use of metal products which are normally viewed from one side only, has stimulated interest in a variation of the conventional mash seam welding operation. This variation, which will be called metal finish seam welding, is illustrated in Fig. 1 below the other basic seam welding processes. The lap and mash seam welds differ because of the amount of forging action used or, as the name implies, mash down. The lap weld has practically no mash down as shown in the top drawing, while the thickness of the mash seam weld, by means of increased electrode force and reduced sheet overlap, approaches that of a single sheet thickness. The bottom sketch schematically describes the variation which is known as a metal finish seam weld, in which mash down occurs on one side only.

From the figure it appears that mash seam welding results in a smooth flat surface on both sides of the weld. This is true only if the major variables involved (current, pressure, speed and overlap) can be held in proper balance and control. For example, the overlap tolerance is quite critical in mash seam welding and, if not held closely, surface defects will develop.

The purpose of this investigation was to compare mash and finish seam welding, to determine the principal variables of metal finish seam welding, and to establish whether or not a smooth surface on one side of a weld could be maintained consistently.

Equipment and Materials

The test welds of this investigation were produced on a 250-kva circular seam welder equipped with an electronic control unit. Electrodes were 10 in. in diameter, $\frac{1}{2}$ in. thick and made from RWMA Class III forged copper alloy. Initially, the full face widths of the contoured and finish electrodes were used, but edge marring of the finish side of the weld resulted. The face width of the upper electrode was reduced to $\frac{3}{8}$ in. prior to contouring and no further edge marring was noted.

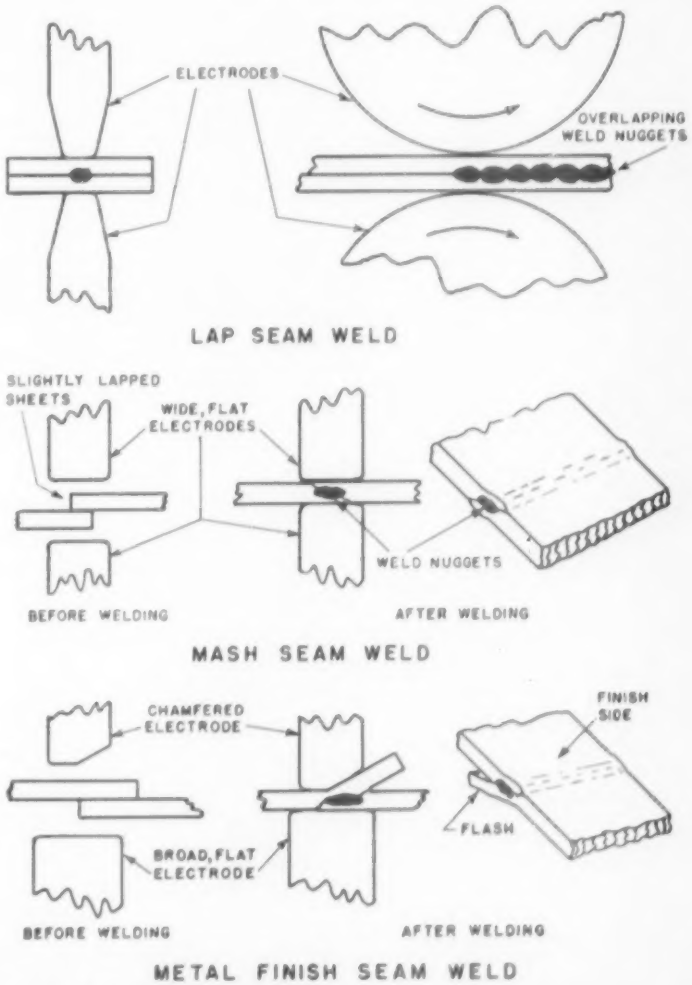

Fig. 1 Types of seam welds

W. J. Allen is Graduate Student, RWMA Fellowship, and M. L. Begeman is Professor, Mechanical Engineering, The University of Texas, Austin, Tex.

Presented at 1956 AWS National Fall Meeting in Cleveland, Ohio, October 8–12.

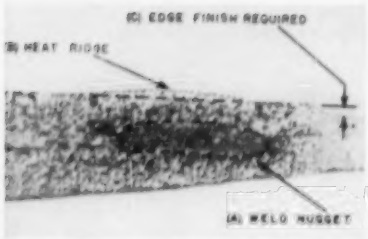

Fig. 2 Terms used on metal finish seam welds

The contours consisted of a $^3/_{16}$-in. flat blended into the desired angle chamfers. The lower electrode, which was used as the finish wheel, was driven by a roller-chain arrangement and the contoured electrode operated as an idler. Water flood cooling was used on the surfaces of the weldments. An adjustable guide bar was mounted in the throat of the welder to provide a means of accurately positioning the weldments under the electrodes and to guide the work through the machine. A calibrated current transformer-ammeter circuit measured the welding current, and the electrode force was measured with an electrode force gage.

The material used was 0.031 in. thick, low-carbon, pickled and oiled, hot-rolled rimmed steel, commonly designated as SAE 1010. An analysis of this steel showed it to contain 0.08% carbon, 0.39% manganese, 0.008% phosphorus and 0.029% sulfur. It was the same thickness and analysis as previously used in an investigation of mash seam welding.

Welding Variables

Two of the principal welding variables associated with a resistance welding process are the current magnitude in the welding circuit and the electrode force. The heat generated by electrical current passing through a constant resistance is proportional to the current magnitude squared, while a constant current passing through a variable resistance will produce heat directly proportional to the magnitude of the resistance. In resistance welding, when working with relatively large currents, a change in current magnitude produces larger heat variations than can be obtained with possible resistance changes in the joint.

In making a two-thickness resistance weld there are seven resistances in series. Two are in the upper and lower electrodes, but have no influence in producing heat at the weld area. Two others are between the upper and lower electrodes and the sheets they contact. Heat generated here is largely dissipated by the cooled electrodes and the flooding of the sheets. The weldment materials provide two more resistances, and the contact resistance between the weldments is the last and most important one. Resistances of a contact nature are subject to change by those factors which may alter the degree of contact. For example, as the electrode force is increased a more intimate contact is made. This causes a decrease in the resistance and results in less heat being generated.

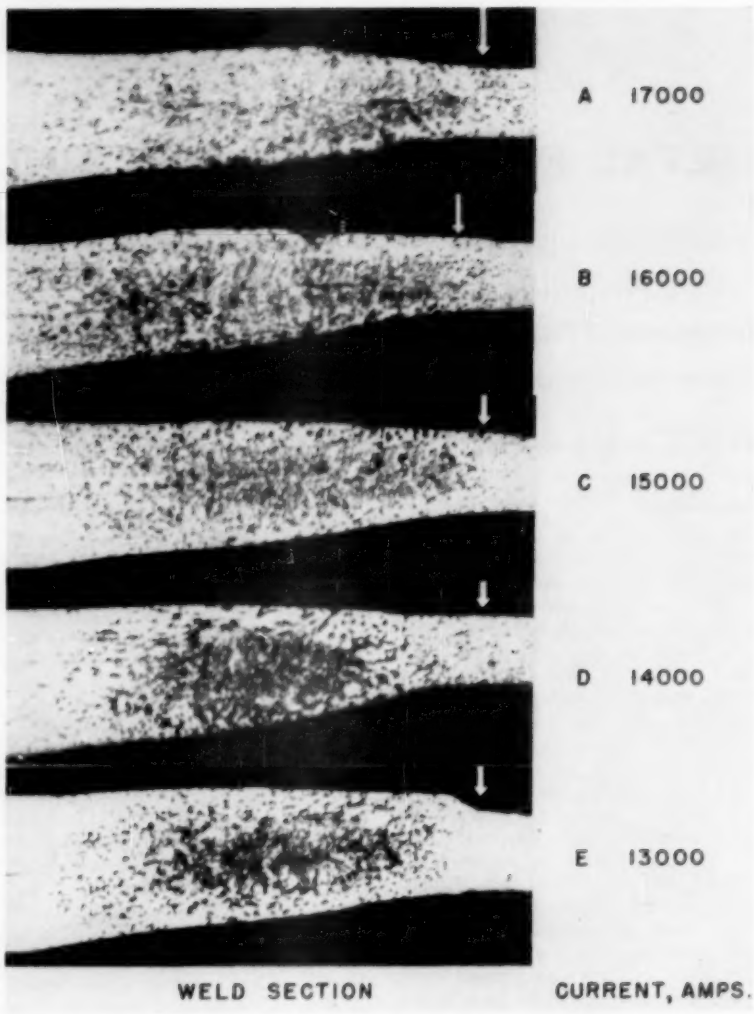

Fig. 3 Effect of current on microstructure of metal finish seam welds
Electrode force 900 lb, speed 140 ipm, contour 7 deg, overlap $^1/_4$ in. X 20. (Reduced by $^1/_4$ upon reproduction.)

Both mash and metal finish seams are produced by welding processes which involve hot-forming. In both cases, the joint thickness and shape are changed considerably while the metal is in a plastic state. The variables involved in the former operation are electrode pressure and initial sheet overlap. As the overlap increases, the volume of metal that must be redistributed increases, which, to a degree, governs the minimum electrode force. The electrode force, in turn, affects both the joint thickness and the contact resistance between the sheets.

Whereas the initial sheet overlap of the mash seam process determines the amount of metal to be redistributed, the position of the weldments under the electrodes determines this volume in the finish seam process. The lower left drawing of Fig. 1 shows that as the lower sheet is removed from under the flat portion of the contoured electrode, there is less material to be mashed down. Also, the use of the contoured electrode has the effect of reducing the electrode pressure in the relieved area and increasing it in the contact zone. This, in turn, brings about changes in the heat zone due to variation in the contact resistance between the sheets. Therefore, position of weldments and angle of contour shall be considered as variables peculiar only to the finish seam process.

The time associated variables are related to both the mash and finish

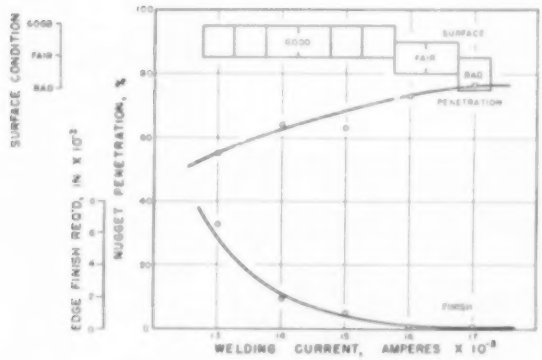

Fig. 4 Effect of current on penetration and surface finish of metal finish seam welds

Electrode force 900 lb, speed 140 ipm, contour 7 deg and overlap 1/4 in.

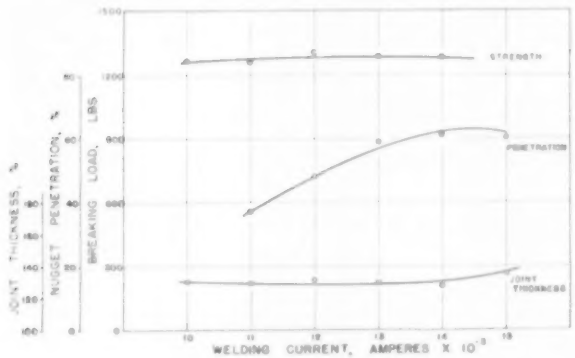

Fig. 5 Mash seam weld characteristics as a function of current

Electrode force 900 lb, speed 130 ipm and initial overlap, 150%

operations and may cause wide variations in the items mentioned above. The factors which normally determine the welding speed are the ability to handle the work in the machine, electrode pickup, and surface condition desired of the weld. The use of continuous current in producing both type welds is recommended.

Procedure

1. All test material was wire brushed, washed with solvent, and lightly oiled prior to spot tacking in an effort to attain a relatively constant contact resistance throughout all tests. The test pieces were then lightly spot tacked to maintain the desired overlap.

2. A welding speed of 140 ipm was selected for all tests. This was the approximate speed used on previously conducted mash seam weld tests.

3. The contour chamfer range on the upper electrode was arbitrarily set from 0 to 10 deg. The values selected for study were 3, 7 and 10 deg.

4. Using a 10-deg contour electrode, a number of current and pressure combinations were run at random to preselect the most satisfactory range for investigation. Surface finish was the principal factor influencing the selection.

5. A detailed investigation was made next to determine the combination of electrode force and current magnitude that would produce the most satisfactory weld, based on surface finish and metallurgical analysis. Welds were made at various electrode forces and with the current varying over a wide range of values. In all cases, the overlap was held at 1/4 in. These welds were then subjected to metallurgical examination and spot physical tests. This procedure was then repeated for the 7- and 3-deg contours and the combined results used in selecting the most favorable force, current and contour combinations.

6. The effects of varying overlap and position of weldments under the electrodes were studied using the above selections. These specimens were subsequently subjected to metallurgical investigation.

Results

The curves and illustrations which follow indicate a range of the principal variables which should produce satisfactory finish seam welds. A comparison between mash and seam welding is also presented so that the two processes may be evaluated.

Metallurgical evaluation of mash seam welds is primarily based on nugget penetration, which is normally defined as the ratio of the thickness of the area exhibiting a columnar dendritic structure to the thickness of the joint. The macrograph of a metal finish weld (cross section) in Fig. 2 shows that this joint thickness varies from a single sheet thickness to twice that value. Nugget penetration for this case will then be defined as the ratio of the nugget thickness to the thickness of the joint at the center of the columnar dendritic structure of the nugget.

The surface quality of metal finish welds in this investigation was gaged on the basis of surface heat effects and edge finish required. The heat effects are rated *good*, *fair* and *bad*, and edge finish is the incomplete mash down at the sheet edge on the finish side. The quantity C of Fig. 2 is representative of incomplete edge mash down.

Effect of Welding Current

Figure 3 shows a series of micrographs of finish seam welds in which the welding current was varied while all other variables were held constant. (The pointer at the right end of each sample indicates the finish side.) The effect of too much heat is shown in Weld A where a void may be seen to the right of the nugget. Voids of this type result from insufficient cooling of the molten metal before the electrode force is removed. This weld also has a definite heat ridge on the surface and there was some electrode pickup. Weld B was made with the current reduced 1000 amp but a small void is present and there is still evidence of surface heat defects. The reduction of welding current to 15,000 amp was sufficient to eliminate the surface defects as shown in Weld C and maintain enough heat to give good penetration. Welds D and E show that with further current reductions, penetration decreases and insufficient heat is generated to give adequate mash down.

The characteristics of the welds of Fig. 3 are shown plotted as a function of current in Fig. 4, and the general condition of the weld surface is indicated. This is important information since surface burning and heat ridges are as much a problem as inadequate mash down. As may be expected, no serious heat effects are encountered until maximum penetration is approached. The heat ridges formed in the fair range could be tolerated in some applications, but at 17,000 amp electrode pickup occurs with some regularity. As seen in the micrographs, the heat-effected zone is sufficiently large at the higher values of current to give complete edge mash down. The edge finish rises sharply as penetration begins to drop and will finally reach the value obtained by cold forging at the given electrode force.

The characteristics of mash seam welds are shown in Fig. 5*. The penetration curve has the same general shape as that in Fig. 4 but has a lower

* This figure taken from "Electrical and Metallurgical Characteristics of Mash Seam Welds," by E. J. Funk and M. L. Begeman. THE WELDING JOURNAL, 35 (6), Research Suppl., 265-s to 274-s (1956).

maximum value. This is due principally to the higher current densities required in finish seam welding for a given electrode force. The joint thickness curves for mash seam welds has a slight concave shape over the current range tested and, at low currents, shows some similarity to the finish curve of Fig. 4. The metal finish seam process appears to be more affected by a current reduction than the mash seam process. The joint thickness increase at maximum penetration is due to surface heat ridges. Increasing the heat beyond the point of maximum penetration results in low quality surface conditions. An investigation of the strength of metal finish seam welds was not made for formal presentation, but spot checks showed that the strength curve of Fig. 5 could be reproduced in the corresponding penetration ranges of the metal finish process.

Comparison of Electrode Force Effects

The micrographs of Fig. 6 show the results of electrode force variation with all other variables held constant. Maximum penetration is obtained at the low values of electrode force, and decreases as the electrode force rises. Little or no penetration is apparent in Weld E, as the joint has been made by solid phase bonding. The temperature of the joint metal was above the transformation line, but below the liquid line on the iron-phase diagram. Even though enough grain growth takes place in this temperature range to produce a welded joint, a columnar dendritic nugget structure will not be produced unless the joint metal is molten. Welds having consistent strength are obtained only when conditions are regulated to produce a weld nugget.

The relation of welding circuit resistance and electrode force is illustrated by the micrographs of Fig. 6. In each case, the electrode force was great enough to provide good electrode contact. This is shown by the lack of serious heat zones at the surfaces of the specimens. The electrode force variation shows up most in the heat generated at the interface of the weldments. Welds A and B indicate that the interface resistances were high and a maximum amount of heat was generated by the welding current. The increases of electrode force in Welds C and D had forced the weldments into closer contact, which reduced the circuit resistance and the heat generated. The electrode force of Weld E had reduced the resistance of the welding circuit to a point that, with the same current flowing, inadequate heat was generated for the joint metal to reach the molten state.

It may be noted that, in all welds shown, the heat and force combinations were capable of complete edge mash down. Figure 7 is a plot of the penetration and surface conditions of these welds as a function of electrode force. Figure 8 is a similar plot for mash seam welds. The penetration curves show a distinct similarity and a comparison of joint thickness, and the surface condition reveals that the increase in joint thickness corresponds with bad surface conditions. Both were due to heat ridges on the joint surface. The strength curve was included to show

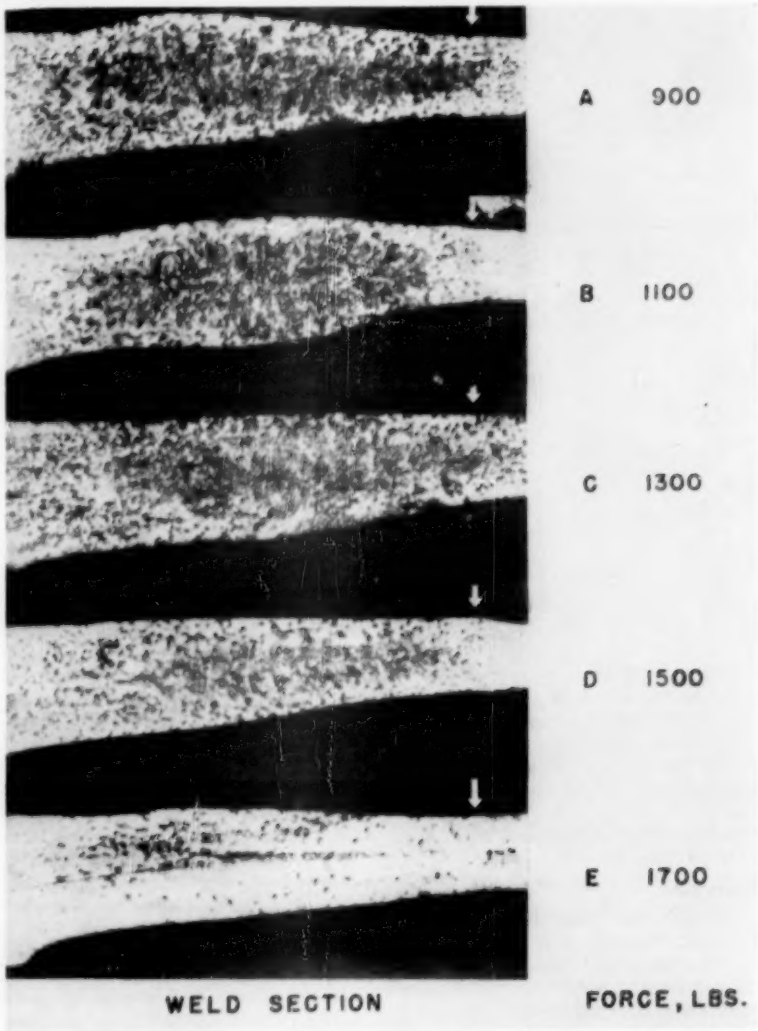

Fig. 6 Micrographs showing results of electrode force variation on metal finish seam welds

Welding current 15,000 amp, speed 140 ipm, contour 7 deg, overlap 1/4 in. X 20. (Reduced by 1/3 upon reproduction.)

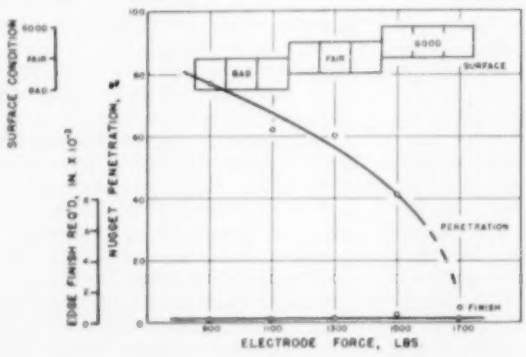

Fig. 7 Influence of electrode force on penetration and surface conditions of metal finish seam welds

Welding current 15,000 amp, speed 140 ipm, contour 7 deg, and overlap 1/4 in.

that little or no penetration is accompanied by a rapid reduction in strength.

Effect of Initial Overlap

The micrographs of Fig. 9 show the effect of varying the amount of overlap of the weldments in the finish seam process. It may be seen that overlap has little effect on the weld structure until the degree of overlap is reduced to approximately 200% of initial sheet thickness. Further reduction results in reduced penetration. As in the mash seam process, this is due to the high current density in the interface contact area. Current densities of these magnitudes cause rapid heating of the weldments and equally fast mash down. A premature mash down results in a lowered current density and an improved heat dissipation, due to increased electrode contact area which, in turn, reduces the heating effect of the weld zone.

Figure 10* is a plot of the characteristics of mash seam welds with varying initial overlap. It may be seen that as overlap increases, the final joint thickness increases. If a smooth surface is required in joining the two sheets, the final joint thickness should be maintained at approximately 120%, or less, as shown by Fig. 10. One of the most difficult operations of production mash seam welding is maintaining this close tolerance on initial overlap. If a smooth surface is required on one side only, a comparison of the results of Figs. 9 and 10 indicate that the metal finish operation permits wide variations of initial overlap in producing consistent quality welds. This is the major advantage of the finish seam process.

Position of Weldments Between Electrodes

The series of micrographs shown in Fig. 11 indicate the effect of varying the position of weldments between the electrodes with other variables held constant. The figures at the side indicates how far the lower sheet edge is to the right of the upper electrode edge. This variation has two major effects. First, as the sheet edge on the finish wheel is moved from the left side to the contoured edge of upper electrode, the amount of finish required on the welded joint is reduced. Second, with this same movement of the weldments, the penetration increases to a point and then rapidly drops off. The increase of penetration is due to the increased current density, through the interface contact area, subjected to the greatest electrode force. As the weldments are moved from under the flat portion of the contoured electrode, this high electrode pressure area is reduced until a maximum amount of heat is generated in the weld zone. Movement of the weldments beyond this point results in the rapid reduction of penetration. This reduction is apparently due to premature deformation, better heat dissipation, and current shunting effects. Maximum penetration is obtained just prior to moving the edge of the bottom sheet into the contoured area. It may be assumed then that further movement causes sufficient deformation of the joint to allow current shunting in the flat area of the contoured electrode.

Weld characteristics influenced by this variation are shown in Fig. 12. It may be seen from the plotted results that the position of the weldments is critical in obtaining adequate mash down and penetration. The finish required is not at a suitably low value until the penetration reaches its critical range. Satisfactory penetration is obtained over a relatively wide range indicating that the position of the weldments may be determined principally by the amount of mash down desired. In obtaining optimum mash down, however, the range is limited to $^1/_{32}$ in. centered on the point of maximum penetration.

Effect of Electrode Contour

The smaller contour angles of the upper electrode influence the amount of heat generated in the weld zone appreciably. A serious heat balance problem exists when using contours of less than 5 deg. The heat-affected zones shift closer to the finish surface and, when sufficient current is used to obtain the desired penetration, overheating near this surface results in heat ridges. For contour angles greater than 5 deg, however, there was relatively little effect noted. During this investigation, quality welds were more consistently obtained using the 7-deg contour than with the 10-deg contour but the margin was so small that under

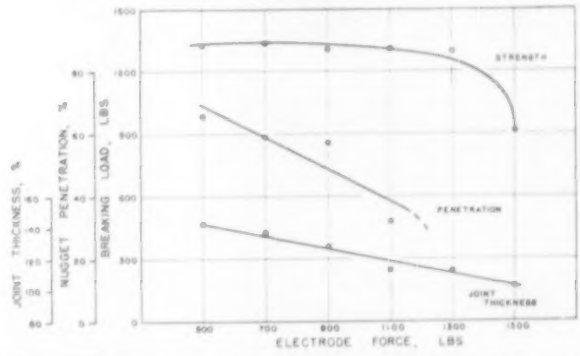

Fig. 8 The effect of electrode force on mash seam welds

Welding current 13,000 amp, speed 130 ipm and initial overlap 150%

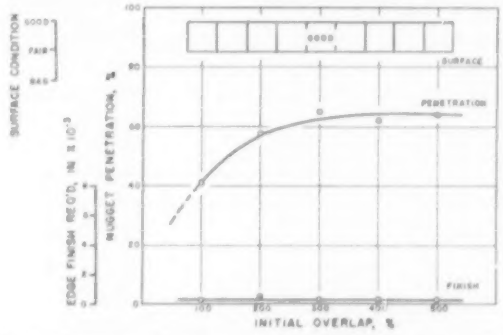

Fig. 9 The effect of overlap on penetration and surface conditions of metal finish seam welds

Electrode force 1300 lb, current 15,000 amp, speed 140 ipm and contour 7 deg

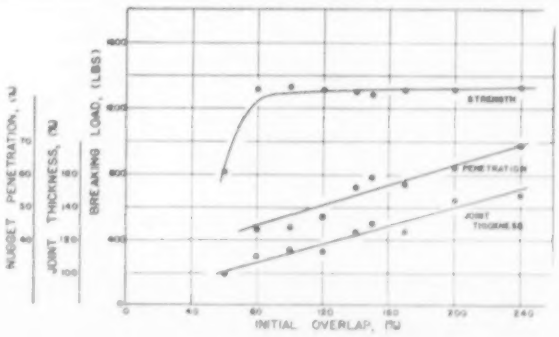

Fig. 10 The effect of initial overlap on mash seam welds

Electrode force 900 lb, current 13,000 amp and welding speed 130 ipm

* This figure taken from "Electrical and Metallurgical Characteristics of Mash Seam Welds," by E. J. Funk and M. L. Begeman, THE WELDING JOURNAL, 35 (6), Research Suppl., 265-s to 274-s (1956).

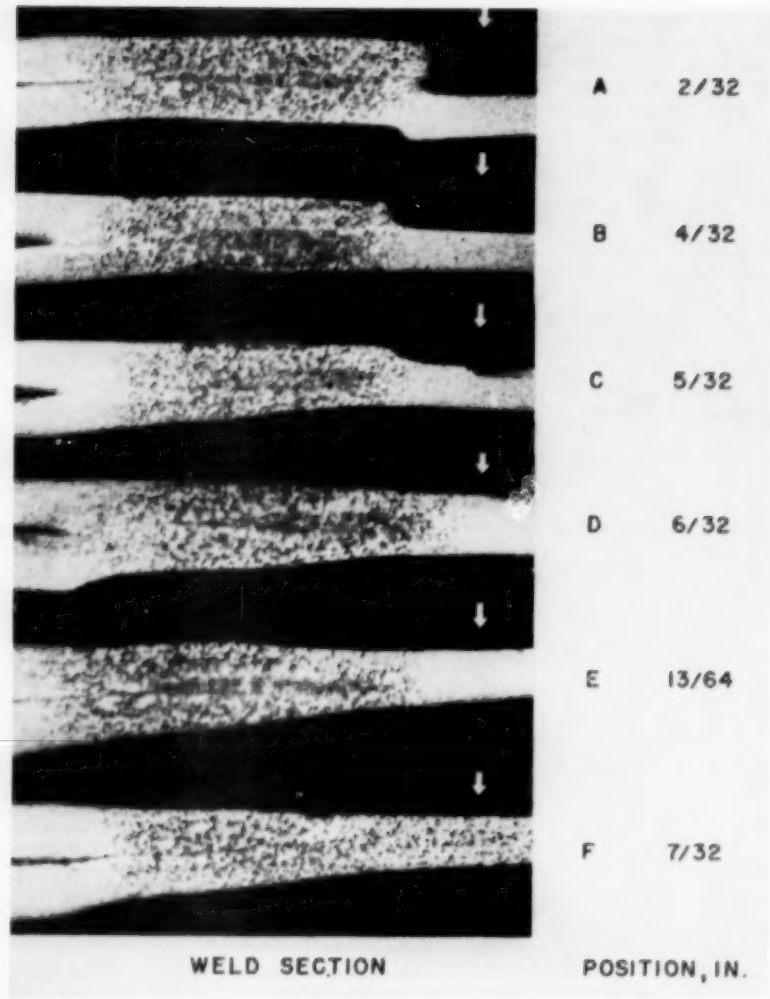

Fig. 11 Effect of position of weldments between electrodes on microstructure of metal finish seam welds

Force 1300 lb, current 15,000 amp, speed 140 ipm, contour 7 deg. X 12. (Reduced by 1/2 upon reproduction.)

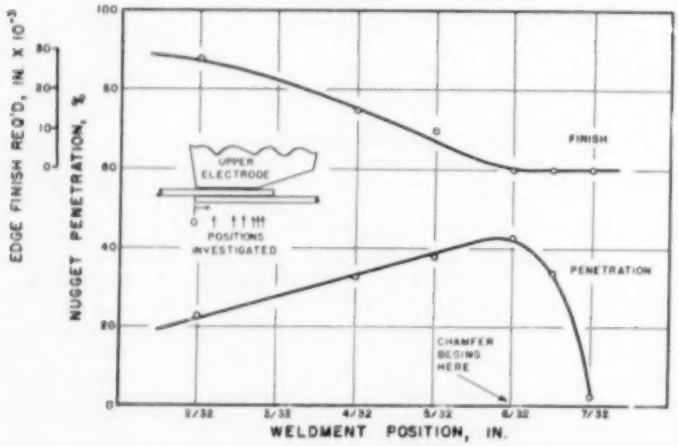

Fig. 12 Effect of lower sheet position on penetration and surface condition of metal finish seam welds

Electrode force 1300 lb, current 15,000 amp, speed 140 ipm and contour 7 deg

slightly altered circumstances this characteristic could be reversed.

The difficulty encountered with the smaller angles resulted primarily from the changes of pressure distribution. As the contour angle was reduced, the electrode force was distributed more evenly over a larger area. Since a portion of this area is not normally affected by the larger contour angles until after the initial deformation of the weldments, the smaller angles require larger electrode pressures. This, in turn, results in lower contact resistances and the requirement of higher welding currents to obtain sufficient penetration. Equally important is the fact that reduction of the contour angle effectively increases the volume of metal to be redistributed by deformation. This also requires the increase in electrode force to obtain adequate mash down. The determination of the action most responsible for the disturbed heat balance was not considered important in this investigation, since welds of good quality could not be obtained over any suitable ranges with contours less than 5 deg.

Conclusions

The following conclusions appear to be justified by the comparative analysis of the metal finish and mash seam welding processes and the examination of process characteristics peculiar only to metal finish seam welds presented in this report:

1. The welding current and electrode force variations under relatively similar conditions for each process result in like characteristics. Slightly higher currents and electrode forces are required by the metal finish process to obtain desired surface finish and penetration. The use of continuous current in producing both types of welds is recommended.

2. The initial sheet overlap must be held to close tolerance in the mash seam process to produce consistently good weld surfaces, but overlap has little effect on the resulting surface of the metal finish seam welds. This appears to be one of the basic advantages of the latter process.

3. The location of the edge of the sheet next to the finish electrode, relative to the contoured electrode, must be held to a tolerance of approximately $\pm 1/64$ in. for metal finish seam welding 0.031 in. low-carbon steel sheet. This would preclude indexing of the work for longer electrode life and would require some form of electrode dressing. The location of the work in the mash seam process has little effect on the quality of weld or surface finish.

4. The electrode contour angle has little effect on weld characteristics for values over 5 deg. Below 5 deg the pressure areas in the weld zone are

significantly changed and the heat balance, required to produce suitable penetration without surface heat effects, is upset.

5. To produce satisfactory metal finish seam welds, using 0.031 in. low-carbon steel (electrode contoured as shown in Fig. 13), the lower sheet should be held just to the left of the electrode center line, the current range from 14,000 to 15,000 amp, the welding speed 140 ipm, and the electrode force at 1300 lb. A micrograph of such a weld is shown in Fig. 6.

In conclusion it can be stated that there is considerable similarity between the schedules for mash seam welding and finish seam welding. Overlap is more critical in mash seam welding while position of the sheets between the electrodes is important in finish seam welding. Both current and electrode force are greater in finish seam welding. The tests demonstrated that a good surface finish could be consistently maintained on one side of the sheets with the proper welding schedule.

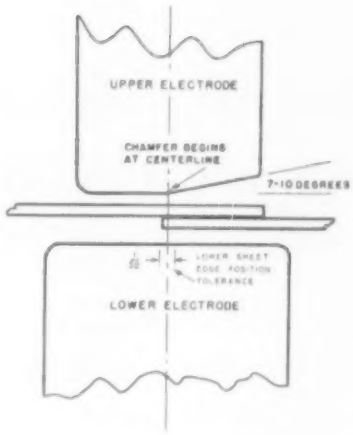

Fig. 13 Recommended circular electrode contour and weldment position for metal finish seam welding of 0.031 low-carbon steel

Acknowledgment

The authors extend their appreciation to the Resistance Welder Manufacturers Association and to the Welding Research Council for sponsoring this investigation. Also, they wish to thank the United States Steel Corp. for supplying the sheet steel, and P. R. Mallory and Co., Inc., for supplying the needed electrodes.

RESEARCH NEWS

New Electron Microscope Announced

A new 100-Kv electron microscope (Type EM-100B) with many operating features including a hinged objective lens for quick change or cleaning of pole inserts, magnetic compensator, objective diaphragm with multiple apertures, and insert screen with binoculars for ultra-thin specimens, has been announced by the Instrument Division, North American Philips Co., Inc., 750 S. Fulton Ave., Mount Vernon, N. Y.

Guaranteed resolving power of the new instrument is better than 20 A. High resolution pole pieces permit continuously variable magnification from the control panel through a range of 5000 to 100,000 diameters. With diffraction pole pieces, the instrument magnifications are 1750 to 35,000 diameters. Camera equipment extends the upper magnification limit to 200,000. Operating magnification level is indicated directly on a panel meter.

For complete details write directly to manufacturer at above address.

X-ray Diffraction Brochure Available

"X-Ray Diffraction for Research, Production Control . . . and Profit!" is the title of a new 4-page brochure released by General Electric's X-ray Department, Milwaukee, Wis.

Discussed are basic theory (Bragg's Law), definitions, analytical advantages and applications in metallurgy, chemistry, mineralogy, physiology, pathology and biology. Included are typical patterns of fundamental methods of crystal study—Laue, rotating crystal and powder method.

Two X-ray diffraction units are illustrated to describe the "building block" principle for acquiring the G-E X-ray diffraction unit desired.

Write directly to company for your copy.

Symposium on Impact Testing

ASTM Special Technical Publication No. 176, 170 pages, heavy paper cover, 6 x 9. In the past few years, engineers and technologists have had increasing interest in the effect of impact and shock on various materials. Both on a theoretical and practical basis, investigations have pushed forward new thinking about impact testing not confined to notch-bar testing.

This symposium, sponsored by Committee E-1 on Methods of Testing, tries to fulfill the larger needs of this area of testing by including papers discussing impact and shock tests for parts, components and complete structures. Five additional papers considered timely and appropriate to the subject are included along with the material presented through the symposium.

Such innovations as the impact tube are discussed and environmental conditions, particularly temperature, are considered. The broad outlook is taken, so as to enhance the practical application of this type of work. The book which contains many graphs, charts and photographs, also contains several bibliographies.

Among the papers included in the symposium are:

Notched-Bar Testing—Theory and Practice—S. L. Hoyt

Transition Behavior in V-Notch

(Continued on page 615-s)

FURTHER STUDIES ON THE EFFECT OF MICROSTRUCTURE ON NOTCH TOUGHNESS AND FRACTURE MORPHOLOGY

Investigation undertaken to determine the influence of some types of discontinuous phases in a nominally constant ferrite matrix on the notch toughness of the aggregate

BY J. C. DANKO, J. H. GROSS AND R. D. STOUT

Introduction

Improvements in design, workmanship and steels have notably reduced the number of brittle failures in welded steels. However, full advantage has not been taken of the improvement obtainable from a proper control of steel composition and heat treatment due at least in part to a lack of understanding of the factors controlling notch toughness. Nominally similar heats of steel exhibit unexplainably large variations in notch toughness, not only as base plate but especially in the welded condition. Many investigators have attempted to correlate notch toughness with microstructural variations. The importance of certain microstructural variables such as ferrite grain size has been established. However, the quantitative influence of all of the important variables has not been determined. Even less is known of the interplay of microstructural variables such as those introduced by welding.

In continuing investigations[1-5] the authors have attempted to determine the effect of microstructural variables on notch toughness. The variation in austenitic grain size, pearlite spacing, and type of pearlite as well as the micromechanism of deformation was investigated in a plain-carbon eutectoid steel. It was observed that notch toughness was reduced with increasing austenitic grain size and decreased pearlite spacing. It was further noted that the mechanism of deformation was a kinking process rather than the usual slip mechanism. Microcracking, that led to ultimate failure, was noted to originate in the kink bands. The kink bands decreased in width with decreasing pearlite spacing and caused cracking at lesser amounts of deformation. This behavior supported the observed decrease in notch toughness with decreased pearlite spacing.

In order to evaluate the effect of complex microstructures produced in weldments, a hypo-eutectoid steel was investigated. Conventional heat treatments producing pearlite of decreasing spacings introduced variations in the ferrite grain size, quantity of pro-eutectoid ferrite, size of pearlite colonies, and carbon content of pearlite. Thus the controlling variables were not properly established. The individual effect of pearlite structure was isolated by annealing the specimen to precipitate all the pro-eutectoid ferrite and produce pearlite containing the equilibrium 0.80% C. Variations in the pearlite were then produced by reheating just above the lower critical and austenitizing only the pearlitic regions. Cooling in various ways to produce differing pearlites in a relatively unchanged ferrite matrix resulted in a negligible variation in notch toughness. Variation in notch toughness was obtained only when the annealing temperature was changed and could be explained in terms of the resulting ferrite grain size changes. This observation was substantiated by examination of the origin and growth of the micro-cracks initiating failure. In general, these microcracks were associated with the ferrite phase and tended strongly to originate at ferrite grain boundaries and at or near ferrite-pearlite interfaces. Moreover, the propagating cracks tended to avoid the discontinuous pearlite phase and secondary cracks were often arrested upon reaching the pearlite areas. Samples deformed in compression resulted in a relatively slight increase in the microhardness of the pearlite compared to the ferrite, indicating only a minor participation of the pearlite phase in the deformation process. These results explain the negligible influence of pearlite spacing on the notch toughness of hypo-eutectoid steels.

The previous investigations were concerned with variations of a lamellar pearlitic phase in a nominally constant ferrite matrix. The present investigation was undertaken to determine the influence of other types of discontinuous phases in a similar ferrite matrix on the notch toughness of the aggregate.

Experimental Procedure

Heat treatment techniques were devised to produce three basic types of microstructures on a C1030 steel of the following analysis: C 0.32%, Mn 0.61%, P 0.016%, S 0.029% and Si 0.18%. The three types were (*a*) pro-eutectoid ferrite and martensite, (*b*) martensite and (*c*) pearlite with a minimum of free ferrite.

All specimens were initially heated to 2000° F to provide a uniform austenitic grain size. For the type (*a*) structures, seven series (Series D2 to D8 in Table 1) of specimens were annealed from the 2000° F temperature, reheated to 1350° F and brine quenched, and Series D3 to D8 were tempered at one of several temperatures to obtain tempered martensite in a pro-eutectoid ferrite matrix. One of the tempering temperatures was chosen to match the microhardness of the martensite to that of the pearlite in a previous series of ferrite and pearlite. By tempering in lead at 1300° F for 1 hr, Series D8 developed a martensite hardness of 227 VHN compared to a pearlite hardness of 214 VHN in Series D1. See Table 1. For the type (*b*) structures, four series (Series D9 to D12) were brine quenched directly from 2000° F, resulting in completely martensitic structures. Series D10 to D12 were then

J. C. Danko, J. H. Gross and R. D. Stout are associated with the Department of Metallurgy, Lehigh University, Bethlehem, Pa.

Presented at the 1956 AWS National Fall Meeting in Cleveland, Ohio, October 8–12.

Table 1—Summary of Heat Treatments, Microstructural Characteristics and Mechanical Properties of C1030 Steel

Series	Heat treatment	Microstructural analysis: Ferrite %	Ferrite Microhardness, VHN	Ferrite Grain size	Pearlite %	Pearlite Microhardness, VHN	Pearlite Aggregate size	Martensite %	Martensite Microhardness, VHN	Martensite Aggregate size	Transition temperature, °F: 10 ft-lb	15 ft-lb	50% fibrous fracture	Tensile properties: Yield strength, kips	Tensile strength, kips	Elongation, %	Reduction of area, %
D1	Annealed 2000° F, aust. 1350° F, transf. 1270° F—4 hr, B. Q.	59.3	150	6.3	44.6	214	5.9				+75	+90	+210	37.6	71.2	33.3	62.4
D2	Annealed 2000° F, aust. 1350° F, brine quenched	55.2	170	5.7				46.4	780	5.5	+340*	+340*	+350	82.8	137.6	2.4	6.6
D3	Annealed 2000° F, aust. 1350° F, B. Q., temp. 400° F—10 min, B. Q.	58.2	126	5.8				45.1	752	5.6	+320*	+320*	+335	70.2	141.8	2.2	4.4
D4	Annealed 2000° F, aust. 1350° F, B. Q., temp. 700° F—10 min, B. Q.	54.2	117	6.0				49.9	460	5.6	+85	+135	+160	53.5	109.0	9.8	22.9
D5	Annealed 2000° F, aust. 1350° F, B. Q., temp. 1000° F—10 min, B. Q.	56.3	114	6.8				48.6	325	6.2	−55	−25	+25	55.6	96.6	17.7	39.2
D6	Annealed 2000° F, aust. 1350° F, B. Q., temp. 1150° F—10 min, B. Q.	50.6	135	6.2				49.2	306	5.4	−50	−35	+30	52.6	84.4	23.7	57.2
D7	Annealed 2000° F, aust. 1350° F, B. Q., temp. 1300° F—10 min, B. Q.	53.3	137	6.6				50.0	236	5.4	−5	+15	+55	50.6	77.7	27.9	64.0
D8	Annealed 2000° F, aust. 1350° F, B. Q., temp. 1300° F—1 hr, B. Q.	54.4	138	7.2				48.0	227	6.4	0	+20	+80	55.0	76.6	33.2	67.6
D9	Aust. 2000° F, brine quenched										+90	+90	+90	184.0	252.0	3.2	1.6
D10	Aust. 2000° F, brine quenched, temp. 700° F—10 min, B. Q.										−130	−100	−15	158.3	170.9	11.5	37.1
D11	Aust. 2000° F, brine quenched, temp. 1300° F—10 min, B. Q.										−170	−145	−70	74.0	93.4	24.6	71.3
D12	Aust. 2000° F, brine quenched, temp. 1300° F—8 hr, B. Q.										−85	−70	−10	53.0	76.5	30.6	75.5
D13	Aust. 2000° F, quenched in salt at 400° F, B. Q.										−45	−25	+215	77.4	115.3	17.8	60.3

* Energy values failed to attain 10 ft-lb in fully ductile condition (100% fibrous fracture). Values reported represent mid-point in energy curve.

tempered to various strength levels. For the type (c) microstructure, one series (Series D13) was quenched from 2000° F in molten salt at 400° F, producing a structure containing essentially pearlite with small amounts of pro-eutectoid ferrite.

Each series consisted of 16 bars $^{7}/_{16}$ x $^{7}/_{16}$ x $3^{1}/_{2}$ in. Fourteen bars were machined into V-notch Charpy specimens and tested to determine the 15 ft-lb transition temperature and the 50% fibrous fracture transition temperature. Two bars were machined into standard half-size tension specimens and tested.

Fracture surfaces of Charpy specimens were nickel plated and ground perpendicular to the fracture surface prior to microstructural examination. Typical micrographs, microhardness values and deformation specimens were obtained from specimens cut from undeformed portions of the Charpy bars.

The quantity and grain size of the various microconstituents were determined individually by lineal analysis.

Results and Discussion

Notch Toughness Behavior

Transition temperatures, grain size of the ferrite, aggregate size of the discontinuous phase, microhardness values and tensile properties of the various microstructural aggregates are compiled in Table 1. Typical microstructures are shown in Fig. 1. The amount and grain size of both pro-eutectoid ferrite and the discontinuous phases were maintained relatively constant by means of the annealing and re-austenitizing technique. However, the microstructural characteristics of the discontinuous phases were varied markedly by the cooling treatments following re-austenitizing. The discontinuous phase ranged from coarse pearlite with a hardness 214 VHN to freshly formed martensite with a hardness of 780 VHN and tempered martensite with a hardness of 227 VHN.

As previously mentioned the type of pearlite, i.e., coarse or fine spacing, in a nominally constant ferrite matrix is unimportant with respect to notch toughness. However, when the character of the discontinuous phase is changed and the strength varied over much broader limits, the discontinuous phase exerts a pronounced influence. This effect is shown in Fig. 2. A severe loss in notch toughness occurs when the tensile strength is increased through the presence of a discontinuous phase of freshly formed martensite. The beneficial effect of tempering martensite is readily observed. However it will be noted that an optimum tempering temperature occurs around 1150° F, well below the lower critical temperature and at a tensile strength well above that obtainable at higher tempering temperatures. This may appear anomalous both from the

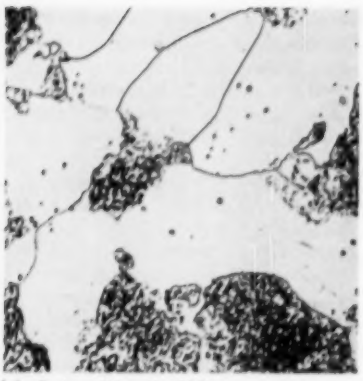

(a) Series D1. X 500.

(b) Series D8. Picral-nital etch.

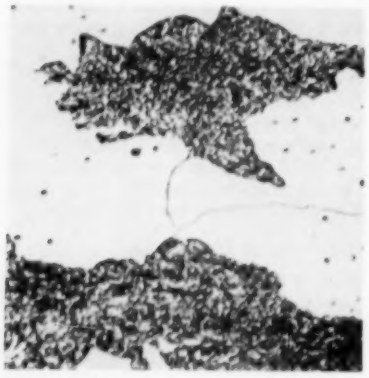

(c) Series D6.

(d) Series D13.

Fig. 1 Typical microstructures produced by various heat treatments of a C1030 steel

negligible effect observed for pearlite variations and from the initial improvement associated with softening due to tempering. This is believed to result from two simultaneous but opposing effects. The pro-eutectoid ferrite in which virtually all of the deformation occurs is restrained by the discontinuous phase. In the case of the untempered martensitic discontinuous phase, this restraint is excessive and a marked reduction in notch toughness occurs. The degree of restraint is reduced materially by the tempering treatment. However, at higher temperatures, the tempering treatment concomitantly embrittles the pro-eutectoid ferrite. This embrittling is temperature dependent and at 1300° F outweighs the beneficial effect of reduced strength. The exact nature of the embrittling effect is not known. However, one manifestation is a tendency for carbides to migrate to the ferrite grain boundaries. This may be observed by comparing Fig. 1(*b*) (1 hr temper at 1300° F) to Fig. 1(*c*) (10 min temper at 1150° F).

It appears from these results that the behavior of a low-carbon steel is controlled principally by the pro-eutectoid ferrite but that its deformation characteristics may be influenced strongly by the constraining environment. In the next section, additional evidence on the effect of the discontinuous structure on deformation is presented to support this concept.

The transition temperature for the ferrite-pearlite series (Series D-1) has been inserted into Fig. 2 and is seen to serve as an extension of the curve obtained for the ferrite-martensite series. The higher transition temperature of the ferrite-pearlite may be explained at least in part by the embrittlement induced in the free ferrite by the 4-hr hold at 1270° F used to obtain isothermal formation of coarse pearlite. The hardnesses and superficial appearance of the microstructure of the pearlite and tempered martensite were very similar, as evident from Fig. 1(*a*) and Fig. 1(*b*).

In Fig. 3, the change in notch toughness of the martensite is shown as a function of its strength level as altered by tempering. Again an optimum is obtained in the tempering series, and a longer time at high temperature produces an embrittlement. It is suggested that the cause for loss of toughness is the same in this case as for the

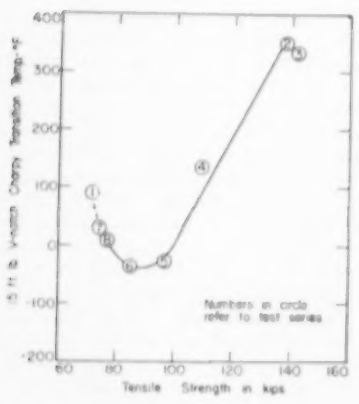

Fig. 2 The effect of tensile strength as varied by tempering on the notch toughness of ferrite-martensite aggregates in C1030 steel

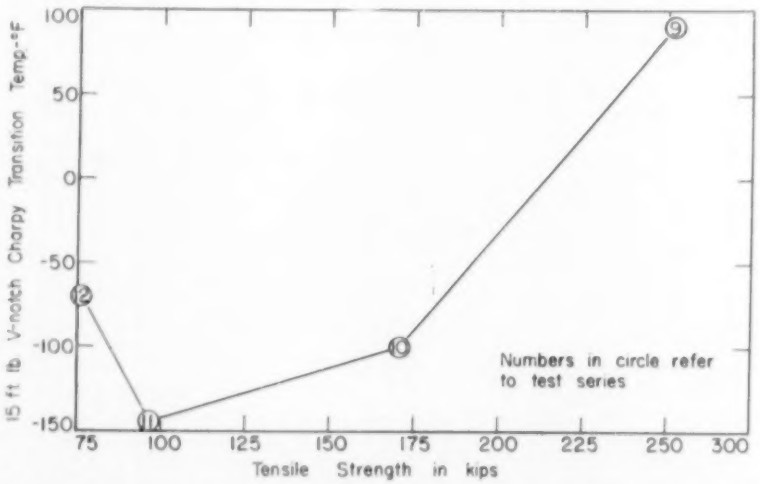

Fig. 3 The effect of tensile strength as varied by tempering on the notch toughness of martensite in C1030 steel

ferrite-martensite series. The ferrite grains developed by a long temper at 1300° F tend to collect carbides at the boundaries, as shown in Fig. 9.

It was previously shown that pearlite containing 0.80% carbon has a transition temperature in the neighborhood of 300° F. An attempt was made to produce 100% pearlite in this 0.32% carbon steel in order to reveal the effect of carbon content. The microstructure obtained by quenching in molten salt at 400° F (Series D13) is shown in Fig. 1(*d*) to contain small amounts of ferrite. The transition temperature was −25° F, considerably better than that of the ferrite −0.80% C pearlite aggregate in the same steel. Thus a reduction in the pro-eutectoid ferrite and a dilution in the carbon content of the pearlite—such as obtained by rapid cooling through the transformation range—is beneficial to the notch toughness of low-carbon steels.

Fracture Behavior

Charpy specimens from several of the test series were selected for microexamination to determine the locus at which cracking originated in the three basic types of microstructure under study. Samples broken at temperatures well in the brittle range below the transition temperature were chosen from the following series: D2, D5, D8, D12 and D13. See Table I for the heat treatments and transition temperatures.

Metallographic observations on a prepolished and etched Charpy bar from Series D2 tested below the transition temperature of the ferrite-untempered martensite aggregate revealed that deformation occurred by slip and twinning in the ferrite. Cracking originated at the ferrite-martensite interfaces. Some cracks were observed extending through the regions of martensite. In cross sections from the interior of the specimen, cleavage behavior of the ferrite was evident whereas the martensite regions exhibited a very irregular fracture path. Cracks were found to initiate at the ferrite grain boundaries and the ferrite-martensite interfaces. A crack initiating at a ferrite grain boundary is illustrated in Fig. 4. The ferrite grain boundaries of this specimen contained appreciable quantities of carbides which may exert an influence on the crack initiation tendency of the grain boundaries. In Fig. 5, cracks that appear at the ferrite grain boundary and ferrite-martensite interface are illustrated.

For the aggregate of ferrite and martensite tempered for 10 min at 1000° F (Series D5), cracks were found initiating at the ferrite grain boundaries and ferrite-tempered martensite interfaces. A crack that appears to initiate at the interface area is illustrated in Fig. 6. The ferrite was cleaved along the fractured edge whereas the tempered martensite revealed a very irregular fracture path. Fracture appeared to be retarded by the areas of tempered martensite.

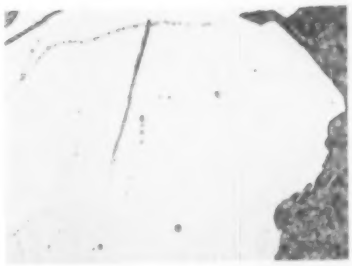

Fig. 4 Crack at ferrite grain boundary in specimen from Series D2 tested at —100° F

X 1000. Reduced by 1/2 upon reproduction. Picral-nital etch.

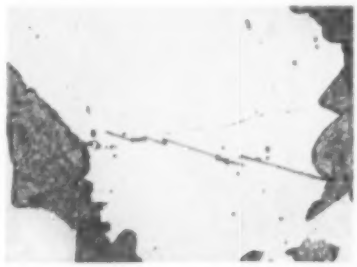

Fig. 5 Cracks at ferrite grain boundary and ferrite-martensite interface in specimen from Series D2

X 1000. Reduced by 1/2 upon reproduction. Picral-nital etch.

Fig. 6 Interface crack in specimen from Series D5 tested at —100° F

X 1000. Reduced by 1/2 upon reproduction. Picral-nital etch.

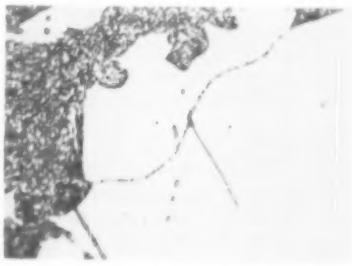

Fig. 7 Microcrack initiating at ferrite grain boundary in specimen from Series D8 tested at —50° F

X 1000. Reduced by 1/2 upon reproduction. Picral-nital etch.

Ferrite and martensite tempered at 1300° F for 1 hr to spheroidite (Series D8) revealed the same fracture initiation behavior as the other ferrite-martensite aggregates. For the specimen tested below the transition temperature (−50° F), cracks were observed to initiate at the ferrite grain boundaries and ferrite-spheroidite interfaces. A ferrite grain boundary serving as a locus of crack initiation from the interior of a specimen tested at −50° F is illustrated in Fig. 7. Appreciable quantities of carbides are discernible in the ferrite grain boundaries. These carbides may play an important role in the initiation of cracks at the ferrite grain boundaries. Microcracks initiating at the ferrite-spheroidite interface from the interior of the specimen are illustrated in Fig. 8. Like the other ferrite-martensite aggregates cleavage behavior of the ferrite was evident but the spheroidite revealed a very irregular fracture edge. Some cracks were observed to stop when they intersected regions of spheroidite.

Observations on the interior surface of the microstructure of 100% spheroidite (Series D12) tested below the transition temperature (−90° F) revealed cleavage behavior of the ferrite. This specimen was tempered for 8 hr after quenching to martensite. Although the evidence is not as conclusive as it was for the mixed structures, it appears that cracks may be initiated at the ferrite grain boundaries. A large crack that is displaced at a ferrite grain boundary is indicated by an arrow in Fig. 9. The crack is widest at the ferrite grain boundary and tapers considerably as it extends into the ferrite. In another region of the specimen microcracks were observed in a continuous and discontinuous manner as illustrated in Fig. 10. The discontinuous cracks extend from one ferrite grain boundary to another. Although carbides were often closely associated with the microcracks, it was difficult to ascertain what influence they would exert either on initiation or retardation of microcracks.

In the specimen (Series D13) consisting mostly of extremely fine pearlite and small amounts of Widmanstätten ferrite in the prior austenite grain boundaries, microcracks were observed to initiate at the pearlite colony boundaries and at the pearlite-ferrite interfaces. A microcrack that apparently initiated at a pearlite colony boundary from a specimen tested at −60° F, below the transition temperature, is illustrated in Fig. 11. Microcracks that appear to initiate at a pearlite colony

Fig. 8 Microcracks at ferrite-spheroidite interface in specimen from Series D8

X 1000. Reduced by 1/2 upon reproduction. Picral-nital etch.

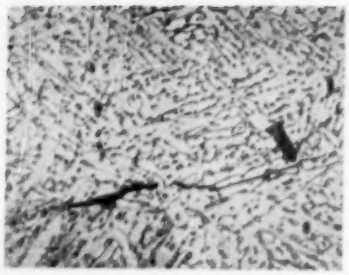

Fig. 9 Microcracks in spheroidite from Series D12 tested at —90° F

X 1500. Reduced by 1/2 upon reproduction. Picral-nital etch.

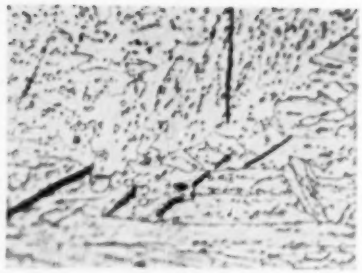

Fig. 10 Microcracks in spheroidite in specimen from Series D12 tested at —90° F

X 1500. Reduced by 1/2 upon reproduction. Picral-nital etch.

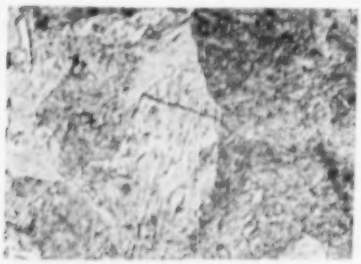

Fig. 11 Microcracks at pearlite colony boundary in specimen from Series D13 tested at —60° F

X 1500. Reduced by 1/2 upon reproduction. Picral-nital etch.

Fig. 12 Microcracks in specimen from Series D13 tested at —60° F

X 1500. Reduced by 1/2 upon reproduction. Picral-nital etch.

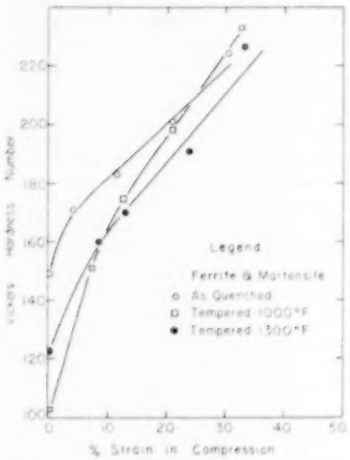

Fig. 13 Strain hardening characteristics of pro-eutectoid ferrite in various C1030 microstructural aggregates

boundary and a pearlite-ferrite interface are shown in Fig. 12.

Strain Hardening Results

Since the transition temperatures of the various aggregate structures varied markedly, strain hardening of each structure of the aggregate was studied in an attempt to explain the transition temperature behavior. Microhardness tests were conducted on the various aggregates after simple compression. The results of the microhardness vs. percent strain in compression for the ferrite of some of the various aggregates are illustrated in Fig. 13. In Fig. 14, the strain hardening of the various discontinuous structures in the presence of ferrite is shown. The as-quenched ferrite-martensite aggregate had the highest transition temperature based on a 15 ft-lb level. The hardness of the ferrite in the undeformed condition was very high as shown in Fig. 13. Furthermore, the martensite did not appear to participate in the over-all deformation since the hardness did not change as shown in Fig. 14. In the ferrite-martensite aggregate tempered at 1300° F for 1 hr, the undeformed ferrite had a much lower initial hardness and the transition temperature of this aggregate was much lower than the as-quenched ferrite-martensite mixture. In addition, the spheroidite that resulted from tempering of the martensite participated appreciably in the deformation of the specimens. Finally, the ferrite-martensite tempered at 1000° F for 10 min, had the lowest transition temperature among the various aggregates of ferrite and martensite whose strain hardening characteristics were studied, and the initial hardness of the ferrite was much lower. From Fig. 14 it can be seen that the tempered martensite participated in the deformation of the aggregate. On the basis of the strain hardening of the individual structures in the various aggregates, the notch behavior appears to be related to the initial hardness of the ferrite, the rate at which it strain hardens, and the participation of the neighboring structure. However, it must be pointed out that the microhardness data were obtained on specimens heated to 250° F during the mounting operation. Thus the previous quenching followed by heating to 250° F probably introduced some aging which would be expected to influence the results.

Ferrite with a high initial hardness would reach the fracture stress by strain-hardening well before ferrite with a lower initial hardness and the same strain hardening characteristics. Furthermore, the limited participation of the neighboring structure during deformation will influence the behavior of the ferrite, and therefore, must, by imposing restraint upon it, be taken into consideration in explaining the notch

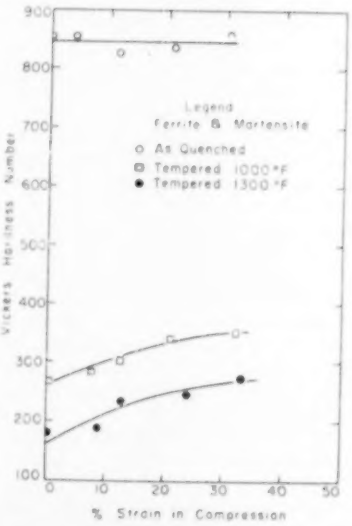

Fig. 14 Strain hardening characteristics of the discontinuous phase in various C1030 microstructural aggregates

toughness behavior of the ferrite aggregates.

Summary

The results of this investigation may be summarized as follows:

1. The notch toughness of a low-carbon steel such as the C1030 studied here is controlled largely by the behavior of the pro-eutectoid ferrite.

2. The presence of a very hard discontinuous phase such as martensite lowers the notch toughness by constraining the flow of the ferrite.

3. Subcritical heat treatments at higher temperatures and longer times appear to embrittle ferrite, possibly by a migration of carbon to the grain boundaries of the ferrite. Embrittlement is not likely to occur during welding, but might be introduced by extended post heat treatment of weldments.

4. In microstructures consisting of pro-eutectoid ferrite and martensite (tempered or untempered) microcracks initiate at ferrite grain boundaries and at ferrite-martensite interfaces.

5. In microstructures consisting mostly of low-carbon pearlite with small amounts of Widmanstätten ferrite, microcracks originate at pearlite colony boundaries and at ferrite-pearlite interfaces.

6. The variation of transition temperature with the softening of the martensite in ferrite-martensite aggregates may be explained on the basis of the initial hardness variation of the ferrite and the degree of participation of the discontinuous structure in the deformation of the aggregate. As the tempering temperature is raised, the martensite participates more in the deformation and the initial hardness of the ferrite is lowered.

Acknowledgments

The authors are grateful to the International Nickel Co. whose support has made possible a continuing investigation at Lehigh University on the problem of brittle fracture in steel.

Bibliography

1. Gross, J. H., and Stout, R. D., "The Effect of Microstructure on Notch Toughness—Part I," THE WELDING JOURNAL, **30** (10), Research Suppl., 481-s to 485-s (1951).

2. Danko, J. C., and Stout, R. D., "The Effect of Microstructure on the Morphology of Fracture—Part I," *Ibid.*, **34** (3), Research Suppl., 113-s to 116-s (1955).

3. Gross, J. H., and Stout, R. D., "The Effect of Microstructure on Notch Toughness—Part II," *Ibid.*, **34** (3), Research Suppl., 117-s to 122-s (1955).

4. Gross, J. H., and Stout, R. D., "The Effect of Microstructure on Notch Toughness—Part III," *Ibid.*, **35** (2), Research Suppl., 72-s to 76-s (1956).

5. Danko, J. C., and Stout, R. D., "The Effect of Microstructure on the Morphology of Fracture—Part II," *Ibid.*, **35** (2), Research Suppl., 77-s to 81-s (1956).

INTERNATIONAL INSTITUTE OF WELDING

The next meeting of the International Institute of Welding will be held in Essen, Germany, June 29th to July 6th. This meeting will be followed by works-visits from July 7th to 14th. The Assembly is preceded by the Great Welding Engineering Convention of the German Welding Engineering Assn. (DVS), to be held in Essen, too, from June 25 to June 28, 1957. Members of both meetings are invited to see the DVS Exhibition "Welding and Cutting" June 23–July 3, 1957, at Gruga-Park in Essen. It is to be a public session in Essen, Germany, July 1st, which will be devoted to all phases of "Metallurgy of Welding."

Any member of the AMERICAN WELDING SOCIETY or Welding Research Council desiring to present a paper at this public session should get in touch at once with the secretary of the American Council of the IIW, William Spraragen, 33 W. 39th St., New York 18, N. Y.

At the meeting in Madrid in 1956 more than 20 American representatives were present. Indications are that more than 30 official American representatives will be present at the meeting in Essen, Germany, and participate in the work of the 15 commissions.

The United States is represented on 14 of these commissions by an official "delegate" and a number of "experts" varying from 3 to 5. The "experts" are being carefully selected by the American Council. The official delegates of the United States on these Commissions are:

Commission	
I	Gas Welding and Allied Processes—J. H. Zimmerman
II	Arc Welding—John J. Chyle
III	Resistance Welding—T. Embury Jones
IV	Documentation
V	Testing, Measurement and Control of Welds—A. Gobus
VI	Terminology—M. A. Cordovi
VII	Standardization—A. N. Kugler
VIII	Hygiene and Safety—H. F. Reinhard
IX	Behavior of Metals Subjected to Welding—R. D. Stout and D. P. Brown
X	Residual Stresses and Stress Relieving—T. McLean Jasper, W. Spraragen, *Alternate*
XI	Pressure Vessels, Boilers and Pipelines—Arthur R. Gatewood
XII	Special Arc Welding Processes—C. J. Sullivan
XIII	Fatigue Testing—A. M. Freudenthal, Expert—LaMotte Grover
XIV	Welding Instruction—Clarence Jackson
XV	Fundamentals of Design and Fabrication for Welding—A. Amirikian

TRIAXIAL TENSION TESTING AND THE BRITTLE FRACTURE STRENGTH OF METALS

Data are presented on the effect of joint thickness on the tensile strength of mild steel and drill rod brazed with silver and copper

BY N. BREDZS AND H. SCHWARTZBART

ABSTRACT. A test has been developed for determining the brittle fracture strength of a metal under triaxial tension. The specimen utilized consists of a composite of a thin disk of soft metal metallurgically bonded to two cylinders of hard metal. When the composite specimen is pulled in tension the thin soft disk is prevented from flowing plastically when its yield point is reached by virtue of the restraint imposed by the adjacent hard cylinders. Thus, a state of triaxial tension is set up in the thin disk. For infinitely thin disks, plastic deformation may be completely suppressed.

The technique herein described involves brazing bars of mild steel and drill rod with silver and copper to obtain the composite specimens. Data on the variations of tensile strength with joint thickness are presented and the significance of these data as to the brittle fracture strength discussed.

Introduction

The ordinary uniaxial tension test is used widely for the evaluation of the mechanical strength and ductility of metals. It is simple to perform and it may be considered adequate in most cases as the first approximation of the way metals react to mechanical loading in service.

Several considerations, however, indicate the deficiencies of the simple tension test and the need for additional means for the study of the flow and fracture of metals. For one thing, the load imposed on a part in service is seldom one of simple tension but is more often one of combined stress. The need for information on the effect of combined stress on flow and fracture is, therefore, apparent. It is this particular consideration which is the subject of this paper.

Usually in tension testing of metals, one is concerned with, first, plastic flow, then fracture. It is, to say the least, especially disconcerting when a material such as mild steel which conventionally behaves in ductile fashion happens to fail in brittle fashion as it sometimes does in ships and other structures. It is useful, therefore, to be able to determine the fracture strength of material in the absence of prior plastic flow. It should be possible to achieve this condition if a material is subjected to equal tension in three mutually perpendicular directions. It would further be desirable if the longitudinal stress could be varied independently of the transverse stresses so that the degree of triaxiality could be varied to determine the effect of triaxiality on properties. Furthermore, it would be desirable if the test were capable of mathematical or experimental analysis so that one could determine quantitatively the principal stresses.

Much work has been done on the effect of biaxial stress systems on flow and fracture. Such data are relatively easy to obtain by loading thin wall tubes under various combinations of longitudinal tension or compression, internal pressure, external pressure or torsion. The hydraulic bulge test on thin sheet has also been used to obtain biaxial stress conditions, circular bulges for equal biaxial stresses and elliptical bulges for unequal biaxial stresses. Still further, the effect of biaxial stresses on fracture has been obtained by bending wide specimens of various width to thickness ratios.

The effort to obtain meaningful quantitative data under conditions of triaxial tension has occupied workers in flow and fracture for some time and has not proved fruitful to date. The obstacle has not been to produce triaxial tension; this is easily done. To produce uncomplicated triaxial tension in a fashion capable of analysis or measurement is the difficult task. The tension testing of a circumferentially notched cylindrical bar yields triaxial tension from some short distance below the notch bottom to the bar center. At the bottom of the notch the stress condition is biaxial since no radial stress exists normal to a free surface. At the bar center the radial stress is equal to the tangential stress. (A review of notch tensile testing and the possibilities of its use in determining the effect of triaxiality on fracturing has been presented by Lubahn.[1])

The notch tensile test is relatively complicated in respect to the combined stresses present and has defied quantitative treatment as yet. In addition, there is an additional complication in the stress concentration which exists at the base of the notch while the specimen is being loaded in the elastic range. After some plastic deformation has occurred, this stress concentration is largely erased and replaced by a strain concentration. Thus stress and strain are nonuniform in distribution and this serves further to complicate the picture. Rather than discuss here in further detail the deficiencies of the notch tension test in determining the effect of triaxiality on fracture, suffice it to say that it has not proved adequate.

Many other triaxial tension tests have been suggested and are reviewed by Nadai.[2] However, to the best of the writers' knowledge no test has yet proved successful in providing the desired results.

One test, however, which has been used by Orowan, Nye and Cairns[3] and Zschokke and Montandon[4] may be capable of fulfilling the conditions required of a triaxial tension specimen. The composite specimen illustrated in Fig. 1 consists of a thin disk of soft metal bonded to two cylinders of hard metal. When the composite specimen is pulled in tension the soft disk reaches its yield point before the hard cylinder but is prevented from contracting plastically by virtue of being bonded to the

N. Bredzs is Research Metallurgist, and **H. Schwartzbart** is Supervisor, Welding Research, Armour Research Foundation, Chicago, Ill.

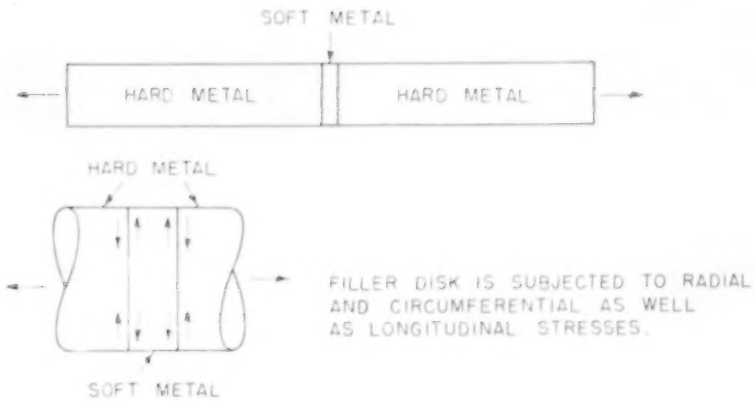

Fig. 1 Butt-brazed specimen pulled in tension

hard cylinders. This condition sets up transverse stresses; the stress state is biaxial at the surface of the thin disk but is triaxial at the center and along a radius almost the whole way to the surface. If the materials are chosen so that the fracture stress of the disk is below the yield strength of the cylinder, and the disk is made infinitely thin, then we may have the triaxial stress specimen required. As will be seen in this paper, the analysis of this specimen is still not simple but it does offer some hope for advancing our knowledge of the fracturing of metals.

In connection with a program on the fundamentals of brazing sponsored at the Armour Research Foundation by the Frankford Arsenal, experimental techniques have been developed for the determination of the effect of joint thickness on the tensile strength of butt brazed specimens. These have been described in a previous paper[5] by one of the present authors and the results obtained up to the date of that paper were presented. The present paper describes, among other things, new techniques which have been developed for extending the data to thicker and thinner joints and presents the newly acquired data, especially in its relation to the above considerations on brittle fracture.

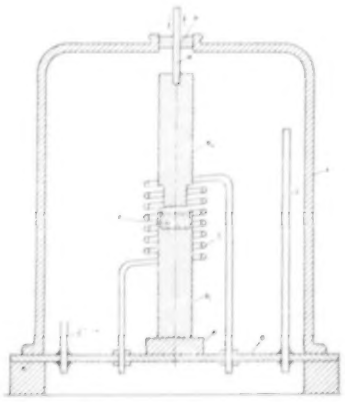

Fig. 2 Apparatus for "brazing" of tensile specimens with extremely thick filler metal joint

B_l, Cylindrical steel bar with a cup machined on the upper end; B_u, upper cylindrical steel bar; C, induction coil; F, molten filler metal; G, glass plate; I, gas inlet tube; J, glass jar; O, gas outlet; P, transite block; R, cork; W, steel wire.

Experimental Procedure

In general, the experimental procedure used in the herein reported investigation are the same as those reported previously and will not be described again. The tensile strength-joint thickness curves previously reported were for joint thicknesses ranging from about 0.0005 to 0.020 in. thick. Although some joints thinner than 0.0005 in. were made sporadically the experimental procedures had not been developed for making absolutely sound and voidless thin joints or joints thicker than 0.020 in. Since the absence of data in the region of very thin and thick joints was a serious handicap in drawing conclusions, it was necessary to develop methods for making consistently sound joints in these regions of thickness. The methods developed are described in the following sections.

"Brazing" of Extremely Thick Joints

The apparatus developed for "brazing" of extremely thick joints is illustrated by Fig. 2. The filler metal wire cut in small pieces is placed in a cup machined on the upper end of the cylindrical steel bar, B_l, which represents the lower half-bar of the tensile bar to be brazed. The upper half-bar, B_u, can be raised and lowered with the help of the steel wire, W, which is drawn through the cork, R, placed in the hole bored into the top of the bell jar, J. During the joining operations the bell jar is filled with 10% H_2 + 90% N_2 gas. Both half-bars, B_l and B_u, are surrounded by the induction coil, C; the positions of the half-bars are adjusted so that the axes of both are exactly concentric with the axis of the coil. By turning on the power in the induction coil, C, the temperature of both half-bars starts to increase quite rapidly. At a certain temperature, depending on the dryness of the 10% H_2 + 90% N_2 gas, the gas will start to reduce the iron oxides on the bottom surface of the steel cup and also on the lower end surface of the upper bar, B_u, so that at the time the melting point of the filler metal is attained, both end surfaces are free from oxides, permitting ready wetting by the molten filler metal.

As soon as the filler metal in the steel cup is completely melted, the power in the induction coil is turned off, and the uppersteel bar, B_u, pushed down until it touches the surface of the molten filler metal. In order to remove the gas bubbles, which are usually entrapped in the molten filler metal just beneath the end surface of the upper bar, B_u, the bar is moved up and down several times in the molten filler metal. Before solidification of the filler metal the position of the upper bar, B_u, is fixed precisely, since the distance between the end surfaces of the two half-bars at the time of solidification of the filler metal determines the thickness of the solidified joint. Both half-bars used in these experiments were 3 in. long and $^3/_4$ in. in diameter. After the joining operation was completed, the "brazed" half-bars were turned down to a standard 0.505-in. tensile specimen (Fig. 3).

With the development of the method for obtaining extremely thick joints, a new problem arose and had to be solved, namely, the elimination of gas inclusions in such joints. Using the new method, joints of any desired joint thickness

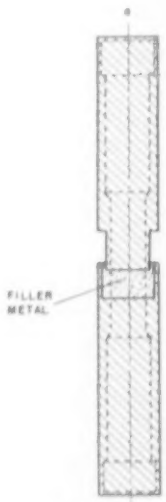

Fig. 3 Tensile test bar (dotted lines) turned down from "brazed" half-bars (continuous lines) with extremely thick filler metal joint

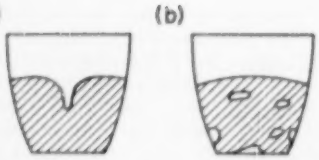

Fig. 4 Cross sections through pure silver melts solidified in porcelain crucibles

(a) Completely degasified pure silver. (b) Commercial silver.

could be easily obtained. However, the exact determination of the tensile strength of the thicker joints was considerably hindered by the large amounts of gas inclusions in these joints. Therefore, the nature and causes of the gas inclusions in very thick joints and the problem of the elimination of such inclusions were investigated in brazed joints made with pure silver filler and low-carbon steel base material.

In order to minimize the problem of gas inclusions, it was attempted to decrease the gas inclusions by means of "degasification" of the silver before brazing. Since the silver used for brazing of steel bars was made from pure, commercial silver which usually is not quite free of oxygen, and since the solubility of oxygen in solid silver is considerable (up to 0.5 volume of oxygen in one volume of silver), it was felt that by melting the silver wire in 10% H_2 + 90% N_2 atmosphere, the reaction $2H_2 + O_2 \rightarrow 2H_2O$ might take place, and thus the formation of water vapor bubbles might be responsible for the formation of voids in pure silver brazed joints.

According to this reasoning, the best way to completely remove oxygen from silver before brazing would be to melt the silver wire in 10% H_2 + 90% N_2 atmosphere and keep it molten under this atmosphere until the development of gas bubbles ceased completely. Certainly, degasification in vacuum would be the most effective way to remove any traces of gas from molten silver. However, since all the brazing operations were performed in 10% H_2 + 90% N_2 atmosphere, because of the necessity of reducing the steel surfaces, it was of no avail to degasify the silver in vacuum since it could again pick up hydrogen during the brazing operation.

On the other hand, the solubility of hydrogen in molten silver compared with the solubility of oxygen, according to Smithells,[8] is very small. It should be especially low in 10% H_2 + 90% N_2 atmosphere, except for very small amounts of hydrogen which might precipitate by solidification of the silver degasified in the 10% H_2 + 90% N_2 atmosphere.

The degasification of silver was accomplished by melting the silver wire in a porcelain crucible under a glass jar filled with 10% H_2 + 90% N_2. During these experiments, it was observed that by remelting the "degasified" silver in 10% H_2 + 90% N_2 gas evolution again occurred. The evolution of gas from molten silver ceased completely only after at least four remelting operations in the 10% H_2 + 90% N_2 atmosphere. It was also observed that the gas-free silver develops a shrinkage pipe in the center of the silver surface during solidification, as shown in Fig. 4. The shrinkage pipe was not observed on solidified surfaces of nondegasified silver (Fig. 4).

Thus, it might be expected that sound brazed joints, completely free from gas inclusions, would be obtained by using degasified silver. Indeed, the first brazed joints made with degasified silver showed a considerable decrease of gas inclusions; and in some thinner joints, no gas inclusions were observed after fracture of the joints.

However, in the center of the thinner silver joints a new type of joint imperfection could be discerned: namely, a characteristic polygon-shaped void with rather sharp edges and corners, as illustrated in Fig. 5. This polygon-shaped void was always found on both surfaces of the fractured joint. In a few cases, smaller voids were also present around the large void in the center of the joint.

Since this type of joint imperfection was present only in the joints made with degasified silver, it was concluded that this type of void is caused by volume contraction* during the solidification of the degasified silver. Since cooling of the steel bars after brazing proceeds from the surface inward, the silver in the center of the bar will be the last to solidify, consequently, the effect of the volume contraction must show up here in the form of a shrinkage cavity.

In order to eliminate the formation of the shrinkage voids, the brazing process was modified so that during the cooling period after brazing, the outer surface layers of the steel bars around the brazed joint could be kept at a higher temperature than the center of the joint and cooling would proceed through the ends of the bars. This condition can be achieved by switching on the high frequency current in the coil around the joint for quite short intervals during the cooling period. In this manner, the cooling conditions in the silver disk could be reversed, so that now the center of the silver disk should be the first portion to become solidified. Under such conditions the shrinkage cavity would not be formed in the center but on the edges of the silver disk which would be removed on the lathe by turning down the brazed

* According to *Metals Handbook* (ASM, 1948), p. 1110, the density of solid silver at 960° C is 9.85 g per cc, and of liquid silver at the same temperature 9.39 g per cc.

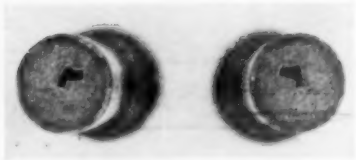

Fig. 5 An enlarged photograph of a fractured brazed joint, X1

The two tensile half-bars were brazed with pure, degasified silver. The typical, polygon shaped shrinkage cavity is present on both end surfaces.

bars to the standard 0.505-in. tensile specimen. Thus, a completely voidless silver disk might be obtained.

To prove this reasoning, a series of brazing experiments was made under strict observance of the outlined procedure. By using the degasified silver as filler metal and the modified brazing procedure for brazing of thicker joints, completely voidless silver joints could be obtained in a wide range of joint thicknesses with the only exceptions the extremely thin joints.

Thus, the next problem to be solved was the development of proper techniques for brazing of extremely thin joints.

Brazing of Extremely Thin Joints

After a great deal of experimentation with brazing technique involving (1) brazing with filler metal electrodeposited on the ends of the cylindrical tensile bars, (2) slow cooling from the brazing operation and (3) improved methods of preparing the bar ends for brazing, it was found that quite perfect joints and sufficiently uniform joint thicknesses of only 0.000005 in. (in some cases even less) could be achieved. Such joints became obtainable through the abandonment of hand polishing of the bar ends and by adopting a precision grinding machine with a subsequent polishing with fine carborundum paper (400A). It was found that preplacing the filler metal by electrodeposition did not improve joint quality, nor did slow cooling from the brazing operation. Therefore, the procedures described previously were used for the brazing of very thin joints, with the exception of the increased care in grinding of the bar ends.

Thus with the development and gradual improvement of the brazing techniques for extremely thin and extremely thick brazed joints the investigation of the tensile strength-joint thickness curves could encompass a range of joint thicknesses from 0.000005 to 0.25 in.

Tensile strength-joint thickness curves were obtained for mild steel and drill rod brazed with both silver and copper.

Experimental Results

The results on the effect of joint thickness on the tensile strength of silver

brazed bars of mild steel and drill rod are presented in tabular form in Tables 1 and 2 and graphically in Fig. 6. A semilogarithmic plot is used in Fig. 6 because of the wide range of joint thicknesses involved. Tables 1 and 2 present the joint thickness measured at four positions around the circumference of the bars as well as the average thickness, the tensile strength and observations on the quality of the bond.

Tensile strength-joint thickness curves for mild steel and drill rod brazed with copper are presented in Fig. 7.

Discussion

The observations and conclusions that can be made from a detailed examination of the data of Fig. 6 are significant in relation to (1) mechanical factors determining the strength of brazed joints and (2) basic mechanical properties of metals. Item (1) is true because silver and iron are practically completely insoluble in each other. This makes it possible to study the mechanical aspects of the problem in the absence of interference of metallurgical phenomena, such as diffusion or precipitations.

It is seen that as joint thickness decreases from 0.100 in. the tensile strength rises, reaches a maximum and decreases. For the data presented, the highest strength is obtained in the range of thicknesses from 0.0001 to 0.0005 in. The reason for the rise in strength with decreasing thickness is primarily the transverse tensions introduced by the difference in yield strength between filler metal and base metal as discussed previously. Sources of transverse stress other than the difference in yield strengths also operate but these are not as potent. One of these is the difference in modulus of elasticity between filler metal and base metal. This difference in modulus of elasticity will give rise to transverse tension at all stresses even below the yield strength of the filler metal. That this factor is not potent in affecting the tensile strength-joint thickness curve can be seen from the review of Bredzs[5] which reveals that in those cases in which there is no difference in strength between bulk filler metal and base metal, joint strength is unaffected by joint thickness, even though a difference in modulus does exist. These same data indicate that the effect of joint thickness on tensile strength is not due to a size effect. It might be reasoned that thin-

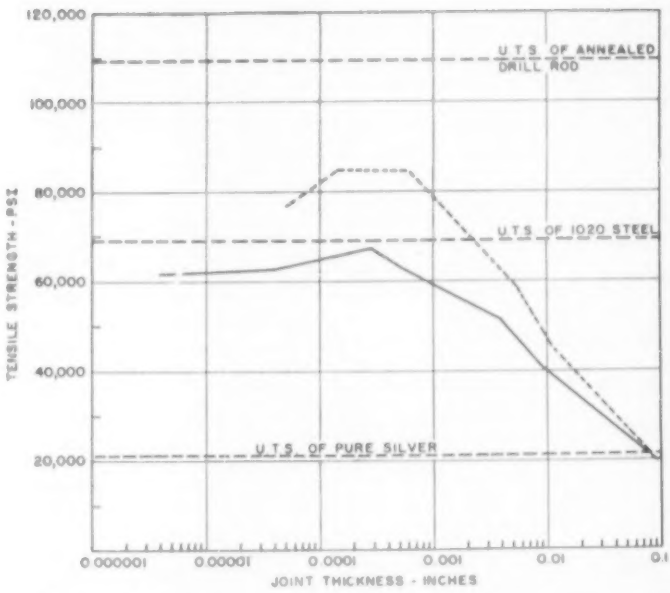

Fig. 6 Tensile strength-joint thickness curves of pure silver joints: (1) in SAE 1020 steel (solid line); (2) in drill rod (dotted line)

Table 1 Tensile Test Results of Low-Carbon (SAE 1020) Steel Bars Brazed with Pure Silver Under 10% H_2 + 90% N_2 Atmosphere

Specimen No.	*Joint thickness, in.* 0°	90°	180°	270°	*Avg*	*Ultimate tensile strength, psi*	*Quality of the metallic bond*
ALCT 119	0.090	0.087	0.092	0.102	0.09275	19,600	Some large bubbles
28 A	0.0093	0.0085	0.0085	0.0083	0.0086	41,300	Almost voidless (2%)
26 A	0.0043	0.0033	0.0043	0.0040	0.0040	50,900	Some voids (10%)
25 A	...	...	...	...	0.0005*	62,900	Absolutely sound and voidless
ALC 128	0.00051	0.00000	0.00012	0.00054	0.00029	67,200	Absolutely sound and voidless
ALC 134	0.00003	0.00003	0.00003	0.00003	0.00003	62,150	Silver film partly destroyed
ALC 143	0.000015	0.00000	0.00000	0.00000	0.000004	61,900	Thin silver film punctured by iron crystals

* Measured after fracture.

Table 2 Tensile Test Results of Drill Rod Bars Brazed with Pure Silver Under 10% H_2 + 90% N_2 Atmosphere (After Brazing the Drill Rod Bars Were Cooled Down in 10% H_2 + 90% N_2 Atmosphere)

Specimen No.	*Joint thickness, in.* 0°	90°	180°	270°	*Avg*	*Ultimate tensile strength, psi*	*Quality of the metallic bond*
ADR 180	0.0115	0.0117	0.0122	0.0113	0.0117	44,150	Shrinkage cavity (5%)
ADR 194	0.00580	0.00580	0.00406	0.00613	0.00545	58,150	Some gas entrapments
ADR 114	0.00025	0.00149	0.00221	0.00080	0.00119	76,600	Almost perfect joint (2% voids)
ADR 115	0.00101	0.00052	0.00075	0.00014	0.00060	84,200	Extremely thin film. Somewhat thicker at edges
ADR 116	0.00055	0.00001	0.00000	0.00002	0.00014	84,350	Extremely thin film. Somewhat thicker at edges

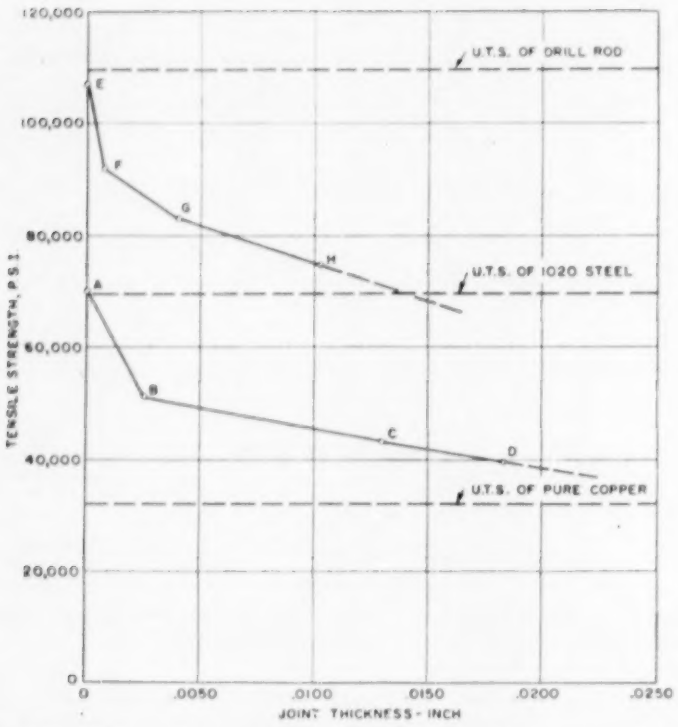

Fig. 7 *ABCD*, tensile strength-joint thickness curve of pure copper joints in SAE 1020 steel. *EFGH*, tensile strength-joint thickness curve of pure copper joints in drill rod bars

ner, therefore smaller, disks might be stronger than thicker disks because of statistical considerations, namely, that there is less likelihood that a serious defect exists in a small volume than in a large volume. However, such a factor operates regardless of the relative strengths of base metal and filler metal and, if the hypothesis were correct, then a rising curve should be obtained even when the strengths of base metal and filler metal were the same.

A further source of transverse tensions is the difference in coefficient of expansion between silver and iron. As the brazement is cooling after solidification, the silver disk is put into radial and circumferential tension by virtue of the fact that it wishes to contract more than the steel, which prevents it from doing so. This residual stress after cooling to room temperature will add to the transverse tensions which arise in subsequent tension testing.

It is pertinent to note that all of the failures were on the plane of symmetry of the silver disk; none of the failures were at the interface between silver and steel, even under a tensile stress as high as 84,350 psi. It is interesting from the fundamental point of view to ponder the reason for the maximum or plateau of the curves of Fig. 6. Plotted on the figure are the values for the ultimate tensile strength of silver, 1020 steel and drill rod. The strengths of the 1020 steel and drill rod were determined for solid, unbrazed bars put through an induction heating cycle identical to that received by the brazed bars. Actually, the plotting of yield strengths under the particular multiaxial stress state existing in the composite specimen would be more pertinent to the ensuing discussion than tensile strength but these data are unavailable. The maximum for the 1020 steel brazements, the solid curve, exceeds the yield strength of the parent steel, almost reaching the tensile strength of 69,000 psi. Thus it is evident that the mild steel deformed plastically, thus decreasing the degree of triaxiality on the silver disk. Thus, in terms of the objective of determining the fracture strength of silver without prior plastic flow, and doing this in a test susceptible to analysis, the picture becomes hopelessly complicated. The curve for the drill rod brazements, the broken curve, lies above that of the mild steel brazements proving the effect of the yield strength of the base metal on the strength of the brazement. Consider now the case of drill rod brazed with silver. Although the maximum of the drill rod curve lies somewhat below the ultimate tensile strength of drill rod, it was observed that some plastic deformation of the drill rod did occur. Thus, even if it might be stated that the yield strength of drill rod in uniaxial tension is higher than 84,350 psi, which is the level of the maximum referred to, this yield strength is depressed by the radial and circumferential compressive stresses present in the layers of drill rod at the braze interface. Therefore, plastic flow of the drill rod, as well as of the mild steel was obtained. Therefore, it would be particularly interesting and pertinent to determine the curve for yet higher strength base metals. Preliminary attempts to accomplish this failed and another program, more precise and comprehensive, is now under way to exploit this experimental method in achieving the desired answers. At any rate, the strength of 84,350 psi achieved for drill rod brazed with silver is four times the tensile strength and 11 times the yield strength of silver.

The questions suggested by these data are intriguing. What is the absolute maximum strength attainable, which cannot be raised by further increase in the yield strength of the base metal? What is the mode of fracture? It is known that iron, a body centered cubic metal, fractures in ductile fashion above the transition temperature on octahedral planes, and in brittle fashion below the transition temperature on cube planes. Face-centered cubic metals, of which silver is one, have not been known to fracture in brittle fashion. A further interesting possibility interjects itself. Presumably, if the joint thickness is so small that it may be considered a thin film in the sense that it no longer possesses a regular lattice but can be considered amorphous, what then? Has this condition actually been achieved with the strength of 84,350 psi?

It is, as the above discussion indicates, premature to rationalize the data of Fig. 6. As discussed above, a more comprehensive program is now under way to obtain the more complete and precise data required to completely understand the phenomena involved. In particular, the tensile strength-joint thickness curves in the region of thin joints must be accurately determined and for systems in which there is no possibility of plastic deformation in the base metal.

For comparison purposes, the data on mild steel and drill rod brazed with copper are presented in Fig. 7. Recall that, whereas in the case of brazing with silver one is concerned principally with mechanical factors due to the lack of solubility between iron and silver, in the case of copper one is concerned with the additional factors of diffusion and grain boundary penetration. The general trend of the tensile strength-joint thickness curves obtained on pure silver and on copper is quite similar. As the joint thickness decreases, the tensile strength gradually increases from the tensile strength of pure filler metal in

extremely thick joints to the tensile strength of the base metal in very thin joints. However, it should be kept in mind that for very thin joints the copper can diffuse completely into the base metal, leaving no discrete joint but only a zone of copper-enriched steel. Thus, steel to steel contact is made across what would be the joint. In pulling such bars in tension, fracture can be obtained in the base metal outside the joint area.

Summary and Conclusions

Methods have been developed for making brazed joints over a wide range of thicknesses, making it possible to study fundamental fracturing behavior under triaxial tension. If a composite specimen consisting of a cylindrical disk of a soft metal such as silver, bonded to two hard cylinders such as steel, is pulled in tension, the soft disk is subjected to large triaxial tensions when the stress reaches the yield point of the soft disk which is prevented from yielding plastically by the adjacent hard cylinders. The degree of triaxiality is higher the thinner the disk and it is felt that the fracture strength of the disk material in the absence of prior plastic flow may be determined by testing or extrapolating to infinitely thin disks.

This paper presents data on the effect of joint thickness on the tensile strength of mild steel and drill rod brazed with silver and copper. The silver brazed joints offer one the opportunity to study mechanical factors in the absence of interfering metallurgical phenomena such as diffusion or grain boundary penetration because there is no mutual solubility between iron and silver.

The following conclusions may be drawn from this work.

1. In pulling the brazed tensile bars in tension, due principally to the suppression of the plastic deformation in extremely thin joints caused by the difference in yield strength between filler and base metal, the stress distribution in the extremely thin filler metal disks might approach a state of very high triaxiality, or a state of almost ideal hydrostatic tension. Under such conditions, the tensile strength of pure silver, which in a standard tensile test is 21,000 psi, can be increased, as the results show, to 84,300 psi. The tensile strength of pure copper, which in a standard test is 32,000 psi, can be increased to 106,500 psi.

2. From the tensile strength-joint thickness curves of pure silver and pure copper joints in SAE 1020 steel and drill rod bars, it is quite evident that the tensile strength of the brazed joints increases with increasing tensile strength of the base metal. In all joint thickness ranges the drill rod curves show much higher tensile strength values than the SAE 1020 steel curves. However, for both mild steel and drill rod some plastic deformation of the base metal was obtained, thus complicating the determination of the brittle fracture strength of the filler metal. In subsequent work it is hoped to exceed the fracture strength of the filler metal before reaching the yield strength of the base metal which is a prime requisite of a specimen capable of determining the brittle fracture strength in triaxial tension.

3. All of the silver brazed joints investigated, even those with the highest tensile strength, broke in the middle of the silver disk. The plane of fracture was identical with the plane of symmetry. Since the fracture never occurred along the steel-silver interface, it is quite obvious that the steel-silver interface was always stronger than the silver itself, even under a tensile strength of 84,350 psi. Thus the formation of an alloy system between the filler metal and the base metal is not an essential prerequisite for obtaining strong brazed joints. Since silver and iron are insoluble in each other, the iron-silver interface must be considered as almost a classic sample of an adhesion bond.

Acknowledgments

This work is part of an investigation sponsored by the Pitman-Dunn Laboratory of the Frankford Arsenal at the Armour Research Foundation and the authors are grateful for their permission to publish it. The constant encouragement and guidance of F. W. Hussey of that organization is gratefully acknowledged.

In addition, the authors wish to acknowledge the contributions of O. T. Barnett and Edward R. Roeder to this work.

References

1. Lubahn, J. D., Notch Tensile Testing, ASM Symposium "Fracturing of Metals" (1948).
2. Nadai, A., *Theory of Flow and Fracture of Solids*, McGraw-Hill Book Co., Inc., New York (1950).
3. Orowan, E., Nye, J. F., and Cairns, W. I., Theoret. Res. Rep. No. 16/56, Arman. Res. Sept. Min. of Supply, London (1945).
4. Zschokke, K., and Montandon, R., *Schweiz. Archiv angew. Wiss u. Tech.*, 10, 1929 (1944).
5. Bredzs, N., "Investigation of Factors Determining the Tensile Strength of Brazed Joints," The Welding Journal, 33 (11), Research Suppl., 545-s to 563-s (1954).
6. Smithells, C. J., *Gases and Metals*, John Wiley & Sons, New York (1937).

RESEARCH NEWS

(*Continued from page 603-s*)

Charpy Slow Bend Tests—Carl E. Hartbower

Effects of Manganese and Aluminum Contents on Transition Temperature of Normalized Nickel Steel—T. N. Armstrong and O. O. Miller

Low Temperature Transition of Normalized Carbon Manganese Steels—T. N. Armstrong and W. L. Warner

Effect of Specimen Width on the Notched Bar Impact Properties of Quenched and Tempered and Normalized Steels—R. S. Zeno

Reproducibility of Charpy Impact Test—David E. Driscoll

Automatic Impact Testing from Room Temperature to −236° C—Thomas S. DeSisto

The Influence of Pendulum Flexibilities on Impact Energy Measurements—Joseph I. Bluhm

The Impact Tube: A New Experimental Technique for Applying Impulse Loads—George Gerad

Longitudinal Impact Tests of Long Bars with a Slingshot Machine—W. Ramber and I. K. Irwin

Stress-Strain Relationships in Yarns Subjected to Rapid Impact Loading—Herbert F. Schiefer, Jack C. Smith, Frank L. McCrackin and W. K. Stone

Shock Tester for Shipping Containers—W. H. Cross and Max McWhirter

Shock Testing with the Rocket Powered Pendulum—R. W. Hager

Properties of Concrete at High Rates of Loading—D. Watstein

Copies may be obtained from the American Society for Testing Materials, 1916 Race St., Philadelphia, Pa., for $3.50 each.

THE WELDING OF HIGH-STRENGTH ALUMINUM ALLOYS IN HEAVY SECTIONS

Investigations indicate that 5154 and 5056 aluminum alloys in heavy sections handle satisfactorily and have mechanical property advantages over 6061 alloy for many applications

BY WILLIS G. GROTH AND RICHARD A. MATUSZESKI

Scope

It has been the purpose of the research reported in this paper to verify the weldability and applicability of the aluminum alloys 5154 and 5056 in the heavy sections and high tensile strengths formerly reserved for the heat-treatable alloys such as 6061. It has been verified that these alloys do handle satisfactorily, and that they do have mechanical property advantages over 6061 for many applications.

Developments of the last two decades in the fields of transportation, chemical process equipment, military armament, and commercial aircraft have focused attention on aluminum in general and high-strength aluminum alloys in particular. The use of aluminum alloys for heavy pressure vessels and machinery elements has been greatly stimulated by the development of the inert-gas welding processes, including both the tungsten-arc process and the newer metal-arc consumable-electrode process.

Unfortunately, the strongest aluminum alloys are not always the best answer to specific industrial problems, nor are they usually considered "weldable" by fusion processes for several reasons. There has been a growing demand for larger and stronger weldments, requiring stronger materials or welds, heavier sections or both.

The fabrication of aluminum alloy railway tank cars for the chemical industry marked, in 1936, the entry of ACF Industries, Inc., into the field of welded aluminum fabrication. Since that time concepts of both "high-strength" and "heavy section" have been relentlessly modified. Today we accept as routine the manufacture of various machinery and pressure-vessel components in base metal thicknesses up to and exceeding six inches. The heaviest welds processed to date have been approximately fourteen inches, face to face. On the "strength" side of the ledger we have alloys providing as-welded tensile strengths ranging from 25,000 to over 40,000 psi. Where postwelding heat treatment is practicable, tensile strengths of 45,000 psi have been accomplished in light sections and it appears entirely practical to provide welds of approximately base-metal strength, with acceptable ductility, in even the heaviest sections.

Willis G. Groth is Senior Welding Engineer and **Richard A. Matuszeski** is Metallurgical Engineer, ACF Industries, Inc., Albuquerque, N. Mex.

Presented at 1956 AWS National Spring Meeting in Buffalo, N. Y., May 7–11.

Alloy Selection

There are a number of basic considerations in the selection of an aluminum alloy and manufacturing procedure where high-strength materials in heavy sections must be used. When heat treatment can be accomplished, that is, where furnace and quenching equipment capacity is adequate and the design is such that such a cycle is feasible, a heat-treatable alloy *may* be the answer. Alloy 6061 is a popular choice of commercial wrought material providing relatively high strength in the heat-treated condition and it is weldable in any condition. However, welding results in the loss of heat-treated mechanical properties in the vicinity of the weld, consequently a balanced design in material heat treated prior to welding must have an increase in section at the weld locations if weight or section economy is a factor. If the weldment can be heat treated after welding, assuming again that equipment is available and the cost is not prohibitive, we must then concern ourselves with the heat-treated properties of the weld deposit. Deposit strength and ductility are considered, of course, as some function of these same properties in the base material. It follows that the heat-treat cycle would almost necessarily be determined by the requirements of the base material, and the susceptibility of the base material to heat treatment (for a given analysis) is a function of the mass of the section to be so treated. Time-temperature plots of hardness (and tensile strength as a function of cooling rate reveal that it may be difficult to obtain optimum cooling rates for the heat treatment of, for instance, 4-in. plate to secure the same mechanical properties as one could expect with, for instance, $^1/_2$-in. plate.

A further complication arises in that the weld deposit in aluminum will not necessarily approximate the chemical analysis or metallurgical condition of the base material. For this reason there is little liklihood that the weld deposit will harden with the same predictability as the base plate. In thin sections the weld nugget may be largely or entirely fused base metal. In this instance, the weld nugget may very well harden satisfactorily (although the ductility has been known to be extremely low). In plate thicknesses of from $^1/_4$ in. to perhaps $^3/_4$ in., using a single-vee weld groove, one must add filler metal, and the degree of dilution of this filler metal will be a function of both the process and procedure used. The tungsten-arc process might be expected to place the most homogeneous deposit and it would ordinarily provide the least dilution. The degree of dilution secured with the metal-arc consumable-electrode process is a function of the depth of arc penetration, and hence of arc power and wire size. In heavier sections it is difficult, if not entirely impractical, to depend upon sidewall penetration to provide base metal alloying of the center of the weld nugget to secure some desirable degree of heat treatability.

The uninitiated might well ask: "why not make the filler wire of the same alloy as the base metal?" This has been largely unsuccessful in the welding of heat-treatable aluminum alloys for several reasons. (1) The analysis may provide poor properties

in a "cast" weld structure because of grain size, orientation, segregation, coring or other metallurgical consideration. The most obvious manifestation of this may be in deposit ductility or impact strength. (2) Cracking difficulties are commonly encountered and may be due to lack of hot strength or hot ductility at or slightly below the temperature of coalescence. In some cases ductility may not be a consideration, and in others it could possibly be improved by special heat treatments or by improving the structure by either hot or cold work. Industry has learned, the hard way, that it costs money to repair cracked welds and perform special heat treatments or forging operations except where weight is a critical factor, as in aircraft. The almost universal approach has been to use an alloy providing freedom from cracking and other troubles, to place a homogeneous weld each and every time if possible and to sacrifice strength if necessary. Economics has also dictated the use, wherever possible, of existing materials. Partially for this reason industry has relied upon alloy 4043 (5% silicon) as a filler material for the joining of many aluminum alloys, including 6061. This filler alloy handles satisfactorily and cracked welds are a rarity when it is properly employed. On the debit side of the ledger, there is the fact that the alloy in itself is not heat-treatable to the strengths desired from the 6061 alloy. Base metal dilution must be depended upon if a strength improvement is to be secured by heat treatment.

Work-Hardening Alloys

We have discussed some basic considerations regarding heat-treatable alloys. Alloys 5056 and 5154 are not heat treatable, although they are definitely in the high-strength category. Here, the tensile strength and other mechanical properties are functions of: (1) alloy content, increasing with increased percentages of magnesium; (2) work hardening, being stronger in the thinner gages where a greater percentage reduction per pass is possible and cold rolling can be satisfactorily accomplished. The beneficial effects of rolling can be secured in sheet and some plate, but at the present it must be conceded that heavy plate (viz., 3 in.) will be supplied in approximately the annealed condition although it may not have been given an anneal after rolling.

The effect of welding on the work-hardened material will be the removal of that strength advantage in the vicinity of the weld. This again is a function of time and temperature and the zone of complete annealing may be very narrow. The weld deposit will also have the properties of the annealed material. Actually these are high-tensile-strength alloys, since their yield strengths in the annealed condition are somewhat below the values for a heat-treatable alloy of the same tensile strength. The high ductility and low yield strength of these alloys in the annealed condition encourages the practice of designing upon the yield strength rather than upon the tensile strength.

As might have been concluded from the above, a survey of the literature leads one to believe that the principal advantages of these aluminum-magnesium alloys are such as to recommend their use where: (1) high ductility and impact strength are primary factors; (2) postwelding heat treatment is impractical or too expensive; (3) their particular corrosion resistant properties (particularly since they use identical filler metal) are desirable.

Prudently, the successful fabricator is sometimes reluctant to commit himself for the fabrication of a new metal or alloy, even though a general similarity to more common materials is obvious. This is particularly true where a material is relatively untried by industry and

Table 1—Chemical Composition Limits

	Alloy	Silicon	Iron	Copper	Manganese	Magnesium	Chromium	Zinc	Titanium	Others Each	Others Total	Minimum remainder
A	6061	0.40–0.80	0.70	0.15–0.40	0.15	0.8–1.2	0.15–0.35	0.20	0.15	0.05	0.15	Al
	5154	0.45	Si and Fe	0.10	0.10	3.1–3.9	0.15–0.35	0.20	0.20	0.05	0.15	Al
	5056	0.30	0.40	0.10	0.05–0.20	4.5–5.6	0.05–0.20	0.10	...	0.05	0.15	Al
	4043	4.5–6.0	0.80	0.30	0.05	0.05		0.10	0.20	0.05	0.15	Al
B	6061-O	0.57	0.35	0.27	0.05*	0.79	0.26	0.10*	0.09	0.05* Ni 0.05* Bi 0.05*		Al
C	6061 + 4043	4.80	0.37	0.10	0.05*	0.18	0.05*	0.10*	0.05*	0.05* Ni 0.05* Bi 0.05*		Al
D	5154-O	0.11	0.25	0.05*	0.05*	3.30	0.21	0.10*	0.11	0.05* Pb 0.10* Ni 0.05* Bi 0.05*		Al
E	5154 + 5154	0.11	0.18	0.05*	0.05*	2.85	0.23	0.10*	0.15	0.05* Pb 0.10* Ni 0.05* Bi 0.05*		Al
F	5056-O	0.10*	0.12	0.07	0.14	4.60	0.10	0.08	0.16	Pb 0.05* Ni 0.05* Bi 0.05*	0.25*	Al
G	5056 + 5056	0.10*	0.05	0.05*	0.10	4.60	0.10	0.08	0.14	Pb 0.05* Ni 0.05* Bi 0.05*	0.25*	Al

Legend: A—Specified chemical composition limits for the respective alloys in this group. B—Actual analysis of base stock (618) from 3-in. Test Ring. C—Actual analysis of weld metal from 3-in. Test Ring (618 with 438 Filler). D—Actual analysis of base stock (548) from 3-in. Test Ring. E—Actual analysis of weld metal from 3-in. Test Ring (548 with 548 Filler). F—Actual analysis of base stock (568) from 3-in. Test Ring. G—Actual analysis of weld metal from 3-in. Test Ring (568 with 568 Filler).

* Denotes "less than."

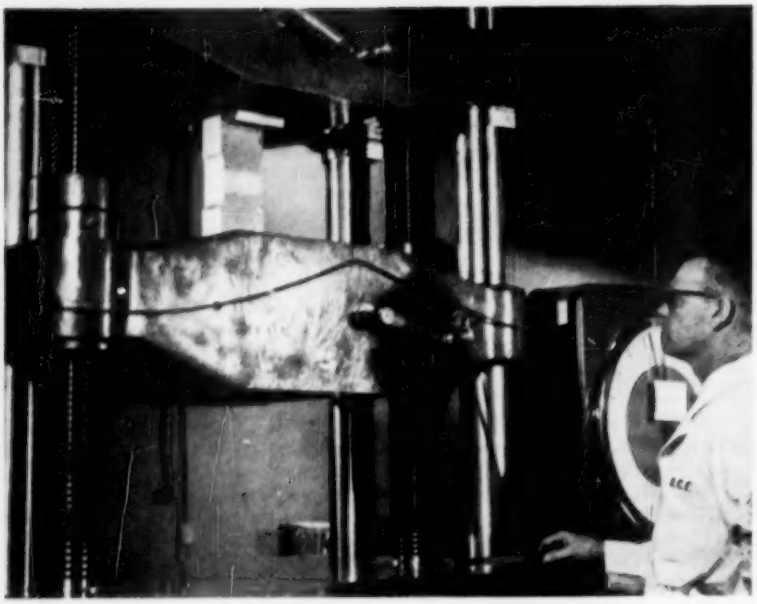

Fig. 1 Tensile testing full-size specimen

there exist comparative doubts of either its workability or application. Such was the reaction to the announcement, several years ago, of the high-strength aluminum alloys 5154 and 5056. At that time the writers' organization decided that: (1) all existing data on the best previous high-strength weldable aluminum alloy (6061) should be compiled and reverified as necessary; (2) upon completion of this, a program should be initiated to investigate those recently developed alloys deemed most likely to gain an important place in welded industrial and military fabrication. The data and information to follow was gleaned from several years of both developmental and production welding.

The criteria by which materials of construction are chosen, or by which a final selection is made, are many. For the purposes of this investigation, it sufficed to make short-time mechanical tests since such factors as creep, stress corrosion or general corrosion were not immediately relevant. Because the general requirement was for "heavy aluminum" it was decided to run test welds, as they might be required, in 3-in. aluminum. Test weldments were cylinders 36 in. OD by 12 in. long, containing one circumferential weld. It had previously been determined that the properties of 3-in. material would generally approximate those of the material range from 2 to 6 in. and also provide sufficient weldment mass to approximate typical fabricating conditions. Since "general" information was sufficient, it was also decided to use 0.505-in. tensile specimens, $^3/_4$-in. free bend specimens and standard vee-notch Charpy specimens.

Radiography

Radiographic standards for production work were used on test welds. All test welds met ASME code requirements for unfired pressure vessels. Generally speaking, the self-imposed porosity standard for critical work corresponded to the ASME Code standard for welds of one fourth the thickness being tested. That is, 2-in. plate welds were checked against porosity standards established for $^1/_2$-in. plate. Radiographs of hundreds of production welds, showing a discrimination of 2% or finer, have been essentially clear.

Conditions and Limitations

There were several limitations to be considered in the test and their evaluation:

1. Commercial alloys in commercially available temper must be used.
2. Commercially available welding and heat-treating equipment must be used.
3. Commercially practicable (although not necessarily conventional) welding and heat-treatment procedures must be used.

These limitations were imposed for several reasons:

1. There existed a conviction that the tests would probably reveal certain joint or deposit shortcomings that would indicate the desirability of filler-metal alloys not commercially available in quantity.
2. It was felt that filler-wire surface condition might be an important factor, but that side research on the subject was not justified.

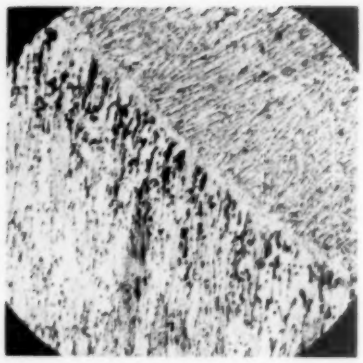

Fig. 2 Fusion line, 4043 weld in 6061-F

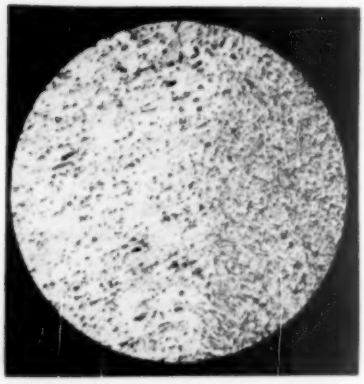

Fig. 3 Fusion line, 4043 weld in 6061, HT to T-6

3. It should be possible to translate the results into mass production procedures using conventional equipment with little or no modification.
4. Procedures should be as simple and straightforward as possible.

For the above and other reasons the following basic procedure variables were initially fixed:

1. Automatic inert-gas consumable-electrode welding would be used wherever practicable.
2. Semiautomatic welding by the same process would be the second choice where deposit rate might be a significant factor.
3. The inert-gas tungsten-arc process would be used for tacking, local repairs and general hand welding.
4. Preheat would not be used.
5. The largest practicable electrode size would be tried for welding at least the initial specimens.
6. Multiple passes of not more than 0.15 lb per foot per pass, and preferably about 0.1 lb per foot per pass, would be used for automatic welding.
7. Stringer bead techniques would be used for all welding, with bead width of approximately four to five times the electrode diameter and not to exceed seven times the electrode diameter.

Table 1 shows the specification

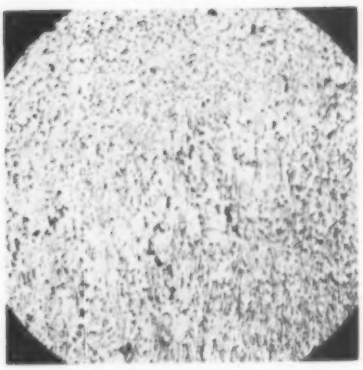

Fig. 4 Fusion line, 5154 in 5154-F

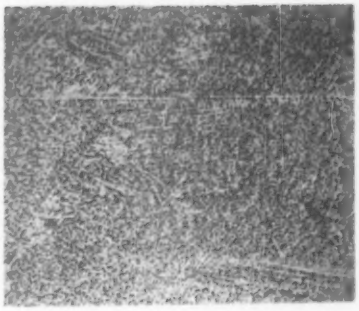

Fig. 5 5154 weld, X 200. (Reduced by 1/3 upon reproduction)

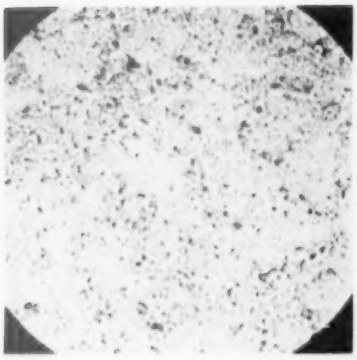

Fig. 6 5056 weld, X 187. (Reduced by 1/3 upon reproduction)

limits and analyses of the base metals and weld deposits considered in this investigation.

Procedures

All welds reported were made by the inert-gas consumable-electrode process using constant wire feed apparatus and constant-potential welding power. The power supply had a droop of approximately one volt per one hundred amperes at the terminals. Arc voltage was maintained at approximately twenty-eight to thirty volts except where the operator encountered macroporosity attributable to the filler wire, where the voltage was increased to approximately thirty-four volts.

Shielding for the consumable-electrode process was 80% helium and 20% argon, with helium flows of from 60 to 100 cfh depending upon ambient conditions. Shielding gas for the tungsten-arc process was welding-grade helium.

Amperages were determined on the bases of deposit rate and arc-handling characteristics. Production department procedures and amperages were satisfactory and the following figures are typical: 1/16-in. electrodes, 275–350 amp; 3/32-in. electrodes, 300–400 amp; and 1/8-in. electrodes, 350–475 amp. Generally speaking, the 5056 and 5154 wires were operated at somewhat greater values than is the practice with 4043 wire. It has been our experience that most experienced welding operators, having a choice, prefer to weld 5056 or 5154 rather than 6061 alloy, although there seems to be an increase in radiation in the ultraviolet spectrum when using either 5154 or 5056 filler wire.

Macroexamination

Macroexamination of the welds for porosity and other internal defects indicated less tendency for macroporosity with the 5056 and 5154 alloys. This could possibly be attributed to a difference in surface condition, however. Conversely, there was an increased susceptibility to the formation of microporosity as will be noted in the section on metallography.

Macro defects were not common to all welds, nor were they necessarily common to all parts of a given weld. For these reasons, a rather careful study was made. Obviously the gaseous elements causing porosity could have been dissolved in the base metal or filler metal before welding. They could also be decomposition products of contaminants on the surface of the wire or base metal. Quite frequently the porosity, or some part of it, can be traced to contaminated shielding gas. More often than not this contamination has been introduced after the gas left the cylinder, by loose connections, leaky hoses, dirty lines and gaskets, or from oil leaks in the equipment. Amperage and voltage were verified to be related factors, particularly where the arc characteristics and porosity could be associated with wire surface condition.

The most common macro defect is spherical porosity of from 1/32 to 3/32 in. in diameter, random distribution. This can be safely attributed to gas dissolved in the weld deposit, whether from unclean wire, dirty gas or plate surface contamination. A second macro pattern is also spherical porosity, sometimes larger, in linear array. This is commonly traceable to mislocation of the weld centerline causing inadequate penetration along one side of the puddle —or entrapment of gas in the papillary penetration groove when using pure argon. A third macro defect, usually of irregular shape, is an oxide inclusion resulting from poor shielding or faulty procedure or machine operation. Due to their size and shape, these defects can be considered incipient cracks and for that reason they should be removed when discovered. It has been our proved conviction that experienced operators can usually indicate the type, magnitude, distribution and location of macro weld defects. When this is the case the defects can be removed before proceeding (at some saving in cost) and recurrences be largely avoided. A pneumatic chipping hammer is one of the most satisfactory tools for continuous production quality control, and when such a tool is available, welding over existing defects is rarely excusable.

There are a number of general approaches to the problem of minimizing porosity from absorbed or entrapped gases:

1. Where it is determined that at least some of the gas is coming out of solution as the puddle cools—increase the cooling rate to keep void size and number down. This can be done by

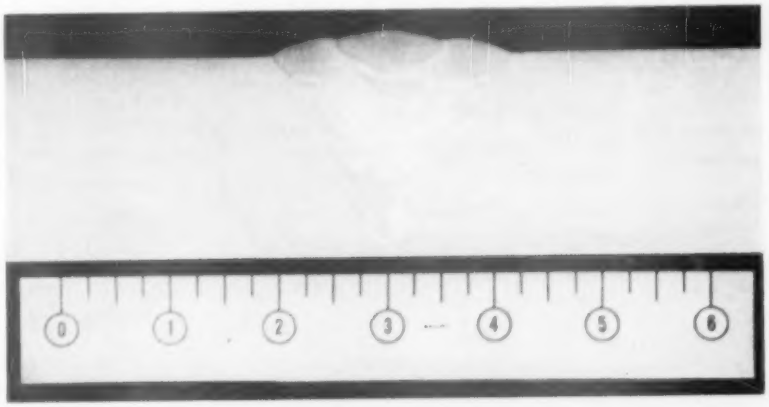

Fig. 7 Typical weld section, as-welded

lowering base-metal temperature, increasing speed, etc.

2. Where the above is not applicable or sufficiently effective, *decrease* the cooling rate in an attempt to provide time for the gas to rise to the puddle surface and dissipate. This can be effected by preheat, lower travel speeds, increased amperages, etc.

3. "Burn-out" defects when making subsequent passes. This involves widening and deepening the penetration profile to "float out" voids in previous passes. This can be done by:

(*a*) Increasing amperage.
(*b*) Increasing voltage.
(*c*) Changing shielding gas or gas mixture.
(*d*) Improving electrode surface condition by using other wire.
(*e*) Changing speed to keep arc on base metal or previous deposit rather than dissipating arc energy in a large puddle.

4. Use materials less prone to porosity or "condition" them by heating them to drive off absorbed or adsorbed gases.

5. Change ratio of absorbed gas (in puddle) to a more favorable one by controlling dilution. Interface porosity can often be decreased by increasing side-wall penetration.

Wire is the first variable suspected in most instances. Where actual tests have indicated the wire to be at least partially at fault, remedial procedures (not always desirable otherwise) can sometimes be devised. In other instances it is not possible to make satisfactory welds with the wire except in the manufacturer's laboratory. It might be noted that there does not ordinarily exist a welding wire quality warranty as such. Some wire manufacturers will certify that a given lot of welding wire was tested (procedure not specified) and found to produce welds of "code" quality. Some suppliers will accept return of new wire found unsatisfactory by a customer. It should be noted that almost any wire will produce "code" welds in some minimum material thickness. Code allowances increase as thickness increases, but many organizations cannot freely accept weld metal voids of $^3/_{16}$ in. or greater diameter merely because they are code acceptable.

Apparently the exact surface condition of an aluminum welding wire is not so critical if the condition—whatever it is—is absolutely uniform from foot to foot, coil to coil, lot to lot, and month to month. "Bad" wire will then always be bad and should eventually disappear from the market. "Fair to good" wire will be matched with appropriate procedures and, if neither wire nor procedure is changed, "shop emergencies" will become less common. "Excellent" wire will do satisfactory work with any minimum procedure and will do premium work for the plant using premium procedures. Fortunately, what has been referred to as an "excellent" wire can be no more expensive to produce than many "fair-to-good" wires, and less expensive than some so-called "premium finish" wires.

Metallographic Study

A number of metallographic studies were made and Fig. 2 shows a section across the fusion line and heat-affected zone of a weld of 4043 alloy in 6061-F base material. It will be noticed in this figure that in the base metal immediately adjacent to the fusion line there is a concentration of segregations of one of the constituents in the material. A comparison with Fig. 3 shows that in reheat treatment of a weld zone of this nature the re-solution and precipitation of these phases had resulted in a general distribution rather than a concentration in the immediate heat-affected zone. This second photomicrograph shows the material and weld in the T-6 condition and shows that the heat treatment has had some effect on the weld deposit itself as the solution and precipitation treatments have somewhat broken up the original columnar structure of the deposit.

The third photomicrograph, Fig. 4 is that of the fusion zone in the 5154 alloy welded in the as-rolled or "F" condition and shows that the weld deposit itself is of generally uniform struc-

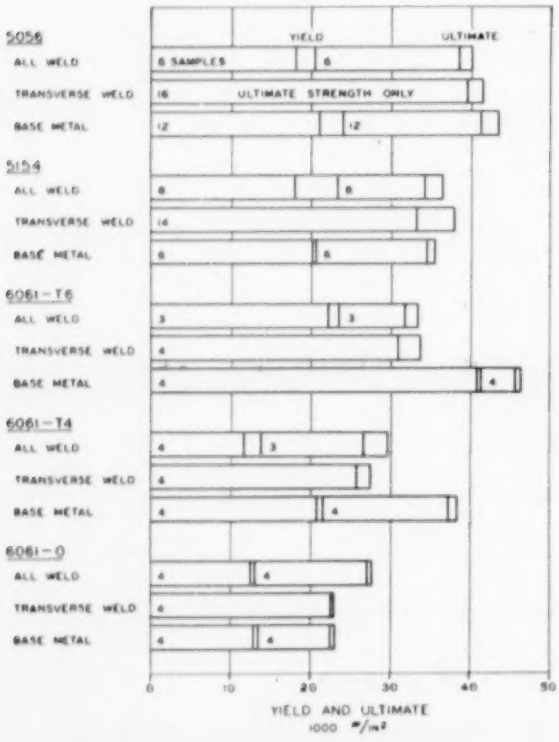

Fig. 8 Tensile and yield strength data

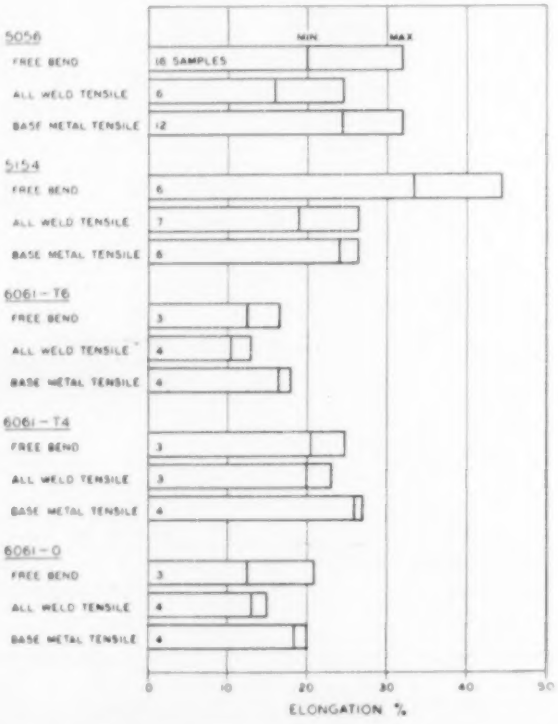

Fig. 9 Ductility comparison data

ture and that there has occurred a general coarsening of the grain structure in the immediate vicinity of the fusion line. Since this is a work-hardening alloy and phase precipitation is not a factor in its hardness and tensile strength, there does not seem to be any great change in the size and distribution of various base-metal and weld-metal constituents. Figure 5 was taken at approximately 200 × and shows a section taken from an area in the approximate center of the weld deposit. It can be seen from this figure that there exist a number of pronounced straight lines indicating the general progress of grain growth upon cooling of the weld nugget. The last photomicrograph, Fig. 6, is that of a weld deposit in the 5056 alloy and two things come to one's attention. First, the development of the grain structure has been somewhat random as though there were a great number of crystal nuclei forming centers of solidification of the weld deposit. Secondly, a number of deposit phase constituents can be identified; which is in keeping with the somewhat higher alloy content of this material. This photomicrograph also reveals the scatter of micro porosity which was found to exist in these welds and which may or may not be a problem in future production work. This porosity was found to be most prevalent along the lower penetration or fusion line profile of each pass and was usually too fine to be detected with the naked eye or ordinary shop optical equipment.

It might be noted that, partially as a result of the findings of this investigation, further work has been and is being done to find more satisfactory filler metal alloys for the welding of heavy 6061 material which is to be heat treated. There are a number of logical courses for such a study, one of them being to modify the 4043 alloy and another to modify the 5052 or 5154 alloy. While both courses lead to adequate strength, there are reasons to believe that the latter course will result in better ductility values. There will undoubtedly be more to report on this subject at a later date.

Test Specimens

A typical weld cross section from a single "U" groove is shown in Fig. 7. All alloys were welded in the as-rolled condition, and the T4 and T6 heat treatments listed for the 6061 alloy were performed after welding. It might be noted again that the 3-in. plate material revealed no beneficial properties which might have resulted from the rolling operation, although this might be the case with thinner material. All 6061 welds were placed using 4043 (5% silicon) filler wire, conforming to conventional industrial practice. The other alloys were welded with

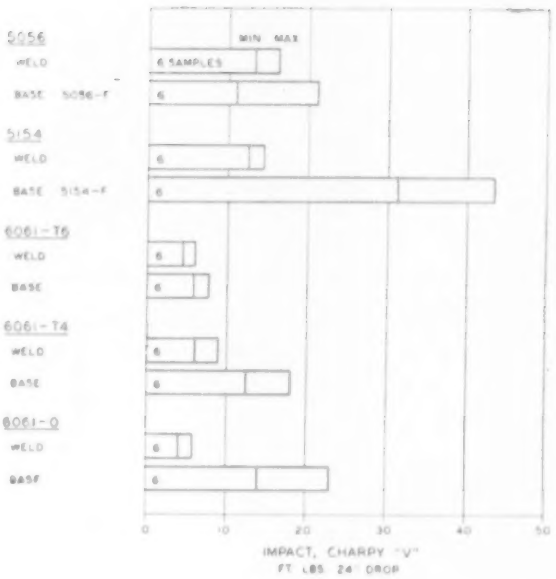

Fig. 10 Impact strength comparison data

filler material of an analysis approximating that of the base material.

Each of the mechanical properties was graphed individually, to better facilitate comparison of that property for each of the alloys or conditions. Figure 8 shows tensile and yield strengths. It is obvious that in the unwelded base metal alloy 6061-T6 is superior. Alloy 5056 is second and 5154 is third. These latter values, as well as their accompanying yield strengths, could be improved if a satisfactory means could be found for work-hardening the sections. Welding changes the picture drastically, and the 6061-T6 weld strength is limited by the strength of the heat treated weld deposit. This value is approximately that of alloy 5154 welds, and below that of 5056 welds. Alloy 6061 in the as-welded and T4 conditions shows no advantage.

Yield strengths of the weld deposits were approximately the same except that here again alloy 6061 in the as-welded and T4 conditions was low.

Figure 9 shows the ductility of the various materials as determined by several conventional methods. Here, it is revealed that alloys 5056 and 5154 show a decided advantage.

Figure 10 includes comparative impact data on the same welds, and again alloys 5056 and 5154 show up very well.

Fabrication Data

The welding of heavy plate is not exactly an everyday occurrence, but the attendant problems are certainly far from insurmountable. Partially because of differences in manpower availability and material costs, the various divisions of a national manufacturing organization may and do use widely differing welding procedures. A few production figures might be of interest. The highest amperage used to date, on 1/8-in. aluminum wire, was 585 amp. On one occasion an arc of 1 hr 55 min. duration was maintained with 4043 filler alloy on 6061 base metal. On another occasion an arc of 3 hr and 15 min duration was maintained with 5154 alloy. It has not been unusual to use 40 lb of wire per machine per 8-hr shift, or 100 lb per machine per three shift cycle, including set-up time.

Such production requires close cooperation between the engineering and producing divisions, with constant surveillance to work out more economical joint designs and more satisfactory procedures. It is often necessary to redesign machine components for access in narrow grooves, and improve head mounting devices to save time in head adjustments. It is also desirable that the operator be able to conveniently make amperage, voltage and slight head position adjustments while the equipment is in operation. This requires that controls be accessible to him, with remote controls and indicating equipment if possible. It is also desirable that this operator be given every opportunity to learn and understand the equipment with which he is working, and that he be given some liberty as to the exact details of the welding procedure which he is required to follow. This somewhat heretical statement does not sound so ridiculous when one notes that some aluminum welds could require hours of almost continuous deposit. At an average power input rate of about twelve thousand watts per hour it is easy to see that the procedure may require changing as the workpiece temperature changes. Considerable change can take place while the operator eats his lunch, or while the equipment is inoperative for

a multitude of other reasons.

Conclusions

Aluminum alloys 5056 and 5154 can be fabricated using conventional equipment and procedures. They are superior to alloy 6061 for heavy weldments which cannot be heat treated to the T-6 condition after fabrication. Where weld ductility and impact strength are factors, they are definitely superior alloys. It is evident that alloy 6061, in the thicknesses tested and using the filler alloy noted herein, shows absolutely no short-time advantages unless heat treated.

Progress is being made in the problems of alloy composition, gas purity, wire cleanliness, machine design and control. Many of the problems first associated with this type of fabrication have been solved by the organizations pioneering this work, and the solutions are available to industry through the hands of the many industrial sales and service organizations who have cooperated in making those equipment and material changes deemed desirable or necessary. The 20-lb coil of aluminum wire, for instance, was born of the necessity to save time where coil changes of up to four times a day were necessary and 50-lb coils were impractical because of their physical size.

Acknowledgment

The authors appreciate the opportunity of presenting this report to American industry, and regret that time and space limitations have prevented a more complete and elaborate presentation. We, the authors, want to thank W. J. Jackel, ACF Industries for his interest and encouragement in the preparation of this paper. We would also like to thank our many coworkers for their invaluable assistance.

A DEW POINT-TEMPERATURE DIAGRAM FOR METAL-METAL OXIDE EQUILIBRIA IN HYDROGEN ATMOSPHERES

New proposed diagram may be used as a working guide for furnace brazing in hydrogen atmospheres

BY W. H. CHANG

Introduction

Furnace brazing, particularly that of heat-resisting materials, often requires a controlled hydrogen atmosphere to reduce the metal oxides present on the surface of the base materials. As a guide to establishing the brazing procedure, it is helpful to have a diagram relating the water-vapor content of the hydrogen atmosphere to its reducing characteristics. Such a diagram may be constructed by plotting log (P_{H_2O}/P_{H_2}) as a function of $1/T$ for the reaction of a particular metal oxide with hydrogen under equilibrium conditions.[1] However, the usefulness of this representation is considerably obscured to the brazing field where the water-vapor content of a hydrogen atmosphere is commonly expressed in dew point rather than in the ratio of the partial pressures. The conversion of $1/T$, where T is in °K, into temperature of ordinary units, also proves to be unnecessarily inconvenient.

For these reasons, a new diagram, intended primarily for brazing, is hereby proposed by relating the dew points of the hydrogen atmosphere to the temperatures at which various metals are in equilibrium with their respective oxides. To provide some understanding of this diagram, a simple derivation and illustration of the principle is included.

Thermodynamic Considerations

The reaction between hydrogen and metal oxides may be represented by the

W. H. Chang is associated with Materials & Processes Lab., General Electric Co., Schenectady, N. Y.

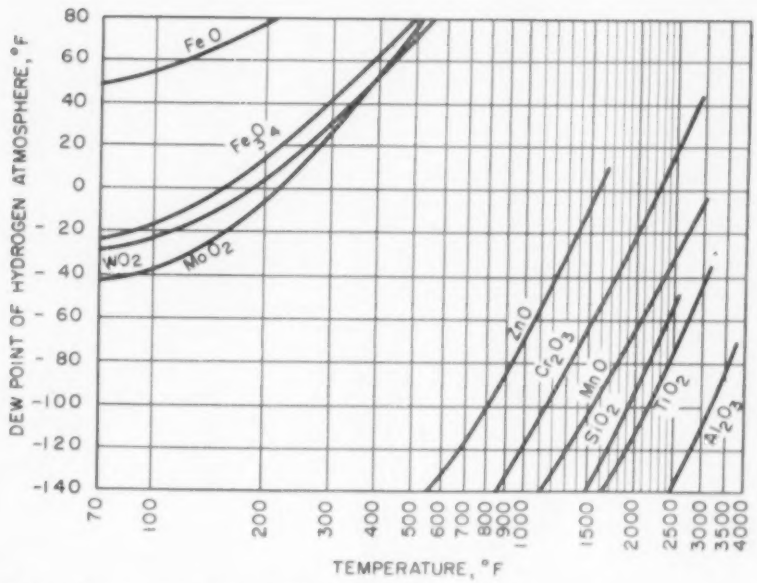

Fig. 1 Metal-metal oxide equilibria in hydrogen atmospheres

equation

$$M_mO_{n(s)} + nH_{2(g)} = mM_{(s)} + nH_2O_{(g)} \quad (1)$$

where M and M_mO_n stand, respectively, for the metal and its oxide in question, m and n are constants for each reaction and s and g indicate solid and gaseous states. Equation 1, in essence, depicts a rivalry for oxygen between the metal and hydrogen. To what extent reduction of the metal oxide will occur depends exclusively on the equilibrium constant, K, which varies with temperature and, for a given temperature, is a constant. For eq 1,

$$K = \frac{a_M{}^m \, a_{H_2O}{}^n}{a_{M_mO_n} \, a_{H_2}{}^n} = \left(\frac{a_{H_2O}}{a_{H_2}}\right)^n = \left(\frac{P_{H_2O}}{P_{H_2}}\right)^n \quad (2)$$

in which the a's denote activities and P_{H_2O} and P_{H_2} are the respective partial pressures of watervapor and hydrogen. It will be noticed that the metal and its oxide are substantially in their standard states. Their activities, a_M and $a_{M_mO_n}$, are correspondingly unity.

The equilibrium constant is related to the standard free energy change, $\Delta F°$, of the reaction, by the expression

$$\Delta F° = -RT \ln K \quad (3)$$

where R is the gas constant. For the reaction represented by eq 1, it follows that

$$\Delta F° = -RT \ln \left(\frac{P_{H_2O}}{P_{H_2}}\right)^n = -4.576nT \log \left(\frac{P_{H_2O}}{P_{H_2}}\right) \quad (4)$$

in which $\Delta F°$ is in calories per mole of M_mO_n and T in ° K. It is apparent that if $\Delta F°$ is known as a function of temperature, the equilibrium relationships between P_{H_2O} and P_{H_2} for any given temperature may be obtained from eq 4.

The temperature dependence of $\Delta F°$ is linear for some reactions and nonlinear for others. Since in either case the construction of the present diagram is valid, a linear temperature dependence will be assumed. This dependence may be represented by

$$\Delta F° = A + BT \quad (5)$$

in which A and B are constants. Combining eqs 4 and 5 gives

$$-4.576nT \log \left(\frac{P_{H_2O}}{P_{H_2}}\right) = A + BT$$

or

$$\left(\log \frac{P_{H_2O}}{P_{H_2}}\right) = \left(\frac{-A}{4.576n}\right)\left(\frac{1}{T}\right) + \left(\frac{-B}{4.576n}\right) \quad (6)$$

By plotting $\log (P_{H_2O}/P_{H_2})$ against $1/T$ a straight line results constituting the basis of representation mentioned in the introduction.[1] The significance of eq 6 will be discussed later.

In accordance with the purpose of the present diagram, it now remains to transform the P_{H_2O}/P_{H_2} ratios into corresponding dew points. This is accomplished by finding the watervapor pressure at each dew point and calculating the ratios $P_{H_2O}/P_{H_2} = P_{H_2O}/(1 - P_{H_2O})$.

Once the relationships between dew point and (P_{H_2O}/P_{H_2}) are known, it is then a simple matter to construct the dew point-temperature diagram. For each section, one dew point is assumed and converted into the corresponding P_{H_2O}/P_{H_2} ratio. The latter is then substituted into eq 6 to obtain the equilibrium temperature. By repeating this procedure, a curve relating dew points to temperatures may be drawn consisting of as many points as may be desired.

Presentation of Diagram

Based on the foregoing principle, a dew point (° F) vs. T (° F) diagram is presented in Fig. 1 for Al_2O_3, TiO_2, SiO_2, MnO, Cr_2O_3, ZnO, MoO_2, WO_2, Fe_3O_4 and FeO. In preparing this diagram, the pertinent standard free energy change equations are obtained from the work of Kubaschewski and Evans.[2] The dew point-log (P_{H_2O}/P_{H_2}) conversions are based on the watervapor pressure data from the *Handbook of Chemistry*.[3]

It will be observed that most of the oxides included in Fig. 1 are those likely to be present on the base materials which are usually furnace-brazed in hydrogen atmospheres. Since this diagram is intended primarily for brazing, the dew-point axis ranges from +80 to −140° F and the temperature axis from 70 to 4000° F. Either dew point or temperatures outside these ranges will seldom, if ever, be encountered in brazing applications. For the same reason, or as a consequence of it, relatively unstable oxides of Cu, Ni, Pb, etc., as well as the very stable oxides of Ca and Be, are not included in this diagram. The curves for the unstable oxides, if drawn, would lie further to the left than the curve for FeO. These oxides may thus be reduced at relatively low temperatures by "wet" hydrogen atmospheres. On the other hand, the curves for CaO and BeO would lie to the right of that for Al_2O_3. To reduce these oxides, unusually high temperatures or extremely pure hydrogen atmospheres are required.

The results given in Fig. 1 are in substantial agreement with those shown by Darken and Gurry,[4] and by Lustman.[5] However, comparing the present diagram with that adopted in the *AWS Brazing Manual*[1] disagreement exists for Cr_2O_3, MnO, MoO_2 and WO_2. Based on the thermodynamic data, Cr_2O_3 is less stable than MnO. This relationship is reversed in the *Brazing Manual* diagram. According to the latter, the equilibrium temperatures for the Cr_2O_3-H_2 system are 3000° F at a dew point of 0° F and 2300° F at a dew point of −50° F. In Fig. 1, the corresponding temperatures are found to be about 2250 and 1600° F.

In addition, the lines for MoO_2 and WO_2 are placed in the *Brazing Manual* diagram close to that for SiO_2. This is in considerable contradiction with the thermodynamic calculations[2] which show that MoO_2 and WO_2 are not nearly as stable as depicted.

Interpretation of Diagram

Each line in Fig. 1 is basically an individual graphical representation of

eq 6,

$$\log\left(\frac{P_{H_2O}}{P_{H_2}}\right) = \left(\frac{-A}{4.576n}\right)\left(\frac{1}{T}\right) + \left(\frac{-B}{4.576n}\right)$$

which determines the equilibrium ratio of P_{H_2O}/P_{H_2} at a given temperature. Under equilibrium conditions, the rate of oxidation of the metal by water vapor is exactly equal to the rate of reduction of the oxide by hydrogen. There is thus no net oxidation or reduction after equilibrium is established, and the ratio P_{H_2O}/P_{H_2} becomes constant, characteristic of that temperature. If the water-vapor content, or dew point, should increase while the temperature remains unchanged, the equilibrium is disturbed. Water vapor, in seeking to reduce its partial pressure, commences to oxidize the metal until the equilibrium ratio of P_{H_2O}/P_{H_2} (which must be constant for a given temperature) is again restored. Conversely, by lowering the dew point from the equilibrium value, hydrogen, being in excess, will reduce the oxide in order to re-establish the equilibrium. The effect of temperature may best be seen from the slopes of the curves shown in Fig. 1. That the slopes are all positive for the systems included therein indicates that at a higher temperature, a greater amount of water vapor may be tolerated in maintaining the equilibrium. Prevention of oxidation or reduction of oxides is thus favored at elevated temperatures.

It follows that each curve in Fig. 1 represents a boundary separating the zone of oxidation (left-hand side) from the zone of reduction (right-hand side). The relative position of each boundary depends on the stability of the oxide, being further to the right of the diagram the more stable the oxide. In actual application of Fig. 1, the significance of each curve may be better grasped from the purpose for which the curve is applied. In brazing, for example, the reduction of oxides is of primary importance. At a given dew point, the corresponding equilibrium temperature is then the minimum temperature required, and at a given temperature, the equilibrium dew point is the maximum dew point allowed to prevent oxidation. In order to reduce the oxides already present, either a higher temperature or a lower dew point than the equilibrium values must be employed. On this basis, the use of Fig. 1 may be illustrated for the case of Cr_2O_3. Assume that a hydrogen atmosphere having a dew point of −40° F is available to reduce Cr_2O_3. From this dew point on the vertical axis of Fig. 1, a horizontal line may be drawn to intersect the Cr_2O_3 curve. If a vertical line is dropped from the intersecting point onto the abscissa, the equilibrium temperature, 1750° F, is located. The chromium oxide will then be reduced by the atmosphere at temperatures slightly above 1750° F, provided the dew point is maintained at −40° F. Conversely, at a temperature of 1750° F, a hydrogen atmosphere having a dew point less than −40° F will be adequate to reduce the oxide. It will be realized that between temperature and dew point, the requirements for one cannot be relaxed without restricting the requirements for the other. In the above example, for instance, if the dew point is raised to −20° F, the oxide will not be reduced until the temperature is above 2000° F. Similarly, by lowering the temperature to 1150° F, a dew point below −100° F becomes essential.

In using Fig. 1, the conditions under which the diagram is constructed should be borne in mind. Since the diagram is based on simple thermodynamic relationships, it does not specify the reaction rate which is determined by the potential barrier or activation energy of the process through which the reaction takes place. Thus, reduction of unstable oxides, which is predicted by Fig. 1 to be possible at relatively low temperatures, may not proceed to discernible extent within a desired length of time. It should be pointed out, however, that for the reactions occurring at high temperatures, the reaction rate is, in general, rather rapid.

Each curve in Fig. 1 is based on a system in which the pure metal and its oxide are taken to be in their standard states. Should the metal exist instead as an alloying element (such as in a base material being brazed), its activity will be less than unity, resulting in dew point-temperature relationships different from those predicted in Fig. 1. Consider, for instance, the oxidation of chromium in its pure state,

$$2Cr_{(s)} + 3H_2O_{(g)} = Cr_2O_{3(s)} + 3H_{2(g)} \quad (7)$$

and as alloying element in steel,

$$2Cr_{(\text{in steel})} + 3H_2O_{(g)} = Cr_2O_{3(s)} + 3H_{2(g)} \quad (8)$$

The equilibrium constants are for eq 7

$$K_1 = \left(\frac{P_{H_2}}{P_{H_2O}}\right)^3 \quad (9)$$

and for eq 8

$$K_2 = \left(\frac{P_{H_2}'}{P_{H_2O}'}\right)^3 \frac{1}{a_{Cr}^2} \quad (10)$$

Since both cases pertain to the reaction of water vapor with chromium, the constants must be identical for a given temperature. Hence,

$$\left(\frac{P_{H_2}}{P_{H_2O}}\right)^3 = \left(\frac{P_{H_2}'}{P_{H_2O}'}\right)^3 \frac{1}{a_{Cr}^2} \quad (11)$$

In eq 11, the value of the activity of chromium, a_{Cr}, depends, among other things, on the chromium content as well as the nature of its existence (such as in solution or as carbides). In any event, it is less than unity so that from eq (11) the relationship

$$\frac{P_{H_2}'}{P_{H_2O}'} < \frac{P_{H_2}}{P_{H_2O}} \quad (12)$$

or

$$\frac{P_{H_2O}'}{P_{H_2}'} > \frac{P_{H_2O}}{P_{H_2}} \quad (13)$$

exists. Equation 13 thus states that, in order to prevent oxidation of chromium, or any other metal included in Fig. 1, a higher dew point may be tolerated when the metal is alloyed than when it is in its pure state. This probably explains why, whereas pure Al_2O_3 or TiO_2 cannot be reduced at 2150° F in a hydrogen atmosphere with a dew point of −90° F, heat-resisting materials which contain small amounts of Al and Ti, may still be brazed under these conditions with a rapid heating.

Returning to the discussion of Fig. 1, it may also be mentioned that when several oxidizable elements co-exist in the base material, it is not unusual for their oxides to form spinels (xM_mO_n-$yM_p'O_q$).[8] The latter may then respond to a given hydrogen atmosphere in a manner unlike that shown by the individual oxides. Finally, it is obvious that the dew point given in Fig. 1 refers to that of the atmosphere surrounding the reacting system in question. Unless prolonged purge of the brazing container is undertaken, any assumption of the actual dew point to be that measured from the exit gas, or of the inlet gas, will lead to serious errors.

The foregoing remarks should have made it clear that a diagram like that shown in Fig. 1 is not tailored to take care of every aspect of brazing. Nevertheless, it serves to describe some basic thermodynamic requirements in temperature and dew point on the oxidation of metals and reduction of their oxides in hydrogen. To the high-temperature brazing field where base materials are, in general, alloys rather than pure metals, these requirements may be considered as limits which need not be exceeded in order to prevent oxidation or to effect reduction. In fact, these requirements, if satisfied in brazing, may be looked upon as providing a margin of safety for the purpose intended. It is on the basis of such understanding that the dew point vs. temperature diagram may be used as a working guide for furnace brazing in hydrogen atmospheres.

References

1. AWS, *Brazing Manual*, 1955, p. 45.
2. Kubaschewski, O., and Evans, E. Ll., *Metallurgical Thermochemistry*, 1955, pp. 305–309.
3. Lange, N. A., *Handbook of Chemistry*, 1939, pp. 1211–1217.
4. Darken, L. S., and Gurry, R. W., *Physical Chemistry of Metals*, 1953, p. 349.
5. Lustman, B., "The Resistance of Metals to Scaling," *Metal Progress*, 850 (November 1946).
6. Preece, A., and Lucas, G., "The High-Temperature Oxidation of Some Cobalt-Base and Nickel-Base Alloys," *J. Inst. Metals*, **81**, 219–227 (1952–53).